UNIVERSITY OF CALIFORNIA
RIVERSIDE

Characterization of a Small Molecule Inhibitor of SUMOylation Pathway as a New Approach to Cancer Treatment

A Dissertation submitted in partial satisfaction
of the requirements for the degree of

Doctor of Philosophy

in

Biomedical Sciences

by

Hilda Wiryawan

June 2014

Dissertation Committee:
Dr. Jiayu Liao, Chairperson
Dr. David Lo
Dr. Ameae Walker

The Dissertation of Hilda Wiryawan is approved:

_____

_____

_____

Committee Chairperson

University of California, Riverside

ACKNOWLEDGEMENTS

Over the past five years, I have received support and encouragement from a great number of individuals. I would like to thank Dr. Jiayu Liao for his mentorship, guidance, and support in my Ph.D. training. I would also like to thank Dr. David Lo for his helpful advice as my committee member. I also received lots of helpful advice from Dr. Ameae Walker both about my project and about future career. She also graciously let me sit in on her lab meetings to learn more about prolactin and cancer research in general.

I would like to thank Dr. Liao's lab members; Dr. Yang Song from whom I inherited this project and learned FRET assays; Dr. Yan Liu, Dr. Ling Jiang, Vipul Madahar, and Sophie He Qu for their camaraderie and help with my project. I would also like to thank Dr. Walker's lab members: Dr. Mary Y. Lorenson for several discussions that helped me to focus on enzyme inhibitors; Dr. Kuan-Hui Chen and Riva Dill for being practice audiences for my presentations. I would like to thank the UCR Graduate Writing Center for their help in my dissertation writing. Thank you Emily, Jennifer, and Adena.

I feel very lucky to have the support and friendship of my fellow UCR Biomed grad students, Dr. Olivia Sakhon, Sanchya Charlu, and Danh Do.. We made it!

To Allan Chan, thank you for serving our country and protecting our freedom! But mostly, thank you for being my Chief Cheerleader-in-Charge.

I'd like to thank my wonderful son, Nicholas, for being the best boy a single mother, Ph.D. student could have. Your love for the "Happy Song" is contagious; you make my life so rich. Last but not least, I would like to thank my mother, Ung Tjhoe Giet; my brother, Roland Wiryawan; and my sister, Grace Wiryawan. Your support and encouragement are priceless.

ABSTRACT OF THE DISSERTATION

Characterization of a Small Molecule Inhibitor of SUMOylation Pathway as a New Approach to Cancer Treatment

by

Hilda Wiryawan

Doctor of Philosophy, Graduate Program in Biomedical Sciences
University of California, Riverside, June 2014
Dr. Jiayu Liao, Chairperson

Small Ubiquitin-like Modifier (SUMO) modification is a post-translational modification affecting many cellular processes, including nuclear transport, transcriptional regulation, cell cycle progression, and protein stability. Upregulation of SUMO, as well as other components of the SUMOylation pathway, has been observed in human cancers such as lung adenocarcinomas, anaplastic large-cell lymphoma, hepatocellular carcinoma, and ovarian tumors. Since SUMO modification changes the activity of a large number of proteins, SUMOylation pathway is one of the cancer-supportive cellular machineries responsible for many aspects of abnormal cell functions in cancer including increased survival of cancerous cells. We hypothesized that targeting

SUMOylation may decrease cancer cells' viability. Recently, our lab used FRET-based high-throughput screening to identify STE as an inhibitor of the SUMOylation pathway.

To elucidate the mechanism of action of STE, we performed SUMO E1 and E2 thioester formation assays and the enzyme kinetic assays. STE inhibits E1~SUMO thioester conjugate formation in a dose dependent manner and this inhibition is specific to the SUMOylation pathway. We developed a quantitative FRET technology to measure the E1 enzyme kinetics and employed this method to measure the inhibition constant of the STE. We found the results of enzyme kinetics assays using the quantitative FRET methods are comparable to those of conventional radioactive assays. The K_m of SUMO2 (3.42 ± 0.91 μM) and SUMO3 (2.76 ± 0.75 μM) are about four to five times higher than the Km of SUMO1 (0.75 ± 0.11 μM). In the presence of STE, the Km for the E1 enzyme is unaltered whereas the V_{max} is decreased as STE concentration increases which indicates that STE is a non-competitive inhibitor of the E1 enzyme. Based on these experiments, the inhibition constant of the STE was calculated to be 1.90μM. Our results also indicated that STE induces cell death in the both Non-Small Cell Lung Cancer (NSCLC) cell lines NCI-H358 and NCI-H460 and inhibit cell cycle progression in HEK293.

We identified and characterized STE, a small molecule inhibitor of the E1 enzyme of the SUMOylation pathway that is active in the cells. Due to the diverse roles of SUMO, the identification of selective inhibitors of the SUMOylation pathway may lead to pharmacological tools for cancer treatment.

TABLE OF CONTENTS

LIST OF FIGURES

LIST OF FIGURES

CHAPTER 1. INTRODUCTION

Small Ubiquitin-like Modifiers (SUMOs) are small proteins from the ubiquitin family that have been implicated in many physiological cellular mechanisms as well as pathological conditions such as cancer and infectious diseases. To date, no specific small molecule inhibitor of the SUMOylation pathway has been found. Therefore, Dr. Liao's lab performed a high-throughput screening to find inhibitors of the SUMOylation pathway and discovered a lead compound STE which is active in a mammalian cell line. This dissertation describes research, from screening to validated hit, to elucidate the mechanism of inhibition of this novel inhibitor of the SUMOylation pathway. We determined that STE acts as a non-competitive inhibitor of the E1 enzyme and is capable of inducing cell death in non-small cell lung cancer cell lines. To provide readers with a comprehensive background in this field, this first chapter is dedicated to describing the research that has been done in the field including studies of SUMO proteins and SUMOylation mechanisms; of dysregulation of SUMOylation pathways in pathological conditions; of high-throughput screening methods; of FRET technology; and of other known small molecule inhibitors of the SUMOylation, ubiquitination, and NEDDylation pathways.

1.1 SUMOylation, SUMO, and the Ubiquitin-like Protein (UBL) Family

The Ubiquitin-proteasome system is responsible for regulating a major proportion of proteolysis in the cell. Several ubiquitin-like proteins have been identified, including SUMO, neural precursor cell expressed, developmentally down-regulated 8 (NEDD8), and Interferon-stimulated gene 15 (ISG15) (1,2). SUMO proteins are 11 kDa proteins and share only 18% sequence identity with Ubiquitin (Ub). Mammalian SUMO2 and SUMO3 share 95% sequence identity with each other and are 50% identical to SUMO1(3). Like ubiquitin, SUMO is found in all eukaryotic cells, including yeast, nematodes, fruit flies, and vertebrate cells. SUMO modulates cytosolic and nuclear protein interaction and function by covalent modification (4).

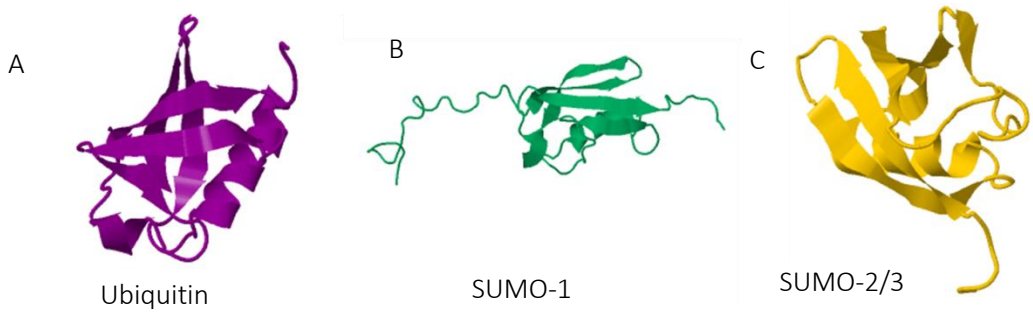

Figure 1.1 Comparison of the Ubiquitin, SUMO1, and SUMO2/3 Structures. Ubiquitin and SUMOs share the same basic β-grasp fold three-dimensional core. Ubiquitin shares 18% structure similarities with SUMO1. SUMO2 and SUMO3 share 95% sequence identity and only share 50% sequence identity with SUMO1. These structural similarities indicate that ubiquitin and SUMO share a common ancestry.

SUMO proteins are expressed as precursor proteins with a short C-terminal peptide that has to be cleaved by Sentrin-specific proteases (SENPs) before they become active. SUMOylation is a cascade of enzymatic processes that involves E1 (5,6), E2 (7), and E3 enzymes (8). Although these enzymes are analogous to those of the ubiquitin pathway, the enzymes of the SUMO pathway are specific to SUMO and have no role in conjugating ubiquitin or any other ubiquitin-like proteins. In contrast, the UbcH8 ubiquitin E2 enzyme is also the E2 enzyme for ISG15 (9). In the SUMOylation pathway, there is only one E1 enzyme (Aos1/Uba2 or SUMO Activation Enzyme SAE1/SAE2 in human), one E2 enzyme (Ubc9), and a few E3 ligases (10). By contrast, the ubiquitin pathway has two E1 enzymes, more than 30 E2 enzymes, and more than 1000 E3 ligase enzymes. This difference in the number of enzymes involved in the pathways is an important consideration in targeting the enzymes in the ubiquitin and ubiquitin-like pathways. For example, inhibiting the

E2 step in SUMOylation will be more efficient compared to inhibiting one E2 enzyme in ubiquitination because of the redundancy in the ubiquitin system.

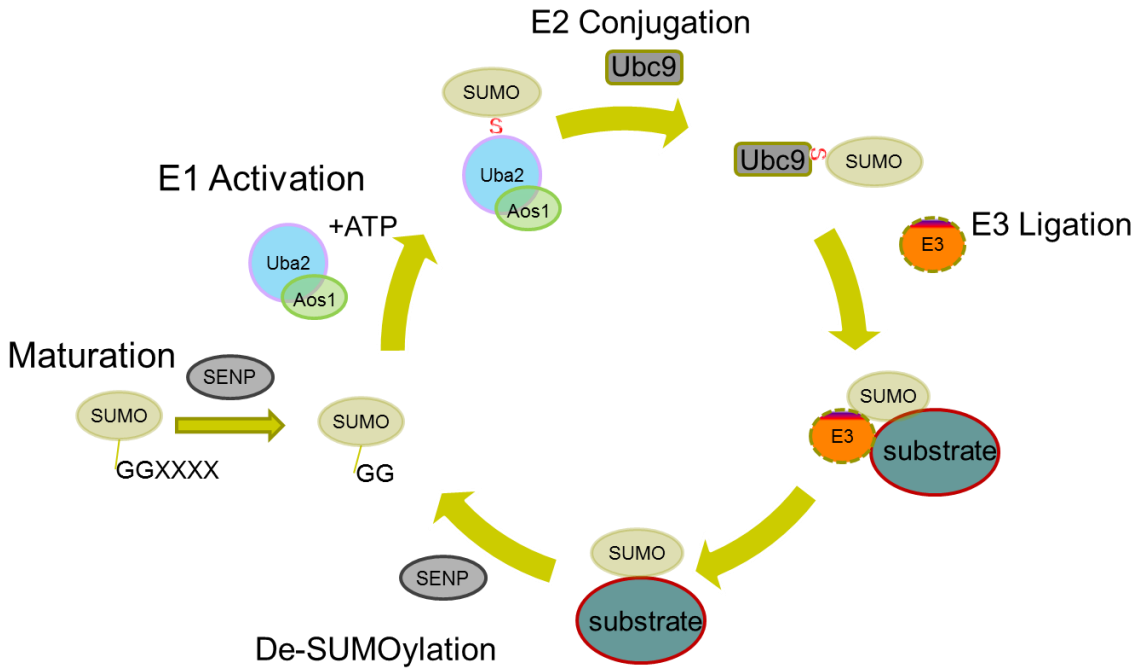

Figure 1.2 The SUMOylation pathway. First SUMO proteins are postranslationally processed by SUMO proteases to expose a C-terminal diglycine motif which can then form a bond with the E1-activating enzyme. Second, this activation step is followed by conjugation of the activated SUMO to the E2-conjugating enzyme, Ubc9. Finally, SUMO modifies its target via a lysine residue by an isopeptide bond. The system is dynamic and reversible by isopeptidases, which can hydrolyze this covalent bond, causing removal of SUMO.

SUMO can recognize short continuous peptide sequences in binding partner(s), known as SUMO motifs. To date, five SUMO motifs have been identified: consensus motif (ϕKXE), inverted consensus motif (ϕϗXƎ), hydrophobic cluster SUMOylation motif (HCSM, ϕϕϕKXE),

phosphorylation-dependent SUMOylation motif (PDSM, ϕKXEXXSP), and negatively-charged amino-acid-dependent SUMOylation motif (NDSM, ϕKXEXXEEE) (11,12). ϕ is a large hydrophobic amino acid, K is the lysine residue that is modified, X is any residue, and E is a glutamic acid) (13,14). Both PDSM and NDSM extensions have a negative charge next to the SUMO consensus site, which enhances SUMOylation (3). Ubc9 has the consensus motif that can bind to SUMO. These SUMO motifs are important for SUMO covalent modifications and can be used as tools to predict SUMO substrates from a set of proteins.

RanGAP1 was the first substrate found to be modified by SUMO. In 1997, Kamitani et al. reported a prominent 90 kDa band (p90) and a series of high molecular weight nuclear proteins that were observed to be modified by Sentrin (SUMO) in a manner similar to ubiquitination (15). In 1998, Mahajan et al. found that glycine 97 of SUMO1 is covalently linked via an isopeptide bond to lysine 526 of RanGAP1 (16). The SUMOylation of RanGAP1 is required for targeting RanGAP1 to the nuclear envelope in cells. This paper also described the importance of the C-terminal domain of RanGAP1, not only because it contains the SUMOylation site, but also because this domain contains nuclear localization signal (17). RanGAP1 is an example of how a substrate that contains a nuclear localization signal (NLS) might be SUMOylated at the nuclear pore by the E3 ligase activity of RanBP2 during nuclear import (18). In our high-throughput screening, we used the C-terminus of RanGAP1 (RanGAP1c) tagged with a yellow fluorescence protein derivative, YPet, as the SUMO substrate.

More than one hundred SUMO target proteins have been found. These proteins are nuclear, cytoplasmic, and membranous. SUMO modification is involved in transcription regulation, intracellular transport, stress responses, the maintenance of genome integrity, and many other biological processes. A major change in level of SUMO substrates, such as p53, RanGAP1, PML,

Sp100, IκBα, 53BP1, BRCA1, MEK1 and MEK2may have a major impact on the fate of cancer cells, making SUMO an attractive cancer drug target (19-21) (22).

1.2 Mechanism of SUMOylation

SUMOylation is a cascade of enzymatic processes that involve E1 activating enzyme (5,6), E2 conjugating (7), and E3 ligase enzymes (8). SUMOylation is a reversible process and SUMO is removed by SUMO-specific proteases SENPs (Sentrin specific peptidase), an enzyme that cleaves the c-terminal peptide from SUMO precursor (13). Figure 1.3 describes the biochemistry of the SUMOylation cascade.

$$\mathrm{Aos1/Uba2_{SH} + ATP + SUMO} \overset{Mg^{2+}}{\rightleftharpoons} \mathrm{Aos1/Uba2}^{\cdot\mathrm{AMP\text{-}SUMO}}_{\mathrm{SH}} + \mathrm{PP_i} \quad (1)$$

$$\mathrm{Aos1/Uba2}^{\cdot\mathrm{AMP\text{-}SUMO}}_{\mathrm{SH}} \rightleftharpoons \mathrm{Aos1/Uba2_{S\text{-}SUMO}} + \mathrm{AMP} \quad (2)$$

$$\mathrm{Aos1/Uba2_{S\text{-}SUMO} + ATP + SUMO} \overset{Mg^{2+}}{\rightleftharpoons} \mathrm{Aos1/Uba2}^{\cdot\mathrm{AMP\text{-}SUMO}}_{\mathrm{S\text{-}SUMO}} + \mathrm{PP_i} \quad (3)$$

$$\mathrm{Aos1/Uba2}^{\cdot\mathrm{AMP\text{-}SUMO}}_{\mathrm{S\text{-}SUMO}} + \mathrm{Ubc9_{SH}} \rightleftharpoons \mathrm{Aos1/Uba2}^{\cdot\mathrm{AMP\text{-}SUMO}}_{\mathrm{SH}} + \mathrm{Ubc9_{S\text{-}SUMO}} \quad (4)$$

Figure 1.3 SUMOylation activation and conjugation scheme. SUMOylation activation and conjugation scheme with non-covalent complexes indicated with a dot and covalent conjugation indicated with a hyphen. S-SUMO refers to the thioester bond between the catalytic cysteine and the SUMO c-terminus.

The E1 activating enzyme is a heterodimer of Aos1 and Uba2 (or SUMO Activating Enzyme, SAE1 and SAE2) (23). Human Aos1 (SAE1) is homologous to the N-terminal of ubiquitin E1, and Uba2 (SAE2) is homologous to the C-terminus of ubiquitin E1. SUMOylation is initiated by an E1 enzyme that catalyzes SUMO adenylation, forms an E1-SUMO thioester bond with a catalytic cysteine in the E1 Cys domain, and transfers thioester to a catalytic cysteine in the E2 conjugating

enzyme (24). Figure 3.8 D shows that the Uba2 consists of a multiple domains, namely an adenylation domain that binds ATP, Mg, and SUMO; a C-terminal ubiquitin-like domain that recruits Ubc9 for thioester transfer; and a catalytic Cys domain that contains the active site cysteine (25). The SUMO E1 activity is controlled by post-translational modification including SUMOylation. SUMO modifies its E1 at the E1 Cys domain and inhibits this domain activity. AutoSUMOylation of E1 at the Lys 236 residue did not affect SUMO adenylation or formation of the E1~SUMO thioester but did inhibit the transfer of SUMO from E1 to E2 (26). In the last step (4) in figure 1.3, activated SUMO is transferred to the E2 (Ubc9) conjugating enzyme (25,27,28). To translocate activated SUMO from E1 to E2, E1 first must undergo significant conformational changes to bring E1 and E2 into close proximity (29). From E2, SUMO is then transferred to a substrate protein that is recruited by E3 ligases such as PIAS proteins, Pc2, and RanBP2 (30-32). This protein-protein reaction cascade is important in SUMOylation.

The E1 activating enzyme is a heterodimer of Aos1/Uba2 (SAE1/SAE2). In the SUMOylation cascade, the E1 enzyme has two substrates namely ATP and SUMO. ATP is the leading substrate because the adenylation process has to happen before the E1~SUMO thioester formation. Because of its action in activating SUMO and transferring the activated SUMO to the E2 enzyme, the E1 enzyme is categorized as a ubiquitin:protein-lysine *N*-ligase (AMP-forming)- EC 6.3.2.19 by the Nomenclature Committee of the International Union of Biochemistry and Molecular Biology (NC-IUBMB) Enzyme Nomenclature (33). This SUMOylation enzymatic cascade is important in characterizing the SUMO inhibitor and thus will be referred to in chapters 2 and 3.

1.3 Alteration of SUMOylation in human pathological conditions

Depending on the target substrate, SUMOylation can regulate target stability, localization, or interaction with a binding partner. These functions are achieved through many events such as

modification by a single SUMO1, modification by polymeric chains of SUMO2/3, a change in conformation of a target protein, appearance of a new allosteric binding pocket, and disruption of a ligand-binding site on targets(34).

1.3.1 SUMOylation in Genome Integrity

SUMOylation's significant roles in genome integrity and carcinogenesis have been established. To guard the integrity of its genome from attack by endogenous and exogenous mutagens, cells perform a highly-coordinated response in DNA replication, gene transcription, DNA repair, and cell-cycle checkpoints (35). Maintaining genome integrity requires activation of the appropriate repair pathways and reversible arrest at cell-cycle checkpoints. The SUMOylation pathway modifies numerous proteins in the genome integrity pathways, such as PCNA, Rad52, Rfa1, Rfa2, and Sgs1 helicase, as well as its human homologues, Bloom syndrome protein (BLM) and DNA helicase WRN, a member of the RecQL family of helicases. Additionally, BRCA1 and 53BP1 are SUMOylated with help of PIAS4, an E3 ligase, before they can be recruited to the DNA damage sites (36). Thus, SUMO is important in protecting cells from genome instability (37). SUMO exerts its functions through various mechanisms, such as affecting protein-protein interactions and regulating enzymatic activity and localization (11,38). All of these processes are important in maintaining genome integrity.

PML protein is a member of the tripartite motif (TRIM) family, which is often fused with the retinoic receptor alpha (RARα) protein in patients with acute promyelocytic leukemia (APL). In normal cells, PML localizes in the nucleus and forms puncta, which are often referred to as PML nuclear bodies (PML-NB). PML-NB formation requires PML SUMOylation and has been implicated in diverse functions, including DNA repair, DNA replication, and DNA transport. The use of arsenic to treat APL patients induces SUMO-dependent ubiquitin-mediated proteasomal degradation of

the PML-RAR fusion protein (39). These protein degradations demonstrate the link between PML, SUMO, and ubiquitin in cancer treatment.

SUMO-targeted ubiquitin ligases (STUbLs) are an emerging E3 ubiquitin ligase family that mediates direct crosstalk between the SUMO and ubiquitin pathways. This family of E3 ubiquitin ligases has been implicated in maintaining genome stability in yeast (40). Slx5-Slx8 heterodimer ubiquitin ligase, the prototype of STUbLs, contains multiple SUMO-binding domains that specifically recognize a SUMOylated substrate through SUMO interaction motifs (SIMs) (41). Unlike the yeast heterodimer STUbL, RING finger protein 4 (RNF4) is a monomer that performs the same STUbL function in mammals (40). In response to arsenic therapy, the N-terminal domain of RNF4 binds to the poly-SUMO2 chain and mediates ubiquitin degradation of PML proteins (39). Structural studies indicate that the RNF4 dimeric RING-type ubiquitin E3 ligases facilitate this catalysis by binding both E2 and ubiquitin, thus activating the E2~Ub thioester bond (42).

The p53 protein is essential for the checkpoint control that arrests cells with damaged DNA in G1, hence the terms “guardian of the genome” and “cellular gatekeeper.” p53 is an inducible, sequence-specific transcription factor that responds to stress signals, such as DNA damage, by regulating cell-cycle progression, apoptosis, DNA repair, cellular metabolism, and autophagy (43). p53 is regulated by many post-translational modifications, including SUMOylation at a single site of K386. SUMOylation of p53 is promoted by members of the PIAS family and Topors (44,45). Even though p53 is one of the first known substrates of SUMO modification, the significance of SUMOylation on p53 remains to be determined (45,46).

PCNA is a homotrimeric, ring-shaped protein that encircles DNA and slides freely upon it in both directions(47). SUMOylation targets K164, which is also modified by monoubiquitination or Lys-63-linked polyubiquitination, thus indicating an interaction between these two modifications

of PCNA regulation, which is often called the "ubiquitin-SUMO switchboard" (48). Both ubiquitination and SUMOylation of PCNA occur during the S phase, but ubiquitination, specifically, occurs when DNA is damaged. PCNA monoubiquitination leads to translesion synthesis (TLS) that is error-prone. However, polyubiquitination occurs when TLS fails and results in recombination-related error-free pathways. In contrast, SUMOylation of PCNA recruits Srs2, a helicase-like enzyme with a much higher affinity, and strips the recombinase Rad51 from chromatin and prevents unwanted recombination between the newly formed sister chromatids (49). Additionally, SUMOylation on Lys-127 inhibits interaction with certain PCNA-binding proteins, such as Eco1(50). These interactions highlight the complementary functions of ubiquitin and SUMO in PCNA regulation of cancer cells.

DNA Damage Response (DDR) pathways involve both SUMO and ubiquitin modifications in regulating their components, and some of the DDR pathways even require crosstalk between SUMO and ubiquitin to coordinate these complex events (48). Double-strand breaks (DSBs) are caused mostly by exogenous agents, such as chemotherapy and ionizing radiation, and are considered the most lethal form of DNA damage (51). In response to DNA damage, DDR proteins are recruited and modulated by post-translational modifications, including phosphorylation, acetylation, methylation, ubiquitination, and poly ADP-ribosylation (52). The two major DNA repair mechanisms that deal with DSB are non-homologous end-joining (NHEJ) and homologous recombination. Morris et al. identified another example of SUMOylation and ubiquitination pathway interactions: BRCA1/BARD1 heterodimers are SUMO-regulated ubiquitin ligases (SRUbl) because SUMOylation of this heterodimer greatly increases its activity as an ubiquitin ligase in a DNA damage response (53). Additionally, Morris et al. and Galanty et al. also identified PIAS1 and

PIAS 4, both SUMO E3 ligases, as requirements for complete accumulation of dsDNA damage-repair proteins subsequent to RNF8 accrual (53,54).

DNA damage induced by UV irradiation is predominantly in the form of a cyclobutane pyrimidine dimer and (6-4) photoproduct bulky adduct. Nucleotide excision repair (NER) is the primary mechanism to remove these bulky lesions [26]. In yeast, Rad4, Rad16, Rad7, Rad1, Rad10, Ssl2, Rad3, and Rpb4 are SUMO modified in the presence of Siz1 and Siz2 E3 ligases in response to DNA damage [33]. Therefore, SUMOs play important roles in genotoxic stress responses.

1.3.2 SUMOylation in Carcinogenesis

Zhang et al. studied SUMO1 functions *in vivo* using SUMO1$^{-/-}$ mice and found that SUMO1 knockout mice are viable with no testis or palate defects. This indicated that SUMO1 function is dispensable in normal mouse development(55). Furthermore, Evdokimov et al. reported that SUMO2/3 provide compensatory substitution for SUMOylation of SUMO1 targets(56). On the other hand, the Ubc9 knockout mouse model indicated that Ubc9-deficient embryos die at the early post implantation stage because of major chromosome condensation, segregation defects, and other severe defects in nuclear organizations(57). Taken together, these studies have shown that to inhibit the SUMOylation pathway, inhibition of one paralog will not be sufficient because of the ability of other SUMO paralogs to substitute. Therefore, taking advantage of the SUMOylation cascade and the limited number of E1 and E2 enzyme in the SUMOylation cascade can provide a better alternative in inhibiting the SUMOylation pathway.

Development of genomic instability in cancer cells is one of the enabling characteristics that allow cancer cells to acquire different functional capabilities during the course of multistep carcinogenesis [34]. Genomic instability generates random mutations, including chromosomal

rearrangements. SUMO involvement in genomic integrity and its interplay with ubiquitin pathway suggests that SUMO plays an important role in carcinogenesis.

Impaired SUMOylation also has been linked to cancers. Kessler et al. recently reported that loss of SAE1/SAE2 enzymatic activity drives synthetic lethality with Myc (58). Microphthalmia-associated transcription factor (MITF) gene mutation (Mi-E418K) inhibits SUMOylation and occurs at a significantly higher frequency in patients with melanoma, renal cell carcinoma (RCC), or both. This gain-of-function mutation has been linked to a fivefold greater risk of developing melanoma, RCC, or both cancers [35].

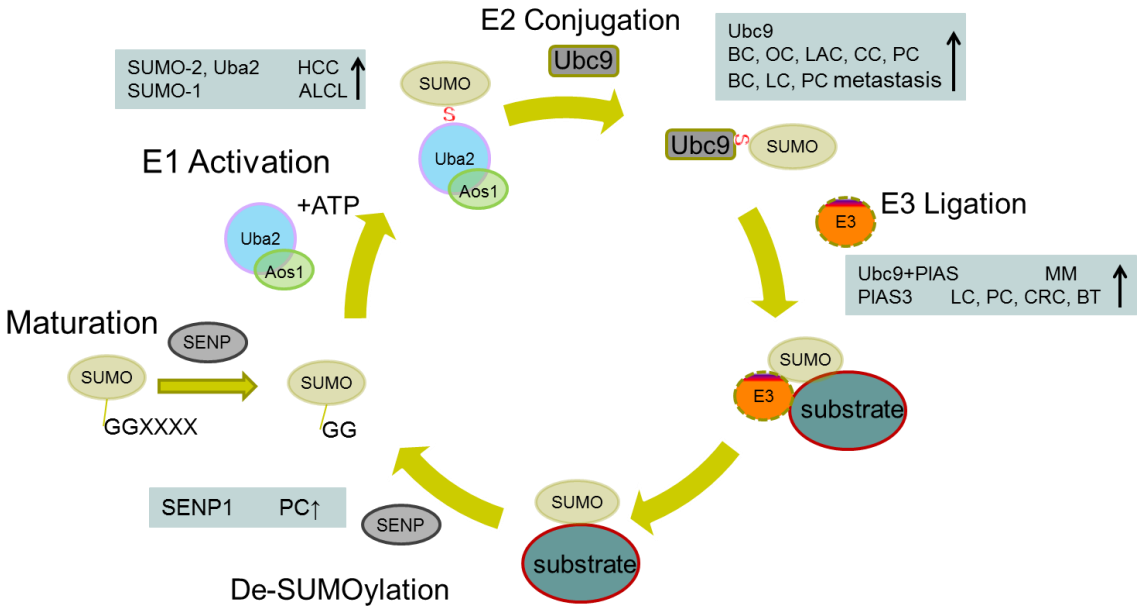

Figure 1.4 The SUMOylation pathway in carcinogenesis. HCC (Hepatocellular carcinoma), ALCL (Anaplastic Large Cell Lymphoma), BC (breast cancer), OC (Ovarian Cancer), LAC (Lung Adenocarcinoma), CC (Cervical Cancer), PC (Prostate Cancer), MM (Multiple Myeloma), CRC (Colorectal Carcinoma) BT (Brain Tumor). Adapted from Betterman K, et al. Cancer Lett. 2012; 316(2):113-25

The SUMO pathway is a suitable target for molecular therapies of cancer because SUMO and the related enzymes involved in the conjugation (E1, E2, and E3) are commonly overexpressed in cancers, and the overexpression state is necessary for the continued maintenance of the cancer. Involvement of the SUMOylation pathway in cancer is depicted in Figure 1.4. In breast cancer patients, those with the 73G > A polymorphism of the Ubc9 gene (Val25Met) have decreased efficacy of DNA double strand breaks repair (59). Higher levels of *Ubc9* mRNA were found in ovarian tumor samples compared to normal ovarian tissue (60). Increased Ubc9 levels are found in a number of human lung adenocarcinoma(61). Chen et al. found that eukaryotic elongation factor 2 (eEF2) was highly expressed in lung adenocarcinoma (LAC), but not in the neighboring non-tumor lung tissue. This finding is important because eEF2 was SUMOylated in LAC cells, and eEF2 SUMOylation correlated with drug resistance (62). Since SUMO modification changes the activity of a large number of proteins, the SUMOylation pathway is one of the cancer-supportive cellular machineries responsible for many aspects of abnormal cell functions in cancer, including increased survival of cancerous cells.

Expression of PIAS3, a SUMO E3 ligase, is altered in a number of different cancer types, such as human breast carcinoma (63) and glioblastoma multiforme (64). Some studies also linked high expression levels of SUMOylation pathway components with poor survival. For example, elevated levels of SUMO E1 enzyme correlated with lower survival rates in patients with hepatocellular carcinoma and multiple myeloma (65).

The de-SUMOylation process has also been linked to carcinogenesis. SENP-3-mediated deconjugation of SUMO2/3 from promyelocytic leukemia has been correlated with accelerated cell proliferation under mild oxidative stress [40]. SENP1 enhances androgen receptor-dependent

transcription through de-SUMOylation of histone deacetylase1 (HDAC1), thus overcoming the HDAC1 repressive function and reducing HDAC1 activity [41]. Additionally, chronic exposure to a synthetic androgen leads to a fivefold induction of SENP1 mRNA expression in prostate cancer cells, which in turn induces changes in AR-mediated cellular proliferation [42].

Lung cancer is the leading cause of cancer deaths in the United States and worldwide. It has high metastatic potential and an overall 5-year survival rate of less than 15%. The two major forms of lung cancer are non-small cell lung cancer (about 85% of all lung cancers) and small-cell lung cancer (about 15%). There are three common forms of NSCLC: adenocarcinomas, squamous cell carcinomas, and large cell carcinomas. Lung cancer susceptibility and risk also increase with reduced DNA repair capacity. p53 mutations are found in 50-75% of lung cancers (66). Overexpression of SUMO1 activates the transcriptional activity of wild-type p53, but not K386R p53 where the SUMO1 acceptor site has been mutated (19,67).

1.4 High-throughput screening in Biomedical Research

High-throughput screening (HTS) is a method of a selecting a few promising possibilities from among thousands of potential candidates in a drug discovery process (68). High-throughput generally refers to the testing of 10,000 to 100,000 compounds per day through the use of mechanized processes ranging from manually operated workstations to fully automated robotic systems. HTS is an *in vitro* assay usually performed robotically in a 384-well microtiter plate (69). There are several parameters of HTS that differ from regular laboratory “bench top” assays, such as simple operations, few (5-10) steps, assays that require only addition of reagents, robotic reagent handling, and automated analysis of all data using statistical criteria (70). HTS success rates are about 50% (71). The understanding of HTS design and the pharmacological impact of the assay design is important to identifying the hit compounds from HTS. In designing an HTS there are many

factors that have to be taken into account: data quality as well as cost and time management. There are several methods that have been developed and applied to ensure data quality such as z trend monitoring, plate pattern recognition algorithms, regular usage of pharmacological standards, and liquid handler and reader performance monitoring (71). The compound screening step typically takes from 1 week to 1-3 months depending on the number of compounds being screened (71). Chapter 2 will describe the specific high-throughput screening that was designed to look for inhibitors of the SUMOylation pathway.

As a complement to biochemical high-throughput screening assays, cellular HTS assays can also be performed. Cell-based luciferase reporter screening and phenotypic cell-based screening are the two main methods in cell-based HTS. Cell-based luciferase reporter screening takes advantage of reporter gene assays to detect metabolites such as cAMP levels or changes in expression of a gene of interest. In phenotypic cell-based screening, HTS measures an observable change in cell physiology and morphology in the presence of active compounds. However, phenotypic assays cannot distinguish direct compound interaction with the specific targets or signaling pathways (71). However, with the advancement of fluorescence technology, a holistic assay can be done with a whole cell assay to measure both the molecular and phenotypical assays.

1.5 Förster Resonance Energy Transfer (FRET) Technology Application

Förster (Fluoresence) Resonance Energy Transfer (FRET) between donor and acceptor fluorophores on two interacting molecules of interest has been utilized in many applications (72). The application of Förster (Fluoresence) resonance energy transfer technology (FRET) takes advantage of non-radioactive energy transfer by means of intermolecular long-range dipole-dipole coupling. The FRET signal is produced by an excited molecular chromophore (donor) that then excites another chromophore (acceptor) over distances ranging from ~10Å to 100Å (73). FRET

technology has been useful in analysis of macromolecular interactions such as molecular interactions in membranes; protein structure and protein-protein interactions in solution; nucleic acids and nucleic acid-protein complexes; and detection of heterogeneous molecular conformations such as oligosaccharides (72). Fluorometric energy transfer assays, or quantitative FRET, are highly sensitive and can be easily automated; therefore, they have been employed for inhibitor screening automation, enzymology studies, and inhibitor evaluations(72). FRET assays with doubly-labeled molecules are useful in measuring continuous protease and peptidase reaction progress and can be performed in a multi-well plate format, a process that can be both economical and time-saving.

In our lab, we labeled the protein of interest with a pair of fluorescent-protein tags optimized for FRET: cyan fluorescence protein, CyPet, and yellow fluorescence protein, YPet. CyPet and YPet are derivatives of cyan fluorescence protein (CFP) and yellow fluorescent protein (YFP) respectively. They exhibit 20-fold stronger FRET signals than unmodified CFP and YFP (74). CyPet acts as a donor and YPet acts as an acceptor. Thus, FRET can be used to determine protein interaction affinity (75), kinetics of protease enzymes (76,77), and for automated inhibitor screening for SUMOylation pathway inhibitors (78). In Chapter 3, I will described how quantitative FRET is used in multiple applications: SUMOylation inhibitor high-throughput screening, enzymology studies to measure the Km of SUMO1, SUMO2, and SUMO3, and STE inhibitor evaluations.

1.6 Small molecule inhibitors of ubiquitin and ubiquitin-like pathways

Biologically active, small molecule compounds can be useful to science as “tools” for dissecting biological mechanisms and testing hypotheses in a model system. They can also be valuable in target and pathway identification and validation of new therapeutic approaches (71).

With the availability of robotic instrumentation and compound libraries, it is often possible to identify relatively specific inhibitors through high-throughput screening. Small molecule inhibitors are useful in studying the kinetics of protein SUMOylation in a more subtle way than gene disruption techniques because it avoids problems with embryonic lethality often observed with genetic knockouts. In addition, small molecules have the advantage of being easily distributed among different laboratories, can tested in different dosage, and may be further developed as therapeutic agents.

In protein–protein interactions, the buried surface area (BSA) is defined as the surface buried away from the solvent when two or more proteins or subunits associate to form a complex (79). In contrast to usual binding sites on an enzyme or receptor surface, which are typically concave, protein–protein interfaces are typically quite flat and indistinguishable from other patches on the protein surface (80). This makes development of small molecule modulators of protein-protein interactions more difficult (80,81). This is true for the protein-protein interactions in the SUMOylation pathway. The SAE2-SUMO interface buries 1650 $Å^2$ of total surface area between SAE2 and SUMO1, which is equal to approximately 20% of the SUMO1 total surface area (82). The Uba2-Ubc9 interaction has a buried surface area of 1293 $Å^2$ (83). The interaction of Ubc9-SUMO1 interface covers a continuous surface, burying 1100$Å^2$ of total buried surface area (84). Therefore, there are some challenges in finding inhibitors of SUMOylation pathway including typical flatness of the protein-protein interaction interface and a lack of small-molecule starting points for drug design. Also, conformational changes upon protein-protein interactions can complicate matters. Another challenge is that there are structural similarities of the proteins involved in the SUMO, ubiquitin, and other ubiquitin-like protein pathways. In terms of the physicochemical properties of small molecules, Lipinski's rule of 5 is often used as a secondary

screen to estimate solubility and permeability in the drug discovery setting. The drug likeliness criteria are molecular weight less than 500, less than 5-H-bond donors, 10-bond acceptors, and calculated Log P (CLogP) less than 5 (85). An ideal small molecule that follows Lipinski's rule has a higher chance to have a good bioavailability.

Numerous small molecule inhibitors of Ubiquitination and NEDDylation pathways have been found by researchers. Of interest to our group were PYR-41, PYZD-4409, and NSC624206. PYR-41 was previously identified as a cell permeable inhibitor of Uba1 that blocks ubiquitin-thioester formation (86-88). Similarly, PYZD-4409 induced cell death in acute myeloid leukemia cells by inhibiting Ubiquitin E1, Uba1 (89). NSC624206 and Largazole were also found to inhibit Ub E1 (87,90). Nutlin-3 targets the Mdm2 protein, a really interesting new gene (RING)-type E3 ubiquitin ligase and antagonizes MDM-p53 interaction with an IC_{50} of only 19nM (91,92). Nutlin-3 is currently in a Phase I clinical trial for the treatment for retinoblastoma, solid tumors, and leukemia (93).

For comparison, MLN4924 was recently found as an inhibitor of the NEDDylation pathway. MLN 4924 is an AMP-mimic that inhibits APPBP1/Uba3, the only E1 enzyme in the NEDDylation pathway, by blocking the enzyme activity through binding the NAE adenylation active site (94). The mechanism of MLN4924 is substrate-assisted inhibition through formation of covalent adducts, NEDD8-MLN4924, which disrupt cullin-RING ligase (CRL)-mediated protein turnover, leading to deregulation of S-phase DNA synthesis, and causing apoptotic death in human cancer cells (95-97). MLN4924 is currently in a Phase I clinical trial for acute myeloid leukemia and solid tumors(98).

To date, there are three natural products that have been reported to inhibit SUMOylation, Gingkogolic acid (MW: 346.5), Anacardic acid (MW 348.5), and Kerriamycin B (MW: 844.89) (99).

Fukuda et al. reported that ginkgolic acid has an IC_{50} of 3.0 µM and Anacardic acid has an IC_{50} of 2.2 µM (99). Ginkgolic acid consists of salicylic acid and a long-carbon chain substituent (99). Since salicylic acid by itself does not have any effect on *in vitro* SUMOylation, Fukuda et al. suggest that the long carbon chain is necessary to inhibit the SUMOylation process(99). Since both of these compounds suppress SUMO1 at 100µM in HEK293 cells, their activity may be the result of off-target action. The same group also found that Kerriamycin B inhibits *in vitro* SUMOylation of RanGAP1 with an IC_{50} of 11.7 µM (100). Recently, Kumar et al. reported their effort to find a small molecule inhibitor through *in silico* screenings and found compound 21 (MW 464.5) to inhibit SUMO E1 with an IC_{50} of 14.4 µM (101). A Google patent search showed that a patent was filed in 2013 for the invention of bicyclic and tricyclic inhibitors of SUMOylation enzymes with the lead compound, MLS0437113, that has an *in vitro* IC50 of approximately 0.25-0.5 µM and a K_d of approximately 180 nM (102). This knowledge of different inhibitors of the SUMO pathway will benefit our research in identifying the mechanism of action of our small molecule inhibitor of SUMOylation pathway.

We found a small molecule inhibitor of the SUMOylation pathway that is active in cells through a FRET-based HTS. Further studies addressed some very fundamental questions about this small molecule inhibitor. Observations from experiments described in this dissertation will have the potential to be used by academic researchers studying cell biology, molecular biology, and tumor biology. In addition, experimental designs that were used in this research project will be useful for any researcher working in the field of drug discovery. Due to the diverse roles and the potent epigenetic modification associated with SUMO, the identification of selective inhibitors of the SUMOylation pathway may lead to pharmacological tools for cancer treatment.

1.7 References

1. Wang J, Taherbhoy AM, Hunt HW, Seyedin SN, Miller DW, Miller DJ, et al. Crystal Structure of UBA2(ufd)-Ubc9: Insights into E1-E2 Interactions in Sumo Pathways. PLoS ONE 2010;5(12):e15805.

2. Au WC, Moore PA, Lowther W, Juang YT, Pitha PM. Identification of a member of the interferon regulatory factor family that binds to the interferon-stimulated response element and activates expression of interferon-induced genes. Proceedings of the National Academy of Sciences 1995;92(25):11657-61.

3. Geiss-Friedlander R, Melchior F. Concepts in sumoylation: a decade on. Nat Rev Mol Cell Biol 2007;8(12):947-56.

4. Johnson ES. PROTEIN MODIFICATION BY SUMO. Annual Review of Biochemistry 2004;73(1):355-82.

5. Desterro JMP, Rodriguez MS, Kemp GD, Hay RT. Identification of the Enzyme Required for Activation of the Small Ubiquitin-like Protein SUMO-1. Journal of Biological Chemistry 1999;274(15):10618-24.

6. Lake MW, Wuebbens MM, Rajagopalan KV, Schindelin H. Mechanism of ubiquitin activation revealed by the structure of a bacterial MoeB-MoaD complex. Nature 2001;414(6861):325-9.

7. Johnson ES, Blobel G. Ubc9p Is the Conjugating Enzyme for the Ubiquitin-like Protein Smt3p. Journal of Biological Chemistry 1997;272(43):26799-802.

8. Kotaja N, Karvonen U, Janne OA, Palvimo JJ. PIAS Proteins Modulate Transcription Factors by Functioning as SUMO-1 Ligases. Molecular Cell Biology 2002;22(14):52222-34.

9. Zhao C, Beaudenon SL, Kelley ML, Waddell MB, Yuan W, Schulman BA, et al. The UbcH8 ubiquitin E2 enzyme is also the E2 enzyme for ISG15, an IFN-α/β-induced ubiquitin-like protein. Proceedings of the National Academy of Sciences of the United States of America 2004;101(20):7578-82.

10. van Wijk SJ, Timmers HT. The family of ubiquitin-conjugating enzymes (E2s): deciding between life and death of proteins. FASEB journal : official publication of the Federation of American Societies for Experimental Biology 2010;24(4):981-93.

11. Gareau JR, Lima CD. The SUMO pathway: emerging mechanisms that shape specificity, conjugation and recognition. Nat Rev Mol Cell Biol 2010;11(12):861-71.

12. Matic I, Schimmel J, Hendriks IA, van Santen MA, van de Rijke F, van Dam H, et al. Site-Specific Identification of SUMO-2 Targets in Cells Reveals an Inverted SUMOylation Motif and a Hydrophobic Cluster SUMOylation Motif. Molecular Cell 2010;39(4):641-52.

13. Hay RT. SUMO: a history of modification. Molecular cell 2005;18(1):1-12.

14. Aasland R, Abrams C, Ampe C, Ball LJ, Bedford MT, Cesareni G, et al. Normalization of nomenclature for peptide motifs as ligands of modular protein domains. FEBS Letters 2002;513(1):141-44.

15. T K, HP N, ETH Y. Preferential Modification of Nuclear Proteins by a Novel Ubiquitin-like Molecule. The Journal of biological chemistry 1997;272(22):14001-4.

16. Mahajan R, Delphin C, Guan T, Gerace L, Melchior F. A small ubiquitin-related polypeptide involved in targeting RanGAP1 to nuclear pore complex protein RanBP2. Cell 1997;88(1):97-107.

17. Mahajan R, Gerace L, Melchior F. Molecular characterization of the SUMO-1 modification of RanGAP1 and its role in nuclear envelope association. J Cell Biol 1998;140(2):259-70.

18. Saitoh H, Sparrow DB, Shiomi T, Pu RT, Nishimoto T, Mohun TJ, et al. Ubc9p and the conjugation of SUMO-1 to RanGAP1 and RanBP2. Current Biology 1998;8(2):121-24.

19. Rodriguez MS, Desterro J, Lain S, Midgley CA, Lane DP, Hay R. SUMO-1 modification activates the transcriptional response of p53. EMBO 1999;18(22):6455-61.

20. Muller S, Dejean A. Viral Immediate-Early Proteins Abrogate the Modification by SUMO-1 of PML and Sp100 Proteins, Correlating with Nuclear Body Disruption. The Journal of Virology 1999;73(6):5137-43.

21. Huang TT, Wuerzberger-Davis SM, Wu Z-H, Miyamoto S. Sequential Modification of NEMO/IKKγ by SUMO-1 and Ubiquitin Mediates NF-κB Activation by Genotoxic Stress. Cell 2003;115(5):565-76.

22. Lamsoul I, Lodewick J, Lebrun S, Brasseur R, Burny A, Gaynor RB, et al. Exclusive Ubiquitination and Sumoylation on Overlapping Lysine Residues Mediate NF-{kappa}B Activation by the Human T-Cell Leukemia Virus Tax Oncoprotein. Molecular and Cellular Biology 2005;25(23):10391-406.

23. Haas AL, Warm JV, Herschko A, Rose IA. Ubiquitin-activating enzyme Mechanism and role in protein-ubiquitin conjugation. The Journal of biological chemistry 1982;257:2543-48.

24. Olsen Shaun K, Lima Christopher D. Structure of a Ubiquitin E1-E2 Complex: Insights to E1-E2 Thioester Transfer. Molecular cell 2013;49(5):884-96.

25. Olsen SK, Capili AD, Lu X, Tan DS, Lima CD. Active site remodelling accompanies thioester bond formation in the SUMO E1. Nature 2010;463(7283):906-12.

26. Truong K, Lee TD, Chen Y. Small ubiquitin-like modifier (SUMO) modification of E1 Cys domain inhibits E1 Cys domain enzymatic activity. The Journal of biological chemistry 2012;287(19):15154-63.

27. Lois LM, Lima CD. Structures of the SUMO E1 provide mechanistic insights into SUMO activation and E2 recruitment to E1. The EMBO journal 2005;24(3):439-51.

28. Bernier-Villamor V, Sampson DA, Matunis MJ, Lima CD. Structural Basis for E2-Mediated SUMO Conjugation Revealed by a Complex between Ubiquitin-Conjugating Enzyme Ubc9 and RanGAP1. Cell 2002;108(3):345-56.

29. Wang J, Hu W, Cai S, Lee B, Song J, Chen Y. The intrinsic affinity between E2 and the Cys domain of E1 in ubiquitin-like modifications. Molecular cell 2007;27(2):228-37.

30. Chung CD, Liao J, Liu B, Rao X, Jay P, Berta P, et al. Specific Inhibition of Stat3 Signal Transduction by PIAS3. Science 1997;278:1803-5.

31. Liao J, Fu Y, Shuai K. Distinct roles of the NH2- and COOH-terminal domains of the protein inhibitor of activated signal transducer and activator of transcription (STAT) 1 (PIAS1) in cytokine-induced PIAS1–Stat1 interaction. Proceedings of the National Academy of Sciences 2000;97(10):5267-72.

32. Tang Z, Hecker CM, Scheschonka A, Betz H. Protein interactions in the sumoylation cascade: lessons from X-ray structures. The FEBS journal 2008;275(12):3003-15.

33. Biochemical Nomenclature and Related Documents. Portland Press; 1992.

34. Everett RD, Boutell C, Hale BG. Interplay between viruses and host sumoylation pathways. Nat Rev Micro 2013;11(6):400-11.

35. Hoeijmakers JHJ. Genome maintenance mechanisms for preventing cancer. Nature 2001;411(6835):366-74.

36. Bekker-Jensen S, Mailand N. The ubiquitin- and SUMO-dependent signaling response to DNA double-strand breaks. FEBS Letters 2011;585(18):2914-19.

37. Muller S, Ledl A, Schmidt D. SUMO: a regulator of gene expression and genome integrity. Oncogene 2004;23(11):1998-2008.

38. Nagai S, Davoodi N, Gasser SM. Nuclear organization in genome stability: SUMO connections. Cell research 2011;21(3):474-85.

39. Geoffroy MC, Jaffray EG, Walker KJ, Hay RT. Arsenic-induced SUMO-dependent recruitment of RNF4 into PML nuclear bodies. Molecular biology of the cell 2010;21(23):4227-39.

40. Heideker J, Prudden J, Perry JJP, Tainer JA, Boddy MN. SUMO-Targeted Ubiquitin Ligase, Rad60, and Nse2 SUMO Ligase Suppress Spontaneous Top1–Mediated DNA Damage and Genome Instability. PLoS Genet 2011;7(3):e1001320.

41. Mullen JR, Brill SJ. Activation of the Slx5-Slx8 ubiquitin ligase by poly-small ubiquitin-like modifier conjugates. The Journal of biological chemistry 2008;283(29):19912-21.

42. Plechanovova A, Jaffray EG, McMahon SA, Johnson KA, Navratilova I, Naismith JH, et al. Mechanism of ubiquitylation by dimeric RING ligase RNF4. Nature structural & molecular biology 2011;18(9):1052-9.

43. Stehmeier P, Muller S. Regulation of p53 family members by the ubiquitin-like SUMO system. DNA repair 2009;8(4):491-8.

44. Kahyo T, Nishida T, Yasuda H. Involvement of PIAS1 in the sumoylation of tumor suppressor p53. Molecular cell 2001;8(3):713-8.

45. Dai C, Gu W. p53 post-translational modification: deregulated in tumorigenesis. Trends Mol Med 2010;16(11):528-36.

46. Melchior F, Hengst L. SUMO-1 and p53. Cell Cycle 2002;1(4):245-9.

47. Moldovan GL, Pfander B, Jentsch S. PCNA, the maestro of the replication fork. Cell 2007;129(4):665-79.

48. Bergink S, Jentsch S. Principles of ubiquitin and SUMO modifications in DNA repair. Nature 2009;458(7237):461-7.

49. Pfander B, Moldovan GL, Sacher M, Hoege C, Jentsch S. SUMO-modified PCNA recruits Srs2 to prevent recombination during S phase. Nature 2005;436(7049):428-33.

50. Moldovan GL, Pfander B, Jentsch S. PCNA controls establishment of sister chromatid cohesion during S phase. Molecular cell 2006;23(5):723-32.

51. Kinsella TJ. Understanding DNA Damage Response and DNA Repair Pathways: Applications to More Targeted Cancer Therapeutics. Seminars in Oncology 2009;36, Supplement 1(0):S42-S51.

52. Dou H, Huang C, Van Nguyen T, Lu LS, Yeh ET. SUMOylation and de-SUMOylation in response to DNA damage. FEBS Lett 2011;585(18):2891-6.

53. Morris JR, Boutell C, Keppler M, Densham R, Weekes D, Alamshah A, et al. The SUMO modification pathway is involved in the BRCA1 response to genotoxic stress. Nature 2009;462(7275):886-90.

54. Galanty Y, Belotserkovskaya R, Coates J, Polo S, Miller KM, Jackson SP. Mammalian SUMO E3-ligases PIAS1 and PIAS4 promote responses to DNA double-strand breaks. Nature 2009;462(7275):935-39.

55. Zhang F-P, Mikkonen L, Toppari J, Palvimo JJ, Thesleff I, Jänne OA. Sumo-1 Function Is Dispensable in Normal Mouse Development. Molecular and cellular biology 2008;28(17):5381-90.

56. Evdokimov E, Sharma P, Lockett SJ, Lualdi M, Kuehn MR. Loss of SUMO1 in mice affects RanGAP1 localization and formation of PML nuclear bodies, but is not lethal as it can be compensated by SUMO2 or SUMO3. Journal of Cell Science 2008;121(24):4106-13.

57. Nacerddine K, Lehembre F, Bhaumik M, Artus J, Cohen-Tannoudji M, Babinet C, et al. The SUMO Pathway Is Essential for Nuclear Integrity and Chromosome Segregation in Mice. Developmental cell 2005;9(6):769-79.

58. Kessler JD, Kahle KT, Sun T, Meerbrey KL, Schlabach MR, Schmitt EM, et al. A SUMOylation-dependent transcriptional subprogram is required for Myc-driven tumorigenesis. Science 2012;335(6066):348-53.

59. Synowiec E, Krupa R, Morawiec Z, Wasylecka M, Dziki L, Morawiec J, et al. Efficacy of DNA double-strand breaks repair in breast cancer is decreased in carriers of the variant allele of the UBC9 gene c.73G>A polymorphism. Mutation research 2010;694(1-2):31-8.

60. Mo YY, Yu Y, Theodosiou E, Ee PL, Beck WT. A role for Ubc9 in tumorigenesis. Oncogene 2005;24(16):2677-83.

61. McDoniels-Silvers AL, Nimri CF, Stoner GD, Lubet RA, You M. Differential Gene Expression in Human Lung Adenocarcinomas and Squamous Cell Carcinomas. Clinical Cancer Research 2002;8(4):1127-38.

62. Chen CY, Fang HY, Chiou SH, Yi SE, Huang CY, Chiang SF, et al. Sumoylation of eukaryotic elongation factor 2 is vital for protein stability and anti-apoptotic activity in lung adenocarcinoma cells. Cancer science 2011;102(8):1582-9.

63. McHale K, Tomaszewski JE, Puthiyaveettil R, Livolsi VA, Clevenger CV. Altered expression of prolactin receptor-associated signaling proteins in human breast carcinoma. Modern

pathology : an official journal of the United States and Canadian Academy of Pathology, Inc 2008;21(5):565-71.

64. Brantley EC, Nabors LB, Gillespie GY, Choi YH, Palmer CA, Harrison K, et al. Loss of protein inhibitors of activated STAT-3 expression in glioblastoma multiforme tumors: implications for STAT-3 activation and gene expression. Clinical cancer research : an official journal of the American Association for Cancer Research 2008;14(15):4694-704.

65. Driscoll JJ, Pelluru D, Lefkimmiatis K, Fulciniti M, Prabhala RH, Greipp PR, et al. The sumoylation pathway is dysregulated in multiple myeloma and is associated with adverse patient outcome. Blood 2010;115(14):2827-34.

66. Herbst RS, Heymach JV, Lippman SM. Lung Cancer. New England Journal of Medicine 2008;359(13):1367-80.

67. Gostissa M, Hengstermann A, Fogal V, Sandy P, Schwarz SE, Scheffner M, et al. Activation of p53 by conjugation to the ubiquitin-like protein SUMO-1. EMBO 1999;18(22):6462-71.

68. America PRaMo. 2014 Biopharmaceutical Research Industry Profile. Washington, DC: PhRMA; 2014 April 2014.

69. Bleicher KH, Bohm HJ, Muller K, Alanine AI. Hit and lead generation: beyond high-throughput screening. Nature reviews Drug discovery 2003;2(5):369-78.

70. Inglese J, Johnson RL, Simeonov A, Xia M, Zheng W, Austin CP, et al. High-throughput screening assays for the identification of chemical probes. Nat Chem Biol 2007;3(8):466-79.

71. Macarron R, Banks MN, Bojanic D, Burns DJ, Cirovic DA, Garyantes T, et al. Impact of high-throughput screening in biomedical research. Nature reviews Drug discovery 2011;10(3):188-95.

72. Clegg R. Fluorescence resonance energy transfer. Current Opinion in Biotechnology 1995;6:103-10.

73. Clegg RM. Fluorescence resonance energy transfer. Current Opinion in Biotechnology 1995;6(1):103-10.

74. Nguyen AW, Daugherty PS. Evolutionary optimization of fluorescent proteins for intracellular FRET. Nature biotechnology 2005;23(3):355-60.

75. Song Y, Rodgers VGJ, Schultz JS, Liao J. Protein interaction affinity determination by quantitative FRET technology. Biotechnology and Bioengineering 2012;109(11):2875-83.

76. Liu Y, Song Y, Madahar V, Liao J. Quantitative Förster resonance energy transfer analysis for kinetic determinations of SUMO-specific protease. Analytical biochemistry 2012;422(1):14-21.

77. Jiang L, Liu Y, Song Y, Saavedra A, Pan S, Xiang W, et al. Internal Calibration Förster Resonance Energy Transfer Assay: A Real-Time Approach for Determining Protease Kinetics. Sensors 2013;13(4):4553-70.

78. Song Y, Liao J. An *in vitro* Forster resonance energy transfer-based high-throughput screening assay for inhibitors of protein-protein interactions in SUMOylation pathway. Assay and drug development technologies 2012;10(4):336-43.

79. Kastritis PL, Bonvin AMJJ. On the binding affinity of macromolecular interactions: daring to ask why proteins interact. Journal of The Royal Society Interface 2013;10(79).

80. Ma B, Elkayam T, Wolfson H, Nussinov R. Protein-protein interactions: structurally conserved residues distinguish between binding sites and exposed protein surfaces. Proceedings of the National Academy of Sciences of the United States of America 2003;100(10):5772-7.

81. Arkin MR, Wells JA. Small-molecule inhibitors of protein-protein interactions: progressing towards the dream. Nature reviews Drug discovery 2004;3(4):301-17.

82. Lois LM, Lima CD. Structures of the SUMO E1 provide mechanistic insights into SUMO activation and E2 recruitment to E1. The EMBO journal 2005;24(3):439-51.

83. Wang J, Hu W, Cai S, Lee B, Song J, Chen Y. The Intrinsic Affinity between E2 and the Cys Domain of E1 in Ubiquitin-like Modifications. Molecular Cell 2007;27(2):228-37.

84. Capili AD, Lima CD. Structure and analysis of a complex between SUMO and Ubc9 illustrates features of a conserved E2-Ubl interaction. Journal of molecular biology 2007;369(3):608-18.

85. Lipinski CA, Lombardo F, Dominy BW, Feeney PJ. Experimental and computational approaches to estimate solubility and permeability in drug discovery and development settings. Advanced Drug Delivery Reviews 2001;46(1–3):3-26.

86. Yang Y, Kitagaki J, Dai RM, Tsai YC, Lorick KL, Ludwig RL, et al. Inhibitors of ubiquitin-activating enzyme (E1), a new class of potential cancer therapeutics. Cancer research 2007;67(19):9472-81.

87. Ungermannova D, Parker SJ, Nasveschuk CG, Chapnick DA, Phillips AJ, Kuchta RD, et al. Identification and mechanistic studies of a novel ubiquitin E1 inhibitor. Journal of biomolecular screening 2012;17(4):421-34.

88. Yang Y, Kitagaki J, Dai R-M, Tsai YC, Lorick KL, Ludwig RL, et al. Inhibitors of Ubiquitin-Activating Enzyme (E1), a New Class of Potential Cancer Therapeutics. Cancer Research 2007;67(19):9472-81.

89. Xu GW, Ali M, Wood TE, Wong D, Maclean N, Wang X, et al. The ubiquitin-activating enzyme E1 as a therapeutic target for the treatment of leukemia and multiple myeloma. Blood 2010;115(11):2251-9.

90. Ungermannova D, Parker SJ, Nasveschuk CG, Wang W, Quade B, Zhang G, et al. Largazole and Its Derivatives Selectively Inhibit Ubiquitin Activating Enzyme (E1). PLoS ONE 2012;7(1):e29208.

91. Vassilev LT, Vu BT, Graves B, Carvajal D, Podlaski F, Filipovic Z, et al. In Vivo Activation of the p53 Pathway by Small-Molecule Antagonists of MDM2. Science 2004;303(5659):844-48.

92. Hoe KK, Verma CS, Lane DP. Drugging the p53 pathway: understanding the route to clinical efficacy. Nature reviews Drug discovery 2014;13(3):217-36.

93. Secchiero P, Bosco R, Celeghini C, Zauli G. Recent advances in the therapeutic perspectives of Nutlin-3. Current pharmaceutical design 2011;17(6):569-77.

94. Brownell JE, Sintchak MD, Gavin JM, Liao H, Bruzzese FJ, Bump NJ, et al. Substrate-Assisted Inhibition of Ubiquitin-like Protein-Activating Enzymes: The NEDD8 E1 Inhibitor MLN4924 Forms a NEDD8-AMP Mimetic In Situ. Molecular Cell 2010;37(1):102-11.

95. Soucy TA, Smith PG, Milhollen MA, Berger AJ, Gavin JM, Adhikari S, et al. An inhibitor of NEDD8-activating enzyme as a new approach to treat cancer. Nature 2009;458(7239):732-6.

96. Milhollen MA, Narayanan U, Soucy TA, Veiby PO, Smith PG, Amidon B. Inhibition of NEDD8-Activating Enzyme Induces Rereplication and Apoptosis in Human Tumor Cells Consistent with Deregulating CDT1 Turnover. Cancer Research 2011;71(8):3042-51.

97. Soucy TA, Smith PG, Milhollen MA, Berger AJ, Gavin JM, Adhikari S, et al. An inhibitor of NEDD8-activating enzyme as a new approach to treat cancer. Nature 2009;458(7239):732-36.

98. Zhao Y, Morgan MA, Sun Y. Targeting Neddylation Pathways to Inactivate Cullin-RING Ligases for Anticancer Therapy. Antioxidants & Redox Signaling 2014.

99. Fukuda I, Ito A, Hirai G, Nishimura S, Kawasaki H, Saitoh H, et al. Ginkgolic acid inhibits protein SUMOylation by blocking formation of the E1-SUMO intermediate. Chemistry & biology 2009;16(2):133-40.

100. Fukuda I, Ito A, Uramoto M, Saitoh H, Kawasaki H, Osada H, et al. Kerriamycin B inhibits protein SUMOylation. The Journal of antibiotics 2009;62(4):221-4.

101. Kumar A, Ito A, Hirohama M, Yoshida M, Zhang KYJ. Identification of Sumoylation Activating Enzyme 1 Inhibitors by Structure-Based Virtual Screening. Journal of Chemical Information and Modeling 2013;53(4):809-20.

102. Chen Y, Li YJ, Divlianska D, Bobkova E, Roth G, PU J, et al. Bicyclic and tricyclic inhibitors of sumoylation enzymes and methods of their use. Google Patents; 2013.

CHAPTER 2. MECHANISM OF ACTION OF STE AS A NOVEL SUMOYLATION PATHWAY INHIBITOR

2.1 Abstract

To date, there have been no specific cell permeable inhibitors of the SUMOylation pathway. To address this problem, our group performed a high-throughput screening to look for small molecule inhibitors for the SUMOylation pathway and identified STE as our lead compound. Because of the generality of the high-throughput screening design, the specific mechanism of the STE in the SUMOylation pathway was not known. To explore the mechanism of the lead compound inhibitor, we analyzed the effect of STE in *in vitro* SUMOylation reactions. Determinations of E1~SUMO1 and E2~SUMO conjugates by gel-Based assays were performed to dissect the effect of STE in the SUMOylation cascade. Additionally, analysis by Western blot to detect SUMO transfer from the E1 to E2 enzyme was also performed. The IC_{50} values for STE was found to be 1.21 µM and 5.17 µM for E1~SUMO and E2~SUMO thioester conjugation, respectively. However, STE treatment does not affect the transfer of SUMO from the E1 to the E2 enzyme. To determine the specificity of STE, the effect of STE treatment in E1 and E2 thioester conjugation of two other pathways, ubiquitin and NEDD8, was also measured. Analysis of STE treatment in Ubiquitination and NEDDylation thioester conjugation revealed that there was no significant difference between STE- treated and DMSO-treated thioester formation. Similar results were found using FRET analysis. This study showed that STE inhibits E1 ~SUMO conjugate formation and that inhibition of the E2~SUMO thioester conjugation was a downstream effect of E1 inhibition.

2.2 Introduction

SUMOylation is catalyzed by the sequential action of SUMO-activating enzyme (E1), a SUMO conjugating enzyme (E2), and an E3 ligase. In humans, there is a single SUMO E1 which is a heterodimer of SAE1/SAE2 (SUMO-Activating Enzyme-1, -2), a single E2 (Ubc9), and many E3 ligases (1). SUMO proteins play multifaceted roles both in physiological and disease conditions(2). Expression of SUMO and its enzymes in the SUMOylation pathway have been found to be significantly increased in many types of cancer(3). Therefore, we hypothesized that inhibition of the SUMOylation pathway could be used as a new approach in cancer therapy.

SUMOylation is a cascade of enzymatic processes that involves E1 (4,5), E2 (6), and E3 enzymes (7). Although these enzymes are analogous to those of the ubiquitin pathway, the enzymes of the SUMO pathway are specific to SUMO and play no role in conjugating ubiquitin or any other ubiquitin-like proteins. SUMOylation is a reversible process and SUMO is removed by SUMO-specific proteases SENPs (Sentrin specific peptidase), enzymes that cleave a c-terminal peptide from the SUMO precursor (8). The mechanism of SUMO activation is:

$$\mathrm{Aos1/Uba2_{SH} + ATP + SUMO} \overset{Mg^{2+}}{\rightleftharpoons} \mathrm{Aos1/Uba2}^{\cdot\mathrm{AMP\text{-}SUMO}}_{\mathrm{SH}} + \mathrm{PP_i} \quad (1)$$

$$\mathrm{Aos1/Uba2}^{\cdot\mathrm{AMP\text{-}SUMO}}_{\mathrm{SH}} \rightleftharpoons \mathrm{Aos1/Uba2_{S\text{-}SUMO} + AMP} \quad (2)$$

$$\mathrm{Aos1/Uba2_{S\text{-}SUMO} + ATP + SUMO} \overset{Mg^{2+}}{\rightleftharpoons} \mathrm{Aos1/Uba2}^{\cdot\mathrm{AMP\text{-}SUMO}}_{\mathrm{S\text{-}SUMO}} + \mathrm{PP_i} \quad (3)$$

$$\mathrm{Aos1/Uba2}^{\cdot\mathrm{AMP\text{-}SUMO}}_{\mathrm{S\text{-}SUMO}} + \mathrm{Ubc9_{SH}} \rightleftharpoons \mathrm{Aos1/Uba2}^{\cdot\mathrm{AMP\text{-}SUMO}}_{\mathrm{SH}} + \mathrm{Ubc9_{S\text{-}SUMO}} \quad (4)$$

Figure 1.3 SUMOylation activation and conjugation scheme. SUMOylation activation and conjugation scheme with non-covalent complexes indicated with a dot and covalent conjugation indicated with a hyphen. S-SUMO refers to the thioester bond between the catalytic cysteine and the SUMO c-terminus.

Numerous small molecule inhibitors of Ubiquitination and NEDDylation pathways have been found by researchers. Of interest to our group were PYR-41, PYZD-4409, and NSC624206. PYR-41 was previously identified as a cell permeable inhibitor of the Uba1 that blocks ubiquitin-thioester formation (9,10). Similarly, PYZD-4409 induced cell death in acute myeloid leukemia cells by inhibiting Ubiquitin E1, Uba1 (11). NSC624206 and Largazole were also found to inhibit Ub E1 (10,12). Nutlin-3 targets the Mdm2 protein, a really interesting new gene (RING)-type E3 ubiquitin ligase, and antagonizes MDM-p53 interaction with IC_{50} of only 19nM (13,14). Nutlin-3 is currently in a Phase I clinical trial for the treatment of retinoblastoma, solid tumor, and leukemia(15).

For comparison, MLN4924 was recently found as an inhibitor of the NEDDylation pathway. MLN 4924 is an AMP-mimic that inhibits APPBP1/Uba3, the only E1 enzyme in the NEDDylation pathway, by blocking the enzyme activity through binding of the NAE adenylation active site (16). The mechanism of MLN4924 is substrate-assisted inhibition by forming covalent adducts NEDD8-MLN4924 which disrupts cullin-RING ligase (CRL) mediated protein turnover leading to deregulation of S-phase DNA synthesis which cause apoptotic death in human cancer cells (17). MLN4924 is currently in phase I clinical trial for AML acute myeloid leukemia and solid tumors(18).

High-throughput screening assays (HTS) for the identification of chemical probes have been used widely in drug discoveries. High-throughput generally refer to the testing of 10,000 to 100,000 compounds per day by employing mechanized processes ranges from manually operated workstations to fully automated robotic system. There are several parameters of HTS that differ from laboratory “bench top” assays, such as simple operations, few (5-10) steps, addition only preferred, assay volume between 1 to 100μl, robotic reagent handling, stable reagents, microtiter plate formats, time of measurements from minutes to hours, fluorescence, luminescence, or absorbance plate reader output formats, and automated analysis of all data using statistical

criteria(19). The understanding of HTS design and the pharmacological impact of the assay design is important to identify the hit compounds from HTS.

Förster (Fluorescence) resonance energy transfer technology (FRET) application takes advantage of non-radioactive energy transfer by means of intermolecular long-range dipole-dipole coupling. The FRET signal is produced by an excited molecular chromophore (donor) that excites another chromophore (acceptor) over distances from ~10Å to 100Å (20). FRET has several advantages in studying enzyme catalyzed reaction. FRET assays can capture reaction progress continuously and can be performed in a multi-well plate format that can be economical and time-saving. CyPet and YPet, derivatives of cyan fluorescence protein (CFP) and yellow fluorescent protein (YFP) respectively, are a protein pair that exhibits a 20-fold stronger FRET signals than the unmodified CFP-YFP pair (21). CyPet acts as a donor, and YPet acts as the acceptor. FRET can be used to determine protein interaction affinity (22), kinetics of protease enzymes (23,24), and automated inhibitor screening for SUMOylation pathway inhibitors (25).

Here, we report the discovery of STE, a small molecule inhibitor of SUMO E1, through high throughput screening to find an inhibitor of SUMOylation pathway. STE inhibits E1~SUMO thioester bond formation and E2~SUMO thioester formation. However, because STE does not affect the transfer of SUMO from E1 to the E2, the E2~SUMO inhibition is a downstream effect of the E1~SUMO thioester inhibition In addition, STE selectively inhibits SUMO E1 activity compared to the closely related ubiquitin-activating enzyme (Uba1) and NEDD8-activating enzyme (NAE) in purified enzyme assays.

2.3 Materials and Methods

Expression and Purification of His-Tagged Proteins E1, Ubc9, and SUMO for SUMOylation studies:

Recombinant plasmids Pet28(b)-Aos1, Pet28(b)-Uba2, Pet28(b)-SUMO1, Pet28(b)-Ubc9, Pet28(b)-Ub, Pet28(b)-Uba1, Pet28(b)-UbcH5α, Pet28(b)-NEDD8, Pet28(b)-APPBP1, Pet28(b)-Uba3, and Pet28(b)-Ubc12 were transformed into E. coli BL21 (DE3) as described previously (22,26). A single colony of freshly transformed cells was cultured in 10ml of Luria Bertani (LB) Broth containing 0.5mg/ml kanamycin with shaking at 225 rpm for 16 hr at 37^{o}C. The 10 ml culture was innoculated into 500ml of 2x Yeast extract and Tryptone (2xYT) broth containing 0.5mg/ml kanamycin. Culture with continuous shaking at 225 rpm at 37^{o}C until OD 600 of 0.6 to 0.7 was reached. Protein expression was induced by adding 0.5ml of 1M isopropyl β-D-1-thiogalactopyranoside (IPTG) for a final concentration of 1mM, and the culture was shaken overnight at 25^{o}C at 180 rpm. The cells were harvested by centrifugation for 15 min at 1250xg. After discarding the supernatant, the cells were resuspended in the binding buffer containing 5mM imidazole, 0.5 M NaCl, 20mM Tris-HCl, pH 7.9. To break the *E. coli* cell wall, the cell suspension was sonicated at 70J for 6 minutes with 5 second on/off cycles. A clear solution was obtained after centrifugation of the cell lysates for 30 min at 20,000xg, 4^{o}C (24).

Proteins of interest were purified from cell lysates using column chromatography and Ni-NTA resin. All the purification steps were carried out in a 4^{o}C cold room. When all the supernatant was loaded, the column was washed with wash buffer I (0.3 M NaCl, 20mM Tris-HCl, pH 7.9), wash buffer II (1.5M NaCl, 20 mM Tris-HCl, pH 7.9, 0.5% Triton), and wash buffer III (0.5M Na Cl, 20mM Tris-HCl pH 7.9), and 10mM imidazole). The protein was eluted with elution buffer containing 0.5M NaCl, 20mM Tris-HCl pH 7.9, and 0.5 M imidazole. The protein samples were dialyzed overnight against dialysis buffer containing 0.5M Na Cl, 20mM Tris-HCl pH 7.9 to reduce imidazole

concentration below 10μM. Five mM dithiothreitol (DTT) was added to the dialysis buffer to prevent oxidation of the Cys residues (27). Protein purities were checked by resolving the samples in 10% SDS-PAGE gels at 100 V for 2 hour. Molecular weights of the His-tagged proteins: H6-SUMO (12kDa), H6-Ubc9 (18 kDa), H6-Aos1 (40 kDa), H6-Uba2 (71 kDa), H6-NEDD8 (9kDa), H6-APPBP1 (61 kDa), H6-Uba3 (52kDa), H6-Ubc12 (18 kDa), H6-Ub (9 kDa), H6-Uba1 (120kDa), H6-Ubc5α (18kDa). Protein concentrations were determined using Pierce® Coomassie (Bradford) protein assay kit. To confirm that the CyPetSUMO1 can modify YPetRanGAP1c with the help of E1 (Aos1/Uba2) and E2 (Ubc9), we performed western blot assays.

Hit confirmation Assays

To confirm the activity of the hit compounds in HEK293 cells, HEK cells were plated at $2x10^6$ cells in 10-cm cell culture dishes. Cells were treated with no DMSO, 0.1%DMSO (control), or 50 μM of compound 7708424, 50 μM STE, and 50 μM STE042 for 4 hours. Cells were harvested and washed in cold PBS, and whole-cell extracts were prepared and normalized by total protein concentration. Total protein (20μg) was separated by SDS-PAGE electrophoresis under reducing conditions. Samples were denatured in 6x sodium dodecyl sulfate (SDS) loading buffer containing 0.1 M DTT and was heated at 90°C for 10 min.

Protein separation was accomplished by electrophoresis in 10% PAGE-SDS minigels for 2 h at 100 V. After electrophoresis, protein was transferred to a nitrocellulose membrane in transfer buffer containing 0.25 mM Tris, 192 mM glycine, and 20% methanol (pH 8.3). Nitrocellulose membranes were blocked with 5% non-fat milk in wash buffer (150 mM NaCl, 20 mM Tris-HCl, pH 7.4, and 0.05% Tween 20) for 2 h and then incubated with rabbit anti-SUMO1 (1:1000) in wash buffer containing 3% non-fat milk overnight. The membranes were rinsed three times with wash buffer and then incubated with secondary horseradish peroxidase–conjugated goat anti-rabbit IgG

in wash buffer containing 3% non-fat milk for 2 h. Membranes were rinsed three times with wash buffer and developed with the enhanced-chemiluminescence system. Images were taken using a UVP Biospectrum A/C Imaging System, and processed using Image J software(28).

Determination of E1~SUMO1 Conjugates by Gel-Based Assay

E1 thioester and E2 thioester formation assays to determine the mechanism of ST025091 inhibition were performed as previously described (6). To analyze E1~SUMO1 thioester bond formation, reaction mixtures containing 3 µM SUMO1 and 1 µM E1 (Aos1/Uba2) were incubated for 5 min at 30°C with or without increasing concentration of STE (0.1, 0.5, 1, 3, 5, 10, 25µM). The reactions were started by the addition of 2µl ATP for a final concentration of 2mM and incubation in ae 37^{o}C waterbath then ensued for 10 mins. The reactions were terminated by the addition of 6x non-reducing SDS loading buffer and the reaction products were fractionated by SDS-PAGE under non-reducing conditions.

Detection of SUMO Thioester Transfer from E1 to E2

The detection of SUMO thioester transfer from E1 to E2 was performed according to the protocol published by Alontaga et al. (27) In the first of two steps to monitor the transfer of SUMO from E1 (Aos1/Uba2) to E2 (Ubc9), E1~S thioester complex was formed by incubating 3 µM SUMO1, 1µM Aos1, and 1µM Uba2 in SUMO assay buffer containing 50mM Tris-Cl pH 7.5, 5mM $MgCl_2$, 2mM ATP in 37^{o}C water bath for 10 mins. After incubation, the reaction was halted by adding ethylenediaminetetraacetic acid (EDTA) to a final concentration of 30mM to remove Mg^{2+}. 1µM Ubc9 was added to different tubes containing DMSO or various concentrations of STE (1, 5, 20, and 50 µM). The E1~SUMO/EDTA mixture was added into each tube to start the reaction. The assay was carried out at room temperature for 5 mins due to fast transfer rate. The reaction was stopped

by mixing one half of the reaction from each tube (25µl) with 5µl 6x non-reducing SDS gel-loading buffer containing 4M urea and the other half was mixed with 5µl 6x reducing SDS loading buffer containing 100mM DTT. The samples were fractionated by 10% SDS PAGE subjected to 100V electrophoresis for 2 hours. The E2~SUMO band intensities were quantified using the ImageJ software (28).

Determination of E2~SUMO1 Conjugates by Gel-Based Assay

To examine inhibition of STE on E2 enzyme, E2~SUMO1 thioester assays, a reaction mix consisting of 3 µM SUMO1, 1 µM E1 (Aos1/Uba2), ATP, and 1 µM E2 (Ubc9) with or without various concentrations ((0, 0.1, 0.5, 1, 3, 5, 10, 25 µM) of STE were incubated for 10 min at 30^{o}C. After mixing the protein mix with STE, solutions were incubated for 10 mins. ATP was added (2µl) to start the reactions and all tubes were incubated in a 37^{o}C water bath for 10 mins.

Determination of E1~Ub, E1~NEDD8, E2~Ub, and E2~NEDD8 Conjugates by Gel-Based Assay

To examine inhibition of STE on E1 and E2 enzymes of the ubiquitination and NEDDylation pathways, E1 and E2 thioester conjugation assays were carried out as described above. For the ubiquitin pathway, the reaction mix consist of 3 µM Ub, 1 µM Uba1, and 1 µM Ubc5α with or without various concentrations (0, 0.1, 0.5, 1, 3, 5, 10, 25 µM) of STE. For the NEDDylation pathway, the reaction mix consist of 3 µM NEDD8, 1 µM E1 (APPBP1/Uba3), and 1 µM Ubc12 with or without various concentrations (0, 0.1, 0.5, 1, 3, 5, 10, 25 µM) of STE.

Western blot analysis

Separated proteins were transferred onto a nitrocellulose membrane using a wet blotter in the transfer buffer (0.25M Tris base, 0.192M glycine, and 20% methanol) for 40 min at a constant voltage of 100V. Nitrocellulose membranes were blocked with 5% non-fat milk in wash buffer (150

mM NaCl, 20 mM Tris-HCl, pH 7.4, and 0.05% Tween 20) for 2 h and then incubated with rabbit anti-SUMO1 (1:1000), mouse anti-His Tag (1:1000) (Sigma Aldrich, St. Louis, MO) in wash buffer containing 3% non-fat milk overnight. The membranes were rinsed three times with wash buffer and then incubated with secondary horseradish peroxidase–conjugated goat anti-rabbit IgG and goat anti-mouse IgG (Sigma Aldrich) in wash buffer containing 3% non-fat milk for 2 h. Membranes were rinsed three times with wash buffer and developed with the enhanced-chemiluminescence system. Thioester bond formations were visualized as a 15-kDa shift by analyzing the respective adducts by Western blot using anti-Uba2, anti-Ubc9, or anti-SUMO1 antibodies (27). Images were taken using a UVP Biospectrum A/C Imaging System.

Quantitative evaluation of the thioester reactions

Image processing and analyses were performed using ImageJ software (National Institute of Health, Bethesda, MD, USA)(28). The intensity of the STE-treated thioester band was expressed as relative thioester band intensity to non-STE-treated reactions. The results of 3 separate measurements for each of the thioester conjugate assays were expressed as mean ±SE. GraphPad Prism software was used for all statistical analysis and graphical illustrations. Any *p*-values less than 0.05 were considered statistically significant. In the presence of inhibition, a dose-response curve was utilized to find the IC_{50} value using GraphPad Prism software.

E1~SUMO and E2~SUMO thioester conjugate analysis by FRET tehcnology

To confirm formation of E1~SUMO and E2~SUMO1 conjugates, we used FRET technology to measure protein-protein interactions in the presence or absence of STE. To detect E1~SUMO formation, 60 µl reactions containing 1 µM YPet-Uba2, 1 µM Aos1, 3 µM CyPet SUMO1, 2mM ATP, and DMSO or various concentration of STE were mixed in a 384-well black plate (Greiner®). A

Flexstation II[384] was used to read the emission wavelength of 530 nm with an excitation wavelength of 414 nm.

2.4 Results

FRET-based High Throughput Screening Design to Identify Small Molecule Inhibitors of the SUMOylation Pathway

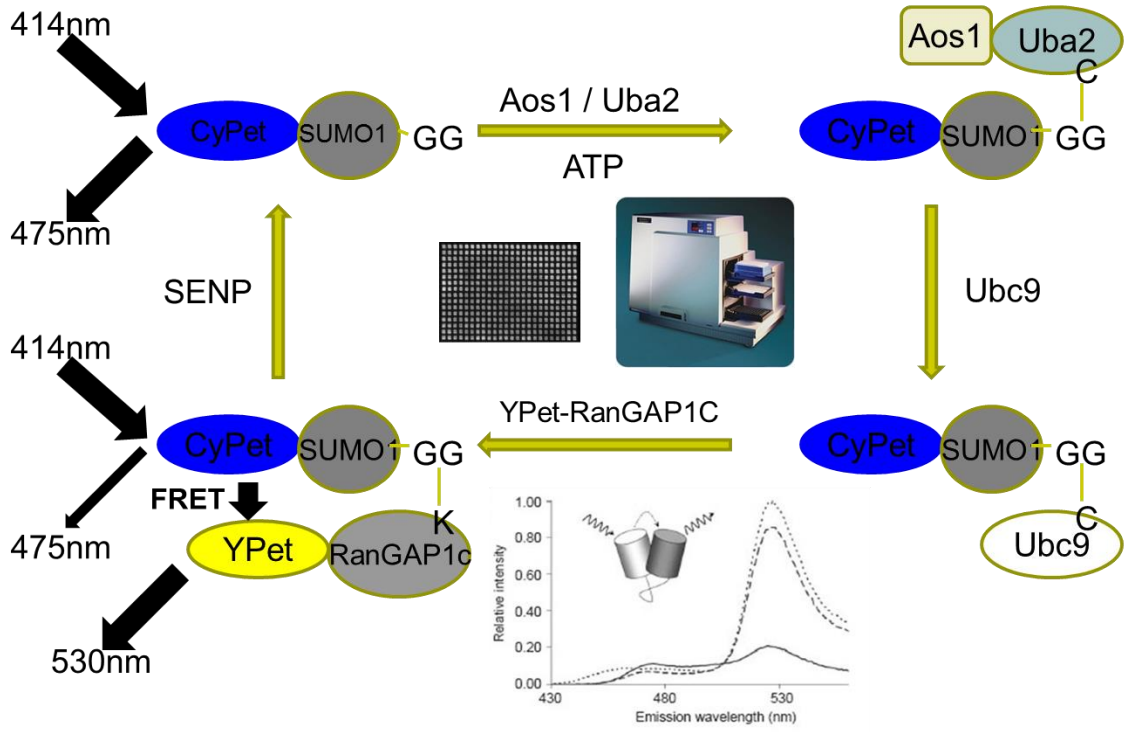

Figure 2.1 Principle of the FRET-based High Throughput Screening to find inhibitors of SUMOylation Pathway. SUMO was fluorescently tagged with CyPet and RanGAP1c was fluorescently tagged with YPet protein. The CyPet has an optimum emission at 475 when excited at 414 nm, whereas YPet has an optimum emission at 530 nm when excited at 475nm. When SUMO interacted with RanGAP1c protein, a FRET signal could be detected. In the presence of an inhibitor of the SUMOylation pathway, RanGAP1c-SUMO formation would be decreased and thus the FRET signal would be decreased accordingly. (Data from Yang Song)

This high throughput screening was performed using FRET. As indicated in Figure 2.1, the screening involved multiple steps of the SUMOylation pathway. First, CyPet-tagged SUMO was incubated with the E1 enzyme (Aos1/Uba2) and ATP. E2 was then added to the solution so SUMO could be transferred from the E1 to the E2 enzyme. Lastly, YPet-tagged RanGAP1c was added as a substrate of SUMO. When RanGAP1c is SUMOylated, a FRET signal can be detected as a 530 nm emission. In the presence of an inhibitor, there will be no interaction between RanGAP1c and SUMO and therefore there will be no FRET signal.

FRET technology is beneficial for high throughput screening because of its sensitivity even in a low concentration. Additionally, the E1, E2, and SUMO substrate involvements were designed to optimize possible hits for small molecule inhibitors of the entire SUMOylation pathway. A small molecule that binds to any of the SUMOylation components would be detected as a decreased FRET signal. We screened 220,000 compounds. 70,000 were from the UCR chemical compounds library and the rest came from the University of Illinois, Urbana-Champaign compounds library. We identified approximately 200 hit compounds and performed confirmation assays to test the compounds' effectiveness in inhibiting SUMOylation in HEK293 cells.

In the first round of confirmation tests, we identified about 60 compounds that were active in HEK 293 cells. Additionally, we performed Western blot to detect formation of RanGAP1c-SUMO *in vitro.* As indicated in Figure 2.2A, compound STE strongly inhibited SUMOylation as indicated by reduced intensity of SUMOylated protein bands in comparison to the effects of other compounds. Additionally, figure 2.2B shows that RanGAP1c-SUMO modifications were inhibited in the presence of 1μM STE or more. Thus, we chose STE as our lead compound for further analysis. Figure 2.2C shows the chemical structure of STE and its derivatives. X, Y, and Z are independently selected

from the group consisting of C, N or O. STE derivatives were designed by replacing the R1, R2, R3, and R4 side chains.

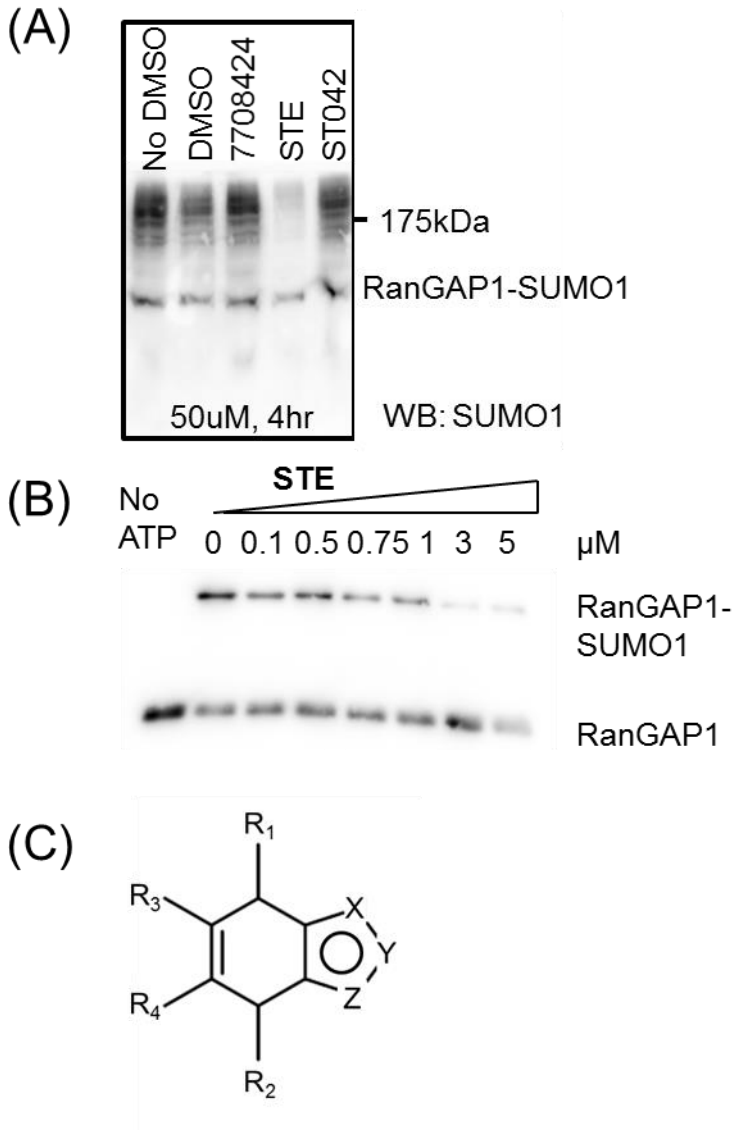

Figure 2.2 Hit Compounds Confirmation. (A) STE was shown to have the highest inhibition of whole cell SUMOylation. Several of the leading hit compounds found in the high throughput screening were used to treat HEK 293 cells. The concentration of each compound was 50μM and the cells were treated for 4 hours. (B) Various concentrations of STE in an *in vitro* RanGAP1c-SUMO

formation assay. The concentration of 1μM was shown to have an inhibitory effect on RanGAP1c-SUMO formation. (A and B data from Yang Song) (C) The chemical structure of STE and its derivatives. X, Y, and Z are independently selected from the group consisting of C, N or O. STE derivatives were designed by replacing the R1, R2, R3, and R4 side chains.

Because STE was found in a high-throughput screening, the exact mechanism of this compound was not evident. To elucidate STE mechanism of action, we dissected the SUMOylation pathway into three major steps: (1) formation of E1~SUMO thioester conjugate, (2) transfer of SUMO from the E1 to E2 enzyme, and (3) formation of the E2~SUMO thioester conjugate. We performed E1~SUMO and E2~SUMO thioester conjugates identification by Western blots. These results will be discussed in the next section.

STE Inhibits E1~SUMO thioester formation in a dose dependent manner

The Cys 173 residue in the active site of the Uba2 subunit of E1 forms a thioester bond with SUMO. The formation of Uba2~SUMO conjugates is shown in Figure 2.3A above. The thioester bond between Uba2 and SUMO can be disrupted by addition of reducing agents such as DTT (right lane). Addition of DTT served as a control to confirm the thioester bond (27). To look for the effect of STE treatment in E1~SUMO thioester conjugate formation, we carried out a thioester formation reaction which consists of E1, SUMO, and ATP in the presence of various STE concentrations or DMSO. We found that STE inhibited E1~SUMO thioester conjugate formation in a dose dependent manner.

As indicated in Figure 2.3A, the Uba2~SUMO band intensities are lower in the STE- treated reactions. Moreover, at concentrations of STE >0.1uM, a dose dependent inhibition was observed.

STE efficiently inhibited E1~SUMO thioester conjugate formation with an IC50 of 1.21µM in three separate experiments (Figure 2.3B).

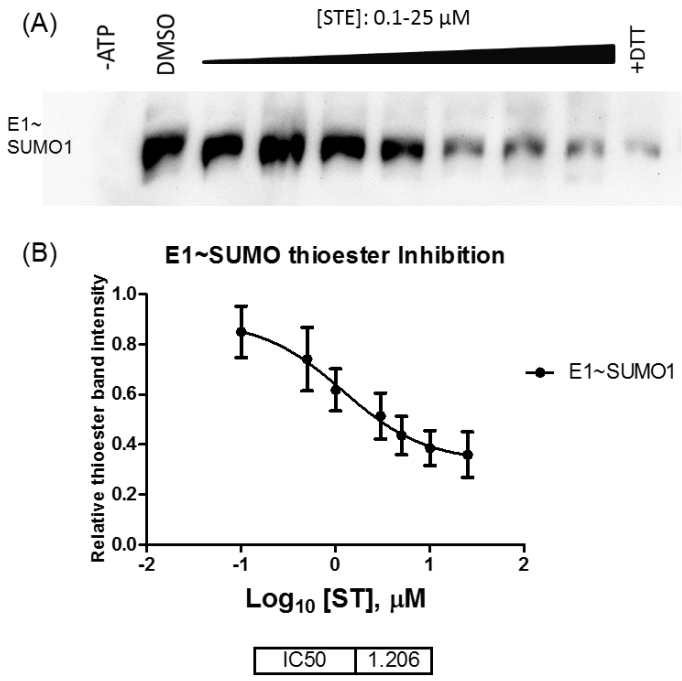

Figure 2.3 Inhibition of E1~SUMO thioester conjugation formation in the presence of increasing dose of STE. (A) Effects of different concentrations of STE on E1~SUMO thioester conjugate formation. (B) The IC 50 calculation was performed using GraphPad Prism software. The bars represent mean ± SE (n=3).

STE Inhibits E2~SUMO thioester formation in a dose dependent manner

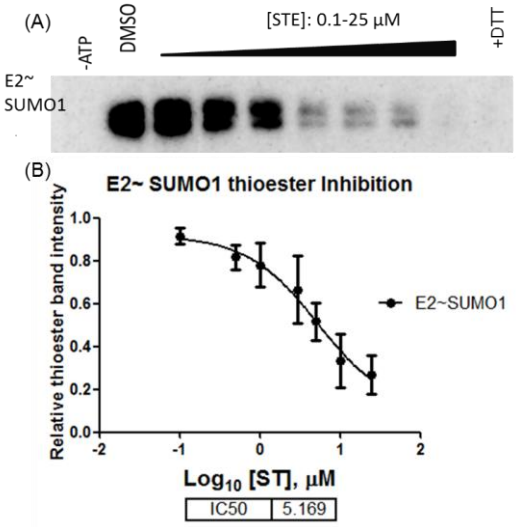

Figure 2.4 Inhibition of E2~SUMO1 thioester conjugation formation in the presence of increasing doses of STE. (A) Effects of different concentrations of STE on E1~SUMO thioester conjugate formation. (B) The IC_{50} calculation was performed using GraphPad Prism software. The bars represent mean ± SE (n=3).

Using the same principal as the E1~SUMO thioester conjugate formation, we performed E2~SUMO thioester conjugate formation assays. In this assay, E1, E2, SUMO, and ATP were incubated in the presence of various concentrations of STE or DMSO. Figure 2.4 shows similar results to the E1~SUMO thioester conjugate assays; we found that STE inhibited the E2~SUMO thioester conjugate formation in a dose dependent manner, as indicated by reduction of the E2~SUMO thioester band intensity (Figure 2.4A). The IC50 of the E2~SUMO was 5.17 µM. This result suggested that STE exhibits selectivity towards SUMO E1. Due to the reaction cascade of the SUMOylation pathway, the E2 thioester reaction does not specify whether STE inhibits SUMO transfer in the apparent inhibition of the E2~SUMO thioester formation. The contribution of STE to the SUMO transfer from E1 to E2 will be elucidated in the next section.

STE does not inhibit SUMO transfer from the E1 to E2 enzyme

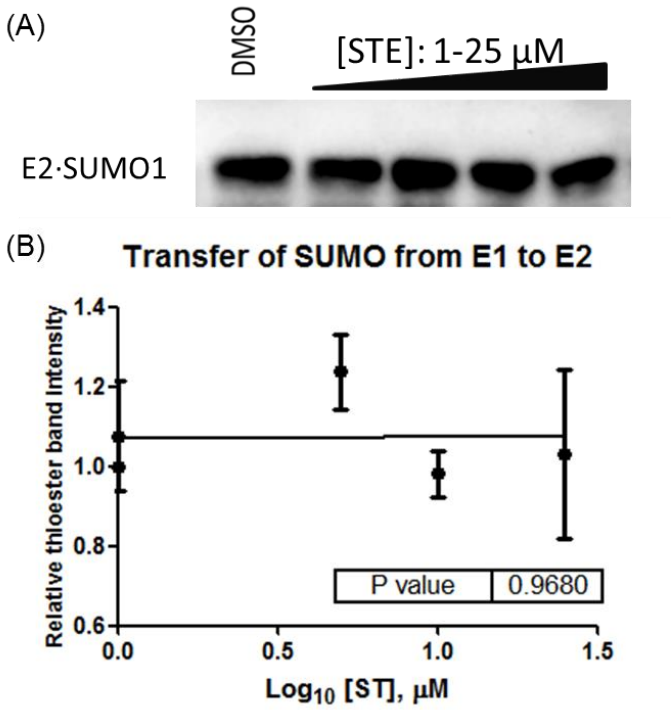

Figure 2. 5 Transfer of SUMO from E1 to E2 is not inhibited by STE. (A) E2~SUMO thioester formation with the preformed E1~SUMO thioester in the presence of DMSO or various concentrations of STE. The absence of changes in the E2~SUMO thioester band intensities indicated that the transfer of SUMO from E1 to E2 is not affected by STE treatment. (B) The relative thioester band intensity comparison is plotted using GraphPad Prism software. The bars represent mean ± SE (n=3).

To dissect whether the E2~SUMO thioester conjugation by STE was a direct effect on the E2 enzyme or whether it was caused by upstream inhibition of the E1~SUMO thioester conjugate formation, we performed a SUMO transfer assay. In this assay, the E1~SUMO was preformed and the reaction was stopped by the addition of the chelating agent, EDTA (ethylenediaminetetraacetic

acid), to form complexes with magnesium ions. The preformed E1~SUMO complex was then added to the E2 enzyme to measure the transfer of the SUMO from E1 to E2, both in the presence of DMSO or increasing concentrations of STE.

As indicated on Figure 2.5, the STE treatment did not have any effect on the E2 thioester formation when the E1~SUMO thioester bond was preformed. Thus, STE did not affect SUMO transfer from E1 to E2. This finding revealed that the inhibition of the E2 enzyme was a downstream effect of STE inhibition of E1~SUMO thioester formation.

FRET confirmation of STE inhibition on the E1~SUMO and E2~SUMO thioester conjugation

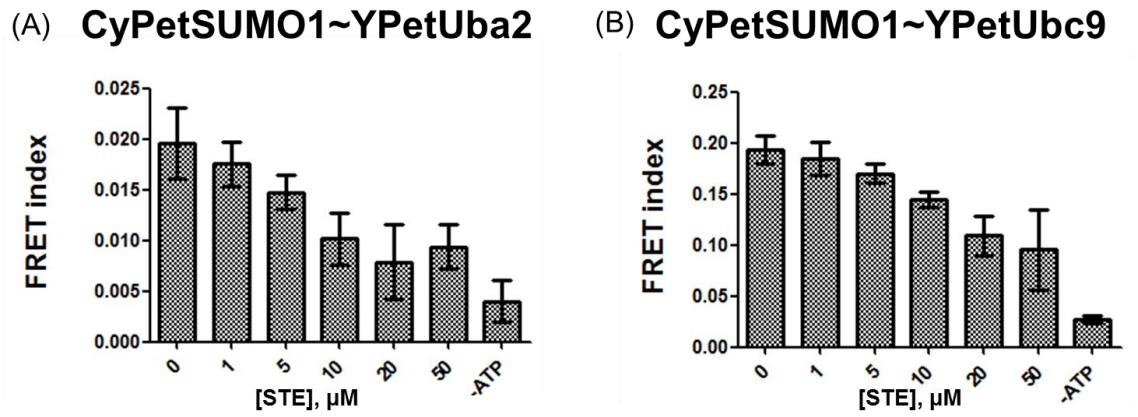

Figure 2.6 FRET confirmation assays of E1~SUMO and E2~SUMO thioester conjugate formation inhibition by STE. (A) STE inhibits CyPetSUMO~YPetUba2 (E1~SUMO) thioester formation in a dose dependent manner. (B) STE inhibits CyPetSUMO~YPetUbc9 (E2~SUMO) thioester formation in a dose dependent manner. (Data from Ling Jiang)

To confirm the results of the Western blot assays of the E1~SUMO and E2~SUMO conjugation by STE, FRET assays were performed using two sets of fluorescently tagged proteins. To detect E1~SUMO conjugation, CyPetSUMO and YPetUba2 pair were used. On the other hand,

to detect E2~SUMO thioester conjugation, CyPetSUMO was paired with YPetUbc9 protein. Similar to the Western blot assays result, the FRET index of both the E1~SUMO thioester (CyPetSUMO~YPetUba2) and E2~SUMO thioester (CyPetSUMO~YPetUbc9) were decreased as the STE concentration was increased. These findings confirm STE inhibition of E1~SUMO and E2~SUMO thioester conjugate formation.

STE does not inhibit E1~Ub and E2~Ub thioester conjugation

After establishing that STE inhibited E1~SUMO thioester formation, we then looked at the effect of STE treatment on the ubiquitination and NEDDylation processes. Since ubiquitin and ubiquitin-like proteins share E1 and E2 enzymes from the same families, the UBA gene family for the E1 enzyme and the UBC gene family for the E2 enzymes, we were interested in testing whether there was any cross-reactivity of the STE inhibition among these pathways. To test for cross reactivity of STE against other pathways, both ubiquitin and NEDD8 E1 and E2 thioester assays were performed.

As shown in figure 2.7, the presence of STE compound in the reaction did not affect the thioester band intensity of the E1~Ub thioester. This indicates that STE had no effect in the formation of the E1~Ub thioester bond. When similar assays were carried out in the presence of the ubiquitin E2 enzyme, we could not detect any significant changes of E2~Ub thioester formation. These experiments showed that STE had no affect on the formation of E1~Ub or E2~Ub thioester conjugates.

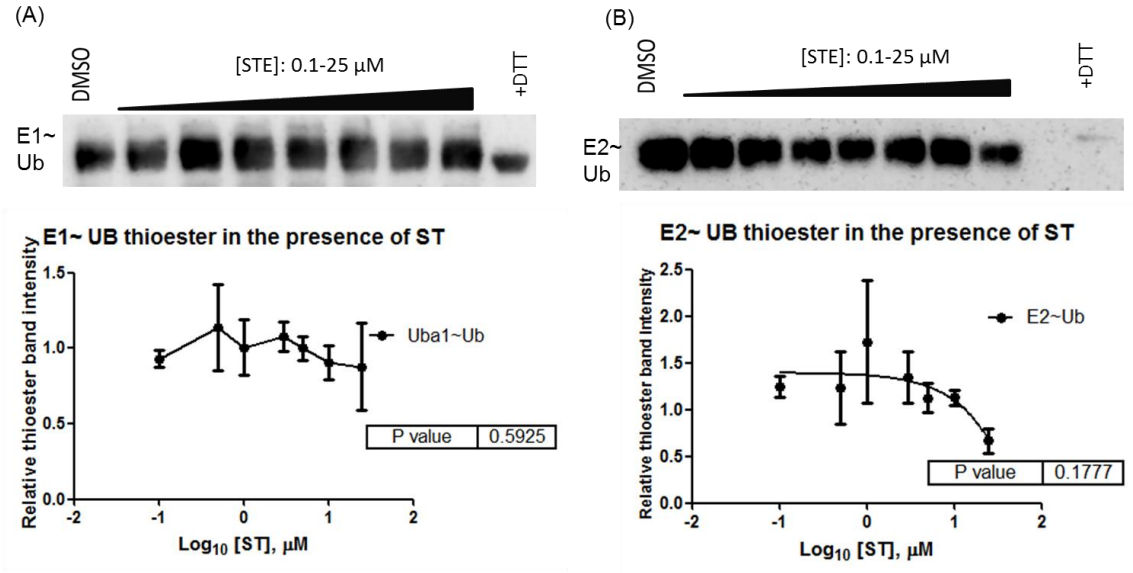

Figure 2.7 STE does not inhibit E1~Ub and E2~Ub thioester conjugate formation. (A) STE treatment does not affect E1~Ub thioester conjugate formation as indicated by the unchanged relative thioester band intensity between the treated and non STE-treated samples. (B) STE treatment does not affect E2~Ub thioester conjugate formation

STE does not inhibit E1~NEDD8 and E2~NEDD8 thioester conjugation

To explore the effect of STE in the NEDDylation pathway, E1~NEDD8 thioester and E2~NEDD8 thioester conjugation assays were performed. Similar to the findings in the ubiquitin pathways, there was no change in the relative thioester bond intensity on Western blot in the presence of STE both in the E1~NEDD8 and E2~NEDD8 thioester formation assays. Since STE did not affect E1 and E2 thioester formation in both the ubiquitin and NEDD8 pathways, STE inhibition was specific to the SUMOylation pathway.

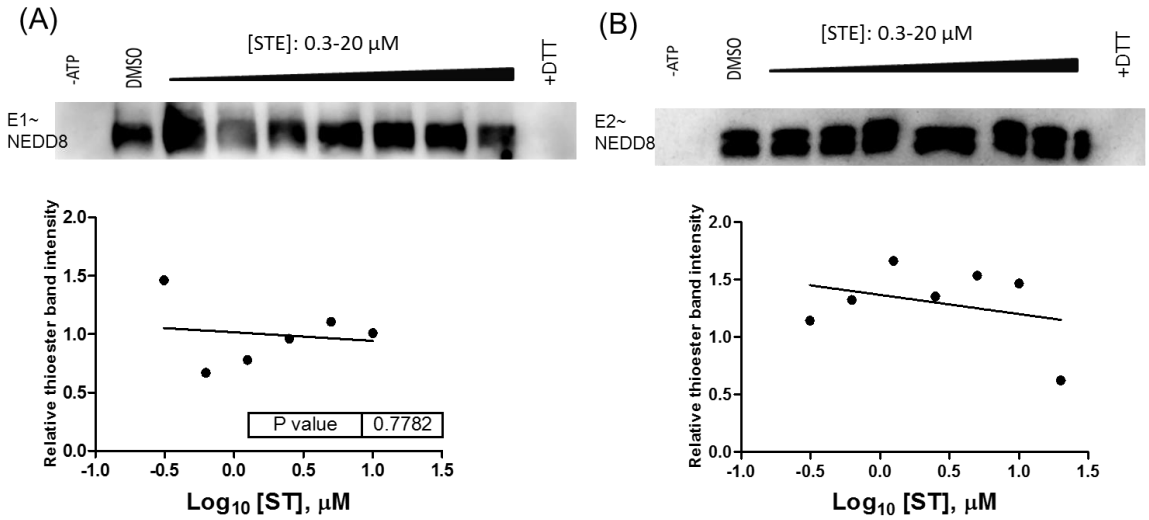

Figure 2.8 STE does not inhibit E1~NEDD8 and E2~NEDD8 thioester conjugate formation. (A) STE treatment did not affect E1~NEDD8 thioester conjugate formation as indicated by the unchanged relative thioester band intensity between the treated and non STE-treated samples. (B) STE treatment did not affect E2~NEDD8 thioester conjugate formation

2.5 Discussion

High-throughput screening is a useful tool to identify small molecule inhibitors of protein-protein interactions. We applied high-throughput screening to identify small molecule inhibitors of the SUMOylation pathway. Highly specific small molecule inhibitors could be a useful tool to study the SUMOylation pathway and may assist in the development of a novel cancer therapy.

Our design of a FRET-based high-throughput assay is unique, not only because the FRET technology is highly sensitive in detecting small changes in the reaction, but also because it provides a higher possibility of identifying hits that may work in any of the different steps of the SUMOylation pathway. Performing the high-throughput screening for inhibitors of the whole SUMOylation pathway is more efficient than screening for inhibitors of a specific step in

SUMOylation pathway. This design is also adaptable for other ubiquitin and ubiquitin-like protein pathways, as well as other signaling pathways that require multiple protein-protein interactions.

To confirm the HTS hits, we performed both whole cell SUMOylation assays and Western blot assays to confirm the inhibition of RanGAP1-SUMO1 formation *in vitro*. In the whole cell SUMOylation assay, STE turned out to be the compound with the most inhibition of SUMOylation in HEK 293 cells compared to other compounds. Thus we further investigated STE inhibition of RanGAP-SUMO formation and found that there was an apparent inhibition at a dose of 1μM. Therefore we decided to pursue STE as our lead compound.

STE inhibited the formation of E1~SUMO thioester conjugate and also E2~SUMO thioester formation in a dose dependent manner. However, further experiments indicated that the E2~SUMO thioester formation was a downstream effect of E1~SUMO thioester inhibition because STE did not affect the transfer of activated SUMO from E1 to E2. This finding is important because SAE2 inhibition switches a transcriptional subprogram of Myc from activated to repressed (29). This suggests that STE may be useful to target Myc hyperactivation through inhibition of SAE2.

There is considerable selectivity of this compound in targeting the SUMO E1 enzyme. STE did not significantly inhibit Ubiquitin E1 (Uba1) or NEDD8 E1 (APPBP1/Uba3). Additionally, STE did not significantly inhibit Ubiquitin E2 (UbcH5α) or NEDD8 E2 (Ubc12). These results also suggest that STE is not simply a thiol-reacting agent. Taken together, these findings suggest that STE is a specific inhibitor of SUMO E1 (Aos1/Uba2), with half-maximal inhibitory concentration (IC_{50}) of 1.20 μM, and that it is selective relative to the closely-related enzymes, Uba1 and APPBP1/Uba3.

A specific inhibitor of NEDD8 E1 has been discovered. MLN4924 was discovered as an inhibitor of NAE (NEDD8 Activating Enzyme) with an IC_{50} of 4.7 nM (17). This compound is structurally related to adenosine 5'-monophosphate (AMP) and binds tightly to the NAE. The

inhibition of NEDDylation at the NAE level reduces the activity of the cullin-RING subtype of ubiquitin ligases and thus inhibits the ubiquitin-proteasome system (17). This compound is currently in a phase I clinical trial for treatment of Acute Myleogenous Leukemia (AML) and solid tumors (30,31). Since there is no specific inhibitor of the SUMOylation pathway, we were interested in elucidating the STE mechanism of action.

In this study, we have uncovered the mechanism of action of STE in inhibition of the SUMOylation pathway. STE inhibited E1~SUMO thioester formation but not the transfer of SUMO from E1 to E2. Western blot assays in combination with FRET studies demonstrated that STE inhibited the SUMO E1 enzyme. Additionally, the STE inhibition of SUMO E1 was specific to the SUMOylation pathway. The details of this enzyme inhibition mechanism will be explored more fully in the next chapter.

2.6 References

1. Johnson ES. PROTEIN MODIFICATION BY SUMO. Annual Review of Biochemistry 2004;73(1):355-82.
2. Seeler J, Bischof O, Nacerddine K, Dejean A. SUMO, the Three Rs and Cancer. In: Pandolfi P, Vogt P, editors. Acute Promyelocytic Leukemia. Volume 313, Current Topics in Microbiology and Immunology: Springer Berlin Heidelberg; 2007. p 49-71.
3. Bettermann K, Benesch M, Weis S, Haybaeck J. SUMOylation in carcinogenesis. Cancer letters 2012;316(2):113-25.
4. Desterro JMP, Rodriguez MS, Kemp GD, Hay RT. Identification of the Enzyme Required for Activation of the Small Ubiquitin-like Protein SUMO-1. Journal of Biological Chemistry 1999;274(15):10618-24.
5. Lake MW, Wuebbens MM, Rajagopalan KV, Schindelin H. Mechanism of ubiquitin activation revealed by the structure of a bacterial MoeB-MoaD complex. Nature 2001;414(6861):325-9.
6. Johnson ES, Blobel G. Ubc9p Is the Conjugating Enzyme for the Ubiquitin-like Protein Smt3p. Journal of Biological Chemistry 1997;272(43):26799-802.
7. Kotaja N, Karvonen U, Janne OA, Palvimo JJ. PIAS Proteins Modulate Transcription Factors by Functioning as SUMO-1 Ligases. Molecular Cell Biology 2002;22(14):52222-34.
8. Hay RT. SUMO: a history of modification. Molecular cell 2005;18(1):1-12.
9. Yang Y, Kitagaki J, Dai RM, Tsai YC, Lorick KL, Ludwig RL, et al. Inhibitors of ubiquitin-activating enzyme (E1), a new class of potential cancer therapeutics. Cancer research 2007;67(19):9472-81.

10. Ungermannova D, Parker SJ, Nasveschuk CG, Chapnick DA, Phillips AJ, Kuchta RD, et al. Identification and mechanistic studies of a novel ubiquitin E1 inhibitor. Journal of biomolecular screening 2012;17(4):421-34.

11. Xu GW, Ali M, Wood TE, Wong D, Maclean N, Wang X, et al. The ubiquitin-activating enzyme E1 as a therapeutic target for the treatment of leukemia and multiple myeloma. Blood 2010;115(11):2251-9.

12. Ungermannova D, Parker SJ, Nasveschuk CG, Wang W, Quade B, Zhang G, et al. Largazole and Its Derivatives Selectively Inhibit Ubiquitin Activating Enzyme (E1). PLoS ONE 2012;7(1):e29208.

13. Vassilev LT, Vu BT, Graves B, Carvajal D, Podlaski F, Filipovic Z, et al. *In Vivo* Activation of the p53 Pathway by Small-Molecule Antagonists of MDM2. Science 2004;303(5659):844-48.

14. Hoe KK, Verma CS, Lane DP. Drugging the p53 pathway: understanding the route to clinical efficacy. Nature reviews Drug discovery 2014;13(3):217-36.

15. Secchiero P, Bosco R, Celeghini C, Zauli G. Recent advances in the therapeutic perspectives of Nutlin-3. Current pharmaceutical design 2011;17(6):569-77.

16. Brownell JE, Sintchak MD, Gavin JM, Liao H, Bruzzese FJ, Bump NJ, et al. Substrate-Assisted Inhibition of Ubiquitin-like Protein-Activating Enzymes: The NEDD8 E1 Inhibitor MLN4924 Forms a NEDD8-AMP Mimetic In Situ. Molecular Cell 2010;37(1):102-11.

17. Soucy TA, Smith PG, Milhollen MA, Berger AJ, Gavin JM, Adhikari S, et al. An inhibitor of NEDD8-activating enzyme as a new approach to treat cancer. Nature 2009;458(7239):732-6.

18. Zhao Y, Morgan MA, Sun Y. Targeting Neddylation Pathways to Inactivate Cullin-RING Ligases for Anticancer Therapy. Antioxidants & Redox Signaling 2014.

19. Inglese J, Johnson RL, Simeonov A, Xia M, Zheng W, Austin CP, et al. High-throughput screening assays for the identification of chemical probes. Nat Chem Biol 2007;3(8):466-79.

20. Clegg RM. Fluorescence resonance energy transfer. Current Opinion in Biotechnology 1995;6(1):103-10.

21. Nguyen AW, Daugherty PS. Evolutionary optimization of fluorescent proteins for intracellular FRET. Nature biotechnology 2005;23(3):355-60.

22. Song Y, Rodgers VGJ, Schultz JS, Liao J. Protein interaction affinity determination by quantitative FRET technology. Biotechnology and Bioengineering 2012;109(11):2875-83.

23. Liu Y, Song Y, Madahar V, Liao J. Quantitative Förster resonance energy transfer analysis for kinetic determinations of SUMO-specific protease. Analytical biochemistry 2012;422(1):14-21.

24. Jiang L, Liu Y, Song Y, Saavedra A, Pan S, Xiang W, et al. Internal Calibration Förster Resonance Energy Transfer Assay: A Real-Time Approach for Determining Protease Kinetics. Sensors 2013;13(4):4553-70.

25. Song Y, Liao J. An *in vitro* Forster resonance energy transfer-based high-throughput screening assay for inhibitors of protein-protein interactions in SUMOylation pathway. Assay and drug development technologies 2012;10(4):336-43.

26. Malik-Chaudhry HK, Saavedra A, Liao J. A linker strategy for trans-FRET assay to determine activation intermediate of NEDDylation cascade. Biotechnol Bioeng 2014.

27. Alontaga AY, Bobkova E, Chen Y. Biochemical Analysis of Protein SUMOylation. Current Protocols in Molecular Biology: John Wiley & Sons, Inc.; 2001.

28. Schneider CA, Rasband WS, Eliceiri KW. NIH Image to ImageJ: 25 years of image analysis. Nature methods 2012;9(7):671-5.

29. Kessler JD, Kahle KT, Sun T, Meerbrey KL, Schlabach MR, Schmitt EM, et al. A SUMOylation-Dependent Transcriptional Subprogram Is Required for Myc-Driven Tumorigenesis. Science 2011;335(6066):348-53.

30. ClinicalTrials.gov. Study of MLN4924 Plus Azacitidine in Treatment-Naïve Patients With Acute Myelogenous Leukemia (AML) Who Are 60 Years or Older. March 18, 2013 ed. Bethesda: National Library of Medicine; 2014.

31. ClinicalTrials.gov. Dose Escalation, Multi-arm Study of MLN4924 Plus Docetaxel, Gemcitabine, or Combination of Carboplatin and Paclitaxel in Patients With Solid Tumors. May 15, 2013 ed. Bethesda: National Library of Medicine 2013.

CHAPTER 3. QUANTITATIVE FRET TECHNOLOGY APPLICATION TO MEASURE KINETICS OF SUMO E1 ENZYME AND TO DETERMINE THE INHIBITION CONSTANT OF STE

3.1 Abstract

SUMOylation has important roles in many key physiological and pathological processes. The SUMOylation cascade involves a heterodimer of the E1 activating enzyme (Aos1/Uba2), the E2 conjugating enzyme (Ubc9), and many E3 ligase enzymes. Previous studies reported the K_m of E1 enzymes in ubiquitin and other ubiquitin-like pathways. However, the K_{ms} of the SUMO paralogs (SUMO2 and SUMO3) are unknown. Here, we used quantitative FRET to measure the SUMO E1 enzyme kinetics of SUMO1, -2, and -3, and ATP under steady state conditions. We found that the enzyme kinetics assay using the quantitative FRET methods produces comparable results to those obtained with conventional radioactive assays. Thus, the K_m, of SUMO2 (3.42 ± 0.91 μM) and SUMO3 (2.76 ± 0.75 μM) are about four to five times higher than the K_m of SUMO1 (0.75 ± 0.11 μM). Previous studies have found that STE inhibits the E1 enzyme, but not the SUMO transfer from E1 to E2. To further characterize the mechanism of action of STE as an inhibitor of the SUMOylation pathway, we investigated the inhibition modalities of this compound. To elucidate this mechanism of inhibition, we employed quantitative FRET technology to measure the Inhibition constant and compared the results with computational docking analysis of STE on the E1 enzyme. The results show that STE acts as a non-competitive inhibitor of the E1 enzyme. We then calculated the inhibition constant of STE and found the K_i of STE on SUMO E1 to be 1.90 μM, which is similar to the number we obtained from docking analysis. These results pinpoint the mechanism of inhibition and the inhibition constant of the SUMO E1 enzyme by STE.

3.2 Introduction

Small ubiquitin-like modifiers (SUMO) have important roles in many physiological processes, including protein stability, DNA repair, chromatic structure regulation, protein translocation, and protein-protein interactions (1-3). On the other hand, SUMO proteins are also involved in many pathological conditions, such as familial dilated cardiomyopathy, diabetes, and carcinogenesis (4,5). There are three SUMO paralogs in humans: SUMO1, SUMO2, and SUMO3. SUMO1 only shares 50% identity with SUMO2 and SUMO3, while SUMO2 and SUMO3 are 97% similar (1). In COS-7 cells, SUMO2 and 3 are more abundant than SUMO1 and are found in a large pool of non-conjugated forms (6). Additionally, unlike SUMO1, SUMO2 and SUMO3 form polymeric chains (7). Similar to ubiquitination and other ubiquitin-like proteins, SUMOylation processes involve an enzymatic cascade that includes E1 activating enzyme, E2 conjugating enzyme, and E3 ligase (8). The mechanism of SUMO activation enzyme is:

$$\mathrm{Aos1/Uba2_{SH} + ATP + SUMO} \overset{Mg^{2+}}{\rightleftharpoons} \mathrm{Aos1/Uba2^{\cdot AMP\text{-}SUMO}_{SH} + PP_i} \quad (1)$$

$$\mathrm{Aos1/Uba2^{\cdot AMP\text{-}SUMO}_{SH}} \rightleftharpoons \mathrm{Aos1/Uba2_{S\text{-}SUMO} + AMP} \quad (2)$$

$$\mathrm{Aos1/Uba2_{S\text{-}SUMO} + ATP + SUMO} \overset{Mg^{2+}}{\rightleftharpoons} \mathrm{Aos1/Uba2^{\cdot AMP\text{-}SUMO}_{S\text{-}SUMO} + PP_i} \quad (3)$$

$$\mathrm{Aos1/Uba2^{\cdot AMP\text{-}SUMO}_{S\text{-}SUMO} + Ubc9_{SH}} \rightleftharpoons \mathrm{Aos1/Uba2^{\cdot AMP\text{-}SUMO}_{SH} + Ubc9_{S\text{-}SUMO}} \quad (4)$$

Figure 1.1 SUMOylation activation and conjugation scheme. SUMOylation activation and conjugation scheme with non-covalent complexes indicated with a dot and covalent conjugation indicated with a hyphen. S-SUMO refers to the thioester bond between the catalytic cysteine and the SUMO C-terminus.

The E1 activating enzyme, a heterodimer of Aos1 and Uba2 (or SUMO Activating Enzyme, SAE1 and SAE2), plays an important role in initiating the cascade by using ATP to form a high-energy

thioester bond similar to the ubiquitin activation by E1 (9). SUMOylation is initiated by an E1 enzyme that catalyzes SUMO adenylation, forms a E1-SUMO thioester bond with a catalytic cysteine in the E1 Cys domain, and transfers thioester to a catalytic cysteine in the E2 conjugating enzyme (10). Human Aos1 (SAE1) is homologous to the N-terminus of ubiquitin E1 (Uba1), and Uba2 (SAE2) is homologous to the C-terminus of ubiquitin E1 (Uba1). Figure 3.8 D shows that Uba2 consists of multiple domains, namely an adenylation domain that binds ATP, Mg, and SUMO; a C-terminal ubiquitin-like domain that recruits Ubc9 for thioester transfer; and a catalytic Cys domain that contains the active site cysteine (11). E1 activity is controlled by post-translational modification. SUMO modifies its E1 at the E1 Cys domain and inhibits this domain activity. AutoSUMOylation of E1 at the Lys 236 residue did not affect SUMO adenylation or formation of the E1~SUMO thioester, but did inhibit the transfer of SUMO from E1 to E2 (12). In the last step (4), activated SUMO is transferred to the E2 (Ubc9) conjugating enzyme (11,13,14). To translocate activated SUMO from E1 to E2, E1 first must undergo significant conformational changes to bring E1 and E2 into close proximity (15). From E2, SUMO is then transferred to a substrate protein that is recruited by E3 ligases such as the PIAS proteins, Pc2, and RanBP2 (16-18).

The application of Förster (Fluoresence) resonance energy transfer technology (FRET) takes advantage of non-radioactive energy transfer by means of intermolecular long-range dipole-dipole coupling. The FRET signal is produced by an excited molecular chromophore (donor) that excites another chromophore (acceptor) over distances ranging from ~10Å to 100Å (19). FRET has several advantages for studying enzyme-catalyzed reactions. FRET assays can capture reaction progress continuously and can be performed in a multi-well plate format that can be both economical and time-saving. The protein pair CyPet and YPet, derivatives of cyan fluorescence protein (CFP) and yellow fluorescent protein (YFP) respectively, exhibit 20-fold stronger FRET

signals than the unmodified CFP-YFP pair (20). CyPet acts as a donor and YPet acts as an acceptor. Thus, FRET can be used to determine protein interaction affinity (21), kinetics of protease enzymes (22-24), and automated inhibitor screening for SUMOylation pathway inhibitors (25).

Enzymes can be characterized kinetically by their k_{cat}, K_m, and k_{cat}/K_m ratio to determine their effectiveness (26). In addition, enzyme kinetics are beneficial in determining and characterizing the binding modality of the inhibitor (27). Conventional methods for measuring the kinetics of E1 in ubiquitination and ubiquitination-like protein pathways involve radioisotopic or fluorescent measurements. Radioisotopic measurements for the adenylation step were performed as ATP:PPi exchange assays, and the [^{32}P]ATP concentrations were measured with activated charcoal powder (28,29) or paper (30). Alternatively, the adenylation process could be followed in a ubiquitin [^{3}H] adenylate assay (29). Oregon green (Og) label can also be used in a steady-state kinetic analysis of human ubiquitin E1 (31). In the present study, we applied a quantitative FRET assay using a CyPet-YPet pair of fluorescently-tagged proteins to determine the SUMO1 and ATP affinity for the E1 activating enzyme in the SUMOylation activation step. From these studies, we concluded that the K_m of SUMO1 and are similar to the values determined by conventional assays.

In the previous chapter, we reported the high-throughput screening discovery of STE, a small molecule inhibitor of SUMO E1. STE inhibits both E1~ and E2~SUMO thioester bond formation. However, the E2~SUMO thioester inhibition is a downstream effect of the E1~SUMO inhibition because STE does not affect the transfer of SUMO from E1 to E2. In addition, STE selectively inhibits SUMO E1 activity as compared to the closely-related ubiquitin-activating enzyme (Uba1) and NEDD8-activating enzyme (NAE) in purified enzyme assays. To further characterize the STE mechanism of action as an inhibitor of the SUMO E1 enzyme, we employed

quantitative FRET-based E1 enzyme kinetic assays. We found that STE is a non-competitive inhibitor of the SUMO E1 enzyme with an inhibition constant of 1.9 μM.

3.3 Materials and Methods

DNA Constructs, Protein Expression and Purification

Expression constructs for Pet28 (b)-CyPet-SUMO1, Pet28(b)-CyPet-SUMO2, Pet28(b)-CyPet-SUMO3, Pet28(b)-YPetUbc9, Pet28(b)-Aos1, and Pet28(b)-Uba2 have been described (21,25). Plasmid constructs were confirmed by DNA sequencing. Expression and purification of proteins were performed as described (21,23,32). The purified proteins were assessed for purity by SDS-PAGE and Coomassie blue staining. Protein concentrations were determined by the Bradford assay, with bovine serum albumin as the standard. Additionally, protein concentrations were adjusted for the level of impurities by quantifying the ratio of the desired protein to impurities, based on band intensities on stained gels.

Gel Electrophoresis and General Western Blotting

To show formation of CyPetSUMO1~YPetUbc9 ('~' indicates a thioester adduct), 0.5 nM E1 (Aos1/Uba2), 4 μM CyPet SUMO, and 2 μM YPet Ubc9 were mixed in SUMOylation buffer (50 nM Tris-HCl, pH7.5, 5 mM $MgCl_2$) in reaction volumes of 300 μl. Reactions were started by adding ATP to a final concentration of 2 mM. Aliquots of 30 μl were taken out at 30, 60, 90, 180, 300, and 2400 seconds, and reactions were stopped by adding 5 μl of 6x SDS loading buffer with 8 M urea. Another aliquot was taken out after 300 s and added to 6x SDS loading buffer (lane labeled as 300*) that contained 0.1 M dithiothreitol (DTT) as a reducing agent to hydrolyze the thioester conjugate and was heated at 90^{o}C for 10 min.

Protein separation was accomplished by electrophoresis in 10% PAGE-SDS minigels for 2 h at 100 V. After electrophoresis, protein was transferred to a nitrocellulose membrane in transfer

buffer containing 0.25 mM Tris, 192 mM glycine, and 20% methanol (pH 8.3). Nitrocellulose membranes were blocked with 5% non-fat milk in wash buffer (150 mM NaCl, 20 mM Tris-HCl, pH 7.4, and 0.05% Tween 20) for 2 h and then incubated with rabbit anti-SUMO1 (1:1000), mouse anti-His Tag (1:1000) (Sigma Aldrich, St. Louis, MO) in wash buffer containing 3% non-fat milk overnight. The membranes were rinsed three times with wash buffer and then incubated with secondary horseradish peroxidase–conjugated goat anti-rabbit IgG and goat anti-mouse IgG (Sigma Aldrich) in wash buffer containing 3% non-fat milk for 2 h. Membranes were rinsed three times with wash buffer and developed with the enhanced-chemiluminescence system. Images were taken using UVP Biospectrum A/C Imaging System and processed using Image J software (33).

In Vitro Kinetic FRET Assay of CyPetSUMO1-YPet Ubc9 Interaction

Multi-well plates were used to measure fluorescence intensity FlexstationII384 fluorimeter (bottom excitation and collection) in Greiner black, clear-bottom 384-well plates. SoftmaxPro was used to write individual programs to perform each task required to run an assay on FlexstationII[384]. Two excitation (Ex) wavelengths were used: 414 nm to excite CyPet and 475 nm to excite YPet. When excited at 414 nm, the CyPet emission peak is 475 nm. On the other hand, when excited at 475 nm, the YPet emission (Em) peak is 530 nm. When FRET is detected, there is an increase of 530 nm emission of the CyPetSUMO1-YPetUbc9 interaction when excited at 414 nm. To examine the baseline and FRET signals, data were collected for each sample at Ex 414/Em 475, Ex 414/Em530, and Ex 475/Em 530.

For the steady-state kinetic experiment, preliminary assays determined the appropriate E1 concentration range in which the rate of CyPetSUMO1~YpetUbc9 conjugation was linearly dependent on the E1 concentration. In addition, the optimal assay duration determined the initial rates of the product formation. To determine initial rates of CyPetSUMO1 activation by E1, 10 nM

E1, 2 μM YPet Ubc9 was mixed in SUMOylation buffer(50 mM Tris-HCl, pH 7.5, 5 mM $MgCl_2$), and serial concentrations of CyPetSUMO1 proteins 0.2, 0.3, 0.4, 0.5, 0.7, 0.9, 1.3, 1.7, 2.2, 3, 4 μM (0.75 dilution factor) in 60-μl reaction volumes. The reactions were started by adding ATP to a final concentration of 2 mM. The same protocol was used to measure the K_m of CyPetSUMO2 and CyPetSUMO3.

To measure the kinetics of ATP as E1 substrate, 10 nM E1, 2 μM CyPetSUMO1, and 2 μM YPet Ubc9 were mixed in SUMOylation buffer (50 mM Tris-HCl, pH 7.5, 5 mM $MgCl_2$ in 60-μl reaction volumes. The reactions were started by adding a serial dilution of ATP to 0.8, 1.15, 1.64, 2.35, 3.36, 4.8, 6.8, 9.8, and 14 μM final concentrations. The initial velocity measurement was performed after addition of ATP by following the changes in 530 nm emission when excited at 414 nm in the first 5 min. The fluorescence intensity was followed for up to 2 h to monitor to determine reaction completion.

Data Processing and K_m Determination

The progression of CyPetSUMO1~YPetUbc9 formed in each reaction was detected by following the changes in 530 nm emission signal when excited at 414 nm. After subtracting the plate background signal, one phase association curves of nonlinear regression of time versus relative fluorescence unit was performed to determine the background signal (Y_0), plateau, and span using GraphPad Prism 5 (GraphPad Software). The Y_0 is the Y value when x (time) is zero. The initial velocity of CyPetSUMO1-YPetUbc9 production was calculated by calculating the change in RFU divided by span times the initial substrate concentration.

For Michaelis-Menten plots, the initial velocity of CyPetSUMO-YPetUbc9 formed per second was plotted against the concentration of CyPetSUMO1, -2, or -3, and the K_m and V_{max} values were extracted from nonlinear least-squares fit of the data (27) with GraphPad Prism 5 software.

Mechanism of STE Inhibition of the SUMO E1 enzyme

The quantitative FRET assays were employed to determine the mechanism of STE inhibition of the SUMO E1 enzyme. The assays were performed according to the "*In Vitro* Kinetic FRET Assay of CyPetSUMO1-YPet Ubc9 Interaction" and "Data Processing and K_m Determination" protocols as described above in the presence of DMSO as a control or various concentrations of STE (0.83, 3.33, 6.67, and 13.33μM). The span determined from the DMSO reactions were used as the reference points for the initial velocity calculations.

In silico (docking) Analysis

The three-dimensional structures of the SAE1/SAE2-SUMO1-Mg.ATP were obtained from RCSB Protein Data Bank 1Y8R(13). In-silico docking was performed by using AutoDock (34) (http://autodock.scripps.edu). The three-dimensional structures of these complexes were displayed using VMD (35). The STE binding position that produced the lowest predicted binding free energy was selected and analyzed.

3.4 Results

Development of a Quantitative FRET Assay to Measure E1 Enzyme Kinetics

The measurement of E1 enzyme kinetics is based on pseudo-first order association kinetics of the interaction between an enzyme and its substrate. Similar to ubiquitin E1, the E1 activating enzyme in the SUMOylation pathway has three substrates: ATP, SUMO, and Ubc9. To design the E1 enzyme kinetic experiments with CyPetSUMO1 as the substrate of interest, we used various concentrations of CyPetSUMO1 and maintained constant high concentrations of the other substrates, ATP and YPet Ubc9. To follow the reaction, we used FRET by exciting the donor protein, CyPet, and observing the resonance energy transfer as the fluorescence emission of the acceptor protein, YPet.

As is shown in Figure 3.1, the principle of kinetic measurement is based on an increase in the absolute FRET signal that corresponds to product formation over time. The absolute FRET signal is determined by measuring the fluorescence emission intensity at 530 nm, which is the peak emission of the YPet protein. Both ATP and SUMO are SUMO E1 substrates (Figure 3.1A). When SUMO is used as the substrate, the first step is the formation of E1~SUMO, an enzyme substrate intermediate, followed by CyPetSUMO~YPetUbc9 as the product. During each time interval, a certain fraction of SUMO1 forms a thioester bond with Ubc9 as a result of SUMO activation by the E1 enzyme. As time advances, more CyPetSUMO1~YPetUbc9 product is formed, and by following the changes of Em 530/Ex 414 of the reaction, we can monitor the reaction progress by plotting the RFU against time (Figure 3.1B).

(A)

$$E + S \leftrightarrow ES \rightarrow E + P$$

$$\text{E1 + ATP+ SUMO} \xrightarrow{Mg^{2+}} \text{E1~SUMO} \rightarrow \text{SUMO~Ubc9}$$

(B)

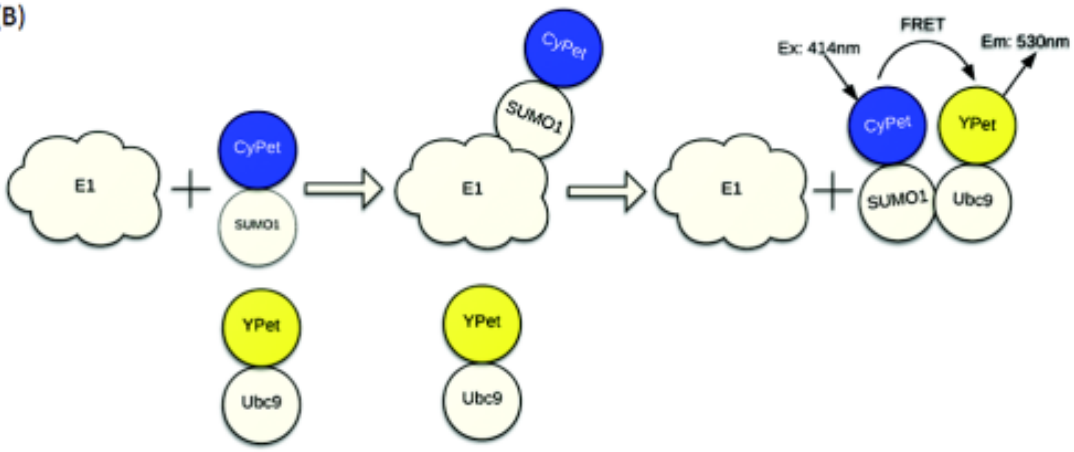

Figure 3.1 A quantitative FRET assay to measure kinetics of the E1 enzyme in the SUMOylation pathway. (A) Reaction scheme of the initial velocity measurement. Either ATP or SUMO can be used as the E1 substrate. When SUMO is the substrate, the first step is the formation of E1~SUMO, an enzyme substrate intermediate, which then forms SUMO~Ubc9 as a product. (B) The kinetic measurement is based on changes in the FRET signal by measuring the fluorescence emission intensity at 530 nm. The peak emission of the YPet protein is 550 nm, at excitation of 414 nm, which is the optimum excitation wavelength of CyPet over a period of time.

E1 Catalyzed the Formation of CyPetSUMO1~YPetUbc9

To confirm that the CyPetSUMO1 can be conjugated by the YPetUbc9, we performed western blot assays and FRET assays. CyPetSUMO1 was used as a substrate by the Aos1/Uba2 E1 enzyme. The E1 catalyzed transfer of CyPetSUMO1 to the E2 protein, YPetUbc9 and was followed

by western blot of nonreducing SDS-PAGE. When E1 was incubated with ATP, YPetUbc9, and CyPetSUMO1, formation of the CyPetSUMO1~YPetUbc9 increased with time over a 40-min period, as detected by western blot (Figure 3.2A). The thioester bond was confirmed by the disappearance of the product upon treatment with reducing agents such as dithioethreitol (Figure 3.2A lane 300*).

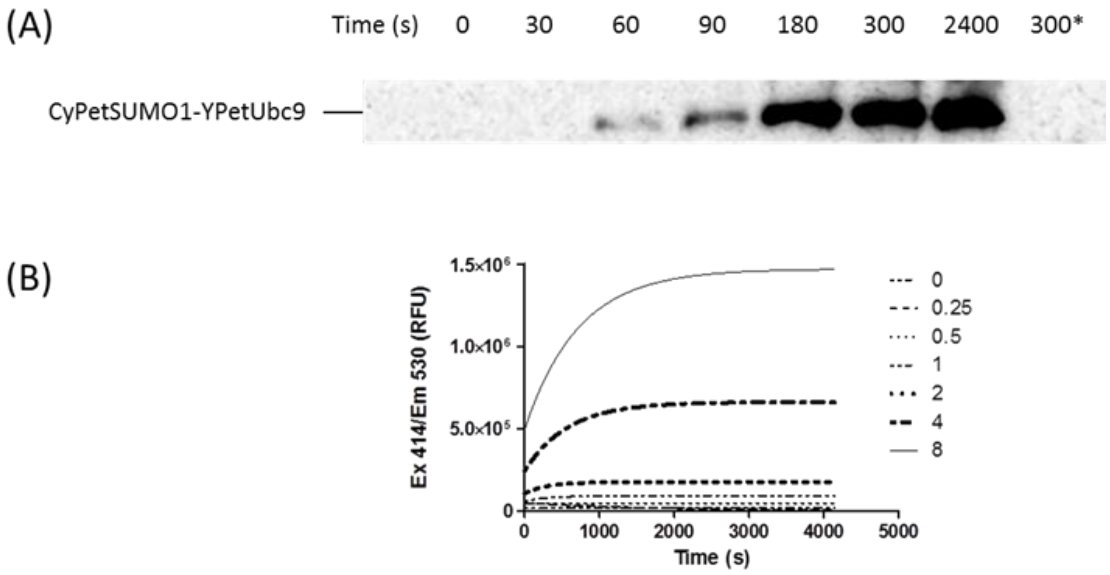

Figure 3.2 Reaction of E1 with CyPetSUMO1 to form CyPetSUMO1-YpetUbc9. Shown is the *in vitro* conjugation of CyPet-SUMO1 to YPetUbc9 in the presence of the E1 enzyme to assess the kinetics of E1 enzymes. (A) *In vitro* conjugation assay to show formation of the CyPetSUMO1~YPetUbc9 thioester. The assay mixture contained 0.5 nM E1, 4 µM CyPetSUMO1, and 2 µM YpetUbc9 in SUMOylation buffer (50 mM Tris, pH 7.5, 5 mM MgCl2). Reaction was started by adding 2 mM ATP and then incubated at 25°C for the indicated time. Aliquots were taken and mixed with a non-reducing gel-loading buffer. Another aliquot of identical volume was taken after 300s of reaction and mixed with the DTT-containing gel-loading buffer (lane labeled as 300*) to hydrolyze the thioester bond. Shown in this figure is a western blot using an anti-SUMO1 antibody. (B) The time course of enzymatic reactions before Y_0 subtraction. The Y_0 is the Y value when x (time) is zero.

With the FRET assay, formation of CyPetSUMO1~YPetUbc9 was evident by the increase in the Em530/Ex414 signal over time. Figure 3.2B shows the relative fluorescence units (RFU) vs. time graph of various CyPetSUMO1 substrate concentrations. Before ATP (time <0) was added, a non-covalent protein-protein interaction between SUMO1 and Ubc9 was observed. The reaction was started by adding ATP, and more CyPetSUMO1~YPetUbc9 product was formed as time progressed until a plateau was reached, as indicated in Figure 3.2B.

Initial Velocity Determination of Aos1/Uba2 with SUMO1 and ATP as Substrates

To determine the K_m of each of these substrates, we performed pseudo-first-order kinetic reactions by using an excess of the other two substrates. The steady state phase required a great excess of the substrate relative to the free enzyme concentration (27). E1 kinetics were measured by determining the initial velocity of CyPetSUMO1~YPetUbc9 formation as a function of each substrate concentration.

Product increases exponentially from t=0, according to the model:

$$[P] = [S]_0 \left(1 - e^{-kt}\right) \quad (1)$$

Accordingly, the pseudo-first order association kinetics from the experiments can be plotted in GraphPad Prism5 software as a one-phase association, according to the equation:

$$Y = Y_0 + (plateau - Y0) * (1 - e^{-k*x}) \quad (2)$$

Y is the relative fluorescence intensity at 530 nm when excited at 414 nm (Em 530/Ex 414 nm signal), plateau is the maximum fluorescence intensity, and x is the time. The Y_0 is the Y value when x (time) is zero. Span is the difference between Y and Y_0. To measure the initial velocity of the SUMO E1-catalyzed reaction, we followed the increase in Em 530/Ex 414 nm signal, which correlates with product formation over time (Figure 3.3A). To observe the linearity of the initial

velocity, the reaction was started by adding ATP and the fluorescence intensity (I, RFU) was measured every 10 seconds. To ensure that the measurements were valid, the initial velocity was calculated when the substrate depletion was between 0 and 10% of the total initial substrate concentration. This can be solved by looking for a time when the fluorescence intensity is less than the total of Y_0 and 10% of the RFU span. The initial velocity is then calculated as:

$$v_0 = \frac{\Delta P}{\Delta t} = \frac{\Delta I}{\Delta t} = slope \times \frac{[S]_0}{span} \quad (3)$$

As depicted in in Figure 3.2b of the CyPetSUMO1~YPetUbc9 reaction progress curves, the initial velocity can be determined from the slope of the linear plot of CyPetSUMO1~YPetUbc9 product concentration versus time. After the initial velocity of each substrate concentration was calculated, the results were plotted by a nonlinear least-squares best fit against the substrate concentrations according to Michaelis-Menten equation to derive K_m and V_{max}.

Further FRET analysis revealed linear initial velocities over a range of E1 concentrations, from 150 pM to 10 nM (Figure 3.3C). This indicates that the velocity of product formation depends linearly on the E1 concentration, as expected for a well-behaved, enzyme-catalyzed reaction. The rest of the experimental data were obtained at a fixed E1 concentration of 500 pM. The YPet Ubc9 concentration was set at 2 μM because previous studies indicated that higher E2 concentrations inhibited E1 activity (36).

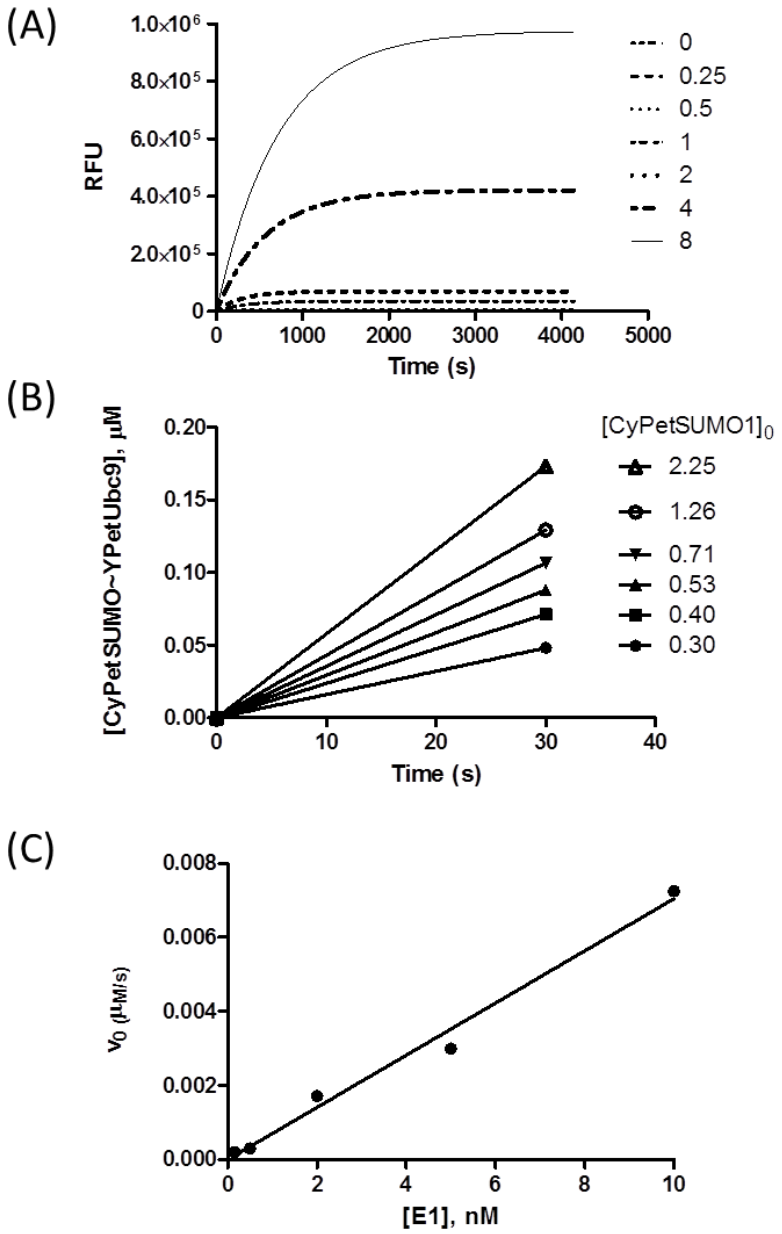

Figure 3.3 Initial velocity determination. (A) The time course of enzymatic reactions after Y0 subtraction. (B) Reaction progress curves for the production of CyPetSUMO1-YPetUbc9 product. The initial velocity can be determined from the slope of the linear plot of CyPetSUMO1-YPetUbc9 product versus time(s). (C) Initial velocity as a function of E1 concentration in E1-catalyzed CyPetSUMO1~YPetUbc9 formation by FRET detection as described in Equation 3.

Kinetic Data for SUMO1, -2, and -3 and ATP

Since K_m varies considerably for a particular enzyme with different substrates, we used the FRET technology to measure K_m for the SUMO E1 enzyme substrates: SUMO1, -2, and -3, and ATP. We measured the velocity of CyPetSUMO1~YPetUBc9 formation as a function of CyPetSUMO1 concentration, while fixing the YPet Ubc9 and ATP concentrations at saturating levels. Titration of E1 with CyPetSUMO1 yielded simple Michaelis-Menten-type kinetics (Figure 3.4A). The CyPetSUMO1 concentration dependence for E1-catalyzed CyPetSUMO1~YPetUbc9 formation was hyperbolic and yielded K_m values 0.75 ± 0.11 μM, indicating high-affinity binding to the Aos1/Uba2 E1 enzyme. Similar strategies were used to measure the K_m for SUMO2 and SUMO3. Using the FRET assay, we found that the K_m was **3.42** ± 0.91 μM for SUMO2 (Figure 3.4B) and 2.76 ± 0.75 μM for SUMO3 (Figure 3.4C).

To measure the K_m for ATP, we measured the velocity of CyPetSUMO1~YPetUbc9 formation as a function of ATP concentration while fixing the saturated CyPetSUMO1 and YPet Ubc9 concentrations. The reaction velocity was also modulated by the ATP concentrations in a hyperbolic fashion as expected from the Michaelis-Menten equation. The K_m for ATP was 7.40 ± 1.77μM (Figure 3.5).

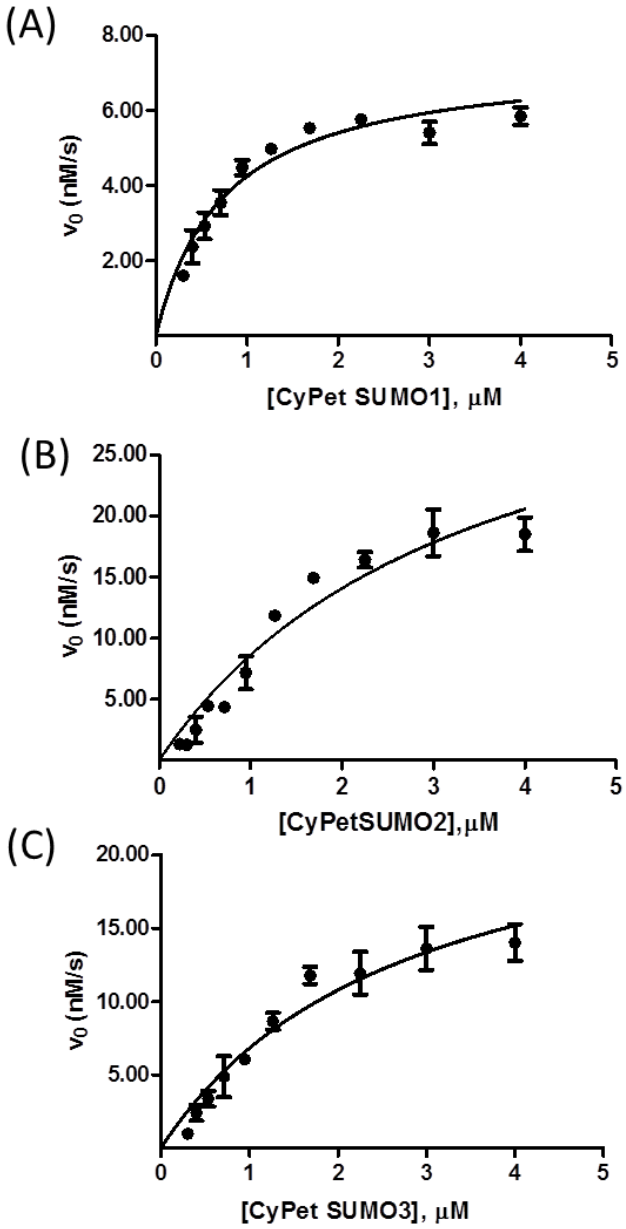

Figure 3.4 Steady-state kinetics of E1-catalyzed CyPetSUMO1-YPetUbc9 formation as a function of CyPetSUMO concentration. Michaelis-Menten Plot of the E1-catalyzed CyPetSUMO1-YPetUbc9 formation based on FRET detection at various (A) CyPetSUMO1, (B) CyPetSUMO2, and (C) CyPetSUMO3 concentrations to examine the kinetics of SUMO E1 enzyme. The solid line through the data points represents the nonlinear least-squares best fit.

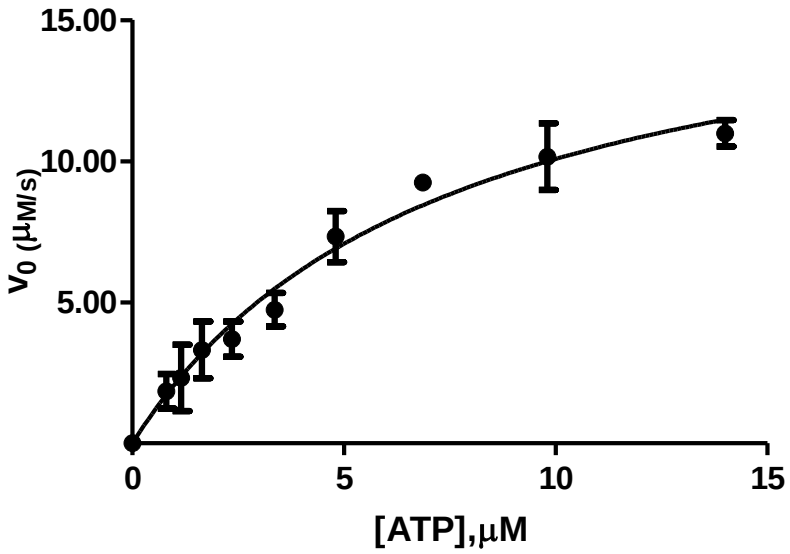

Figure 3.5 Steady-state kinetics of E1-catalyzed CyPetSUMO1-YPetUbc9 formation as a function of ATP concentration. Each reaction contains 0.5 nM E1 enzymes, 2 μM CyPetSUMO1, 2 μM of Ypet Ubc9, and different starting concentrations of substrates (ATP). Michaelis-Menten plot of the reaction velocities as a function of [ATP] at 0.5 nM E1 enzyme. The solid line through the data points represents the nonlinear least-squares best fit.

The catalytic efficiency of an enzyme is defined as the ratio of its kinetic constants k_{cat}/K_m. k_{cat} is known as the turnover number for an enzyme and is calculated by dividing the experimentally determined value of V_{max} by enzyme concentration. To determine the catalytic efficiency of the SUMO E1, we used the K_m and V_{max} data above to calculate the kinetic constants k_{cat}/K_m (Table 1).

Table 1. Kinetic constants for SUMO E1

	K_m (μM)	K_{cat} (s^{-1})	K_{cat}/K_m ($M^{-1}s^{-1}$)
CyPet-SUMO1	0.75 ± 0.11	14.85 ± 0.80	1.99×10^7
CyPet-SUMO2	3.42 ± 0.91	76.23 ± 12.19	2.23×10^7
CyPet-SUMO3	2.76 ± 0.75	51.35 ± 7.85	1.86×10^7
ATP	7.40 ± 1.77	35.09 ± 4.30	4.70×10^6

Determination of the Type of STE Inhibition and STE Inhibition Constant

In an enzymatic reaction, a small compound can act as a competitive, non-competitive, or uncompetitive inhibitor. The type of inhibition can be determined by a careful kinetics study, which then can be confirmed with a more definitive study such as crystallography. STE has been found to inhibit E1~SUMO thioester formation, which suggests that STE binds to E1. To test the type of STE inhibition, we used quantitative FRET technology to look for the apparent K_m and v_{max} in the presence of various doses of STE. Previous data have suggested that the IC_{50} of the STE is about 1.60 μM. Thus, in performing the kinetics analysis, we used STE concentrations of 0.8 μM to 13.33 μM.

In the presence of STE, the apparent K_m does not change as compared to the control DMSO. However, the apparent V_{max} values for the reaction were lower as the concentration of STE increased (Figure 3.6). Taken together, these data indicate that STE is a non-competitive inhibitor of the SUMO E1 enzyme (27).

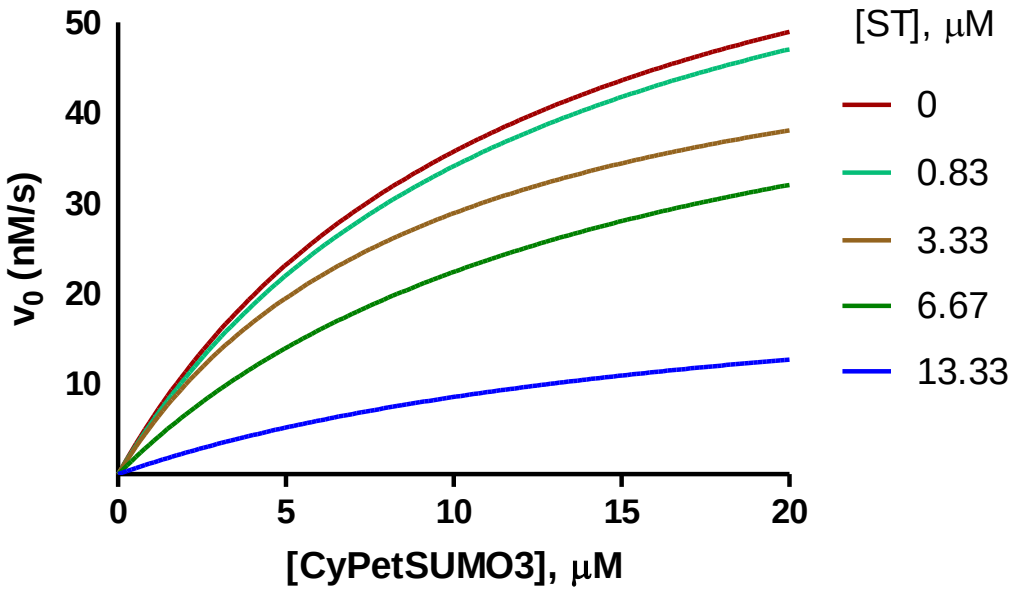

Figure 3.6 Untransformed plots for the effects of STE inhibitor on the velocity of CyPetSUMO3~YPetUbc9 reaction catalyzed by SUMO E1 enzyme. The apparent effect of STE is to decrease the value of v_{max} without affecting the apparent km for the substrate.

Calculation of the inhibition constant (Ki) was performed by constructing two secondary plots. The Dixon plot graphs $1/v_{max}$ at saturating substrate concentration as a function of inhibitor concentrations to extract the value of $-\alpha K_i$ (37). From the Dixon plot (Figure 3.7A), the $-\alpha$Ki value was calculated to be 4.4. In the second plot (Figure 3.7B), the slopes of the double reciprocal lines from the Lineweaver-Burk plot were plotted as a function of inhibitor concentrations to determine the $-K_i$, which is equal to the x intercept (27). From the second graph, the calculated inhibition constant was found to be 1.90 μM. The alpha value of 2.32 indicated that STE acts as a non-competitive inhibitor.

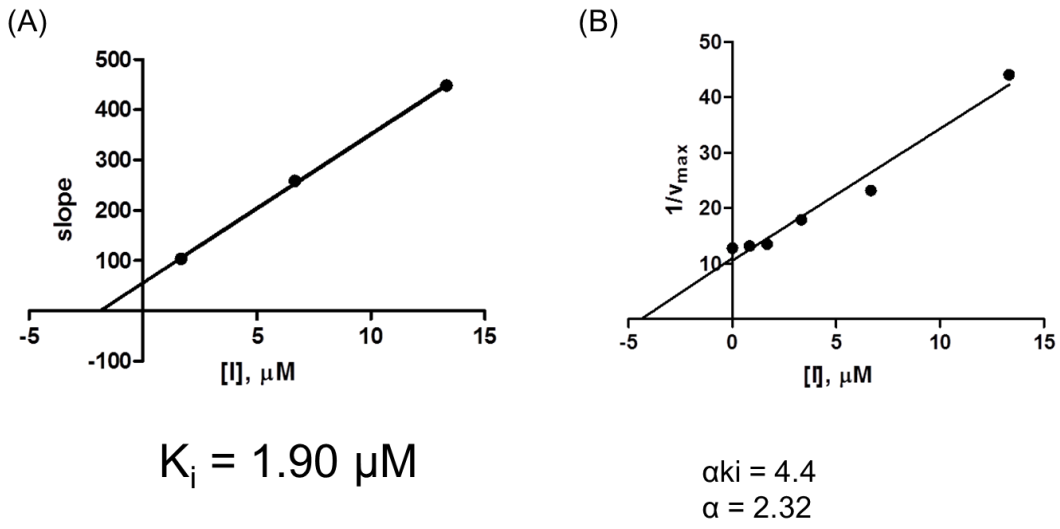

Figure 3. 7 Graphic Determination of Inhibition Constant. (A) Dixon plot ($1/v_{max}$ as a function of [I] for a non-competitive inhibitor and the value of $-\alpha K_i$ is determined from the x intercept of the line. (B)The value of $-K_i$ is determined from the x intercept of a plot of the slope of the lines from the double reciprocal (Lineweaver-Burk) plot as a function of [I]

Docking analysis

Since the crystal structure of the SUMO E1 enzyme is known, computational tools were used to visualize the possible location of the STE binding site. Using AutoDock software and SUMO E1 structure from pdb (1Y8R), we looked for the lowest binding energy of the STE binding. The lowest binding energy was found to be -7.69 kcal/mol, with the calculated inhibition constant of 2.30 μM. This value has a very good correlation with the K_i=1.90 μM obtained from the *in vitro* enzyme kinetics assays.

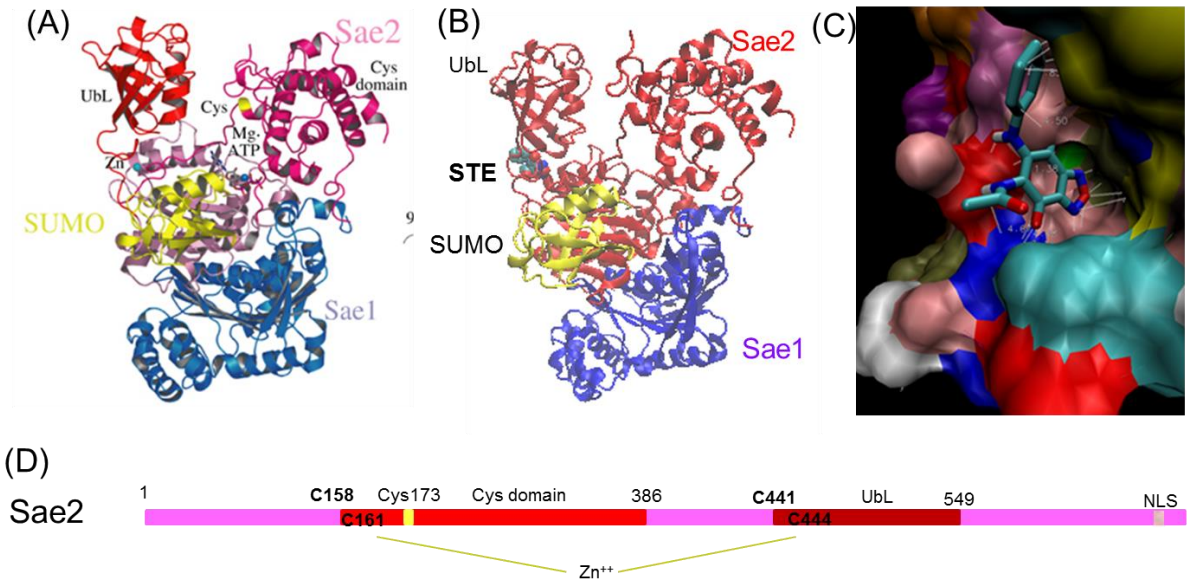

Figure 3.8 STE Docking Simulation. (A) The three-dimensional structure of the SAE1/SAE2-SUMO1-Mg.ATP (PDB: 1Y8R) (B) STE binding position that produces the lowest predicted binding free energy (-7.69 kcal/mol) with the calculated inhibition constant of 2.3μM. The same view and color scheme has been used to highlight the protein chains as in (A). (C) Surface views of the STE-Uba2 interaction with the protein depicted as surface colored by its amino acid chain. (D) Schematic representation of SAE2 (Uba2) colored as in (A).

To understand the interaction between STE and Uba2 in this docking analysis, we measured the distance between the STE and different Uba2 amino acids. Figure 3.8 shows the STE docking simulation. There are three major parts of Uba2 that interact with STE: the adenylation domain, zinc motif, and UbL domain (Figure 3.8 B and D). Arg 127, Leu 130, and Ala 131 are part of an alpha helix from the UBA2 adenylation domain. Val 443, Cys 444, Ser 446, Lys 447, Pro 448 are close to the Zinc motif (Cys 441-X-X-Cys 444)(28). Asp 525, Tyr 526, and Thr527 are part of a beta strand from the UBA2 UbL domain. The closest appositions are made mostly between the

oxygen atoms from the STE to Ala 131 (3.16Å), Lys 447 (3.69Å), and Tyr 526 (3.35Å), as shown in Figure 3.8 C. This docking simulation indicates that STE binds to an allosteric binding site close to the second crossover strand that links the catalytic Cys and UbL domains via the zinc motif.

3.5 Discussion

Development of quantitative FRET technology to measure E1 enzyme kinetics

In this study, we used FRET technology to measure the intrinsic kinetic values of the E1 enzymes and applied this technology to determine the inhibition modality and calculate the inhibition constant of STE. Using CyPet and YPet as FRET donor and acceptor proteins, we followed the steady state E1-catalyzed transfer of SUMO to the E2 protein. Our results demonstrate that quantitative FRET analysis of CyPetSUMO1~YPetUbc9 formation can be used to measure the initial velocity to determine the kinetic constants of the E1 enzyme. The results from the FRET assays are comparable to classical enzymatic assays, such as the radioactive ATP:PPi exchange assay.

The ability to directly follow production of CyPetSUMO1-YPetUbc9 by detecting changes in FRET emission provides us with a convenient method for studying the steady-state kinetics for enzymes of the SUMO transfer cascade. In addition to the convenience of the fluorescence reading, FRET assays can be done in a multi-well plate platform that can increase the efficiency of the steady state kinetics assays by reading multiple samples simultaneously (38). Currently, most FRET applications in enzyme kinetics follow deSUMOylation by isopeptidases, such as SENPs (22,23,39). Here, for the first time, we detailed the steady state kinetic studies for the E1 activating enzyme of the SUMOylation pathway. Our study showed that the K_m of SUMO1 as a substrate is 0.75±0.11 μM and the K_m of ATP is 7.40 ± 1.77 μM. These values agree with those reported for ubiquitin E1 (31,40).

The similar values for the K_{ms} of SUMO2 and SUMO3 can be explained by their structural homology. Since SUMO2 and SUMO3 are about 95% similar, we can attribute the higher SUMO2 and SUMO3 K_m compared to the SUMO1 K_m to the substrate identity that define perturbations that affect the chemical steps in enzymatic catalysis. As described by Lois and Lima, there are two divergent amino acids out of 11 SUMO side chains that make direct contact to SAE2. The two amino acids are Asn60 and Arg70 in SUMO1 and Arg60 and Pro70 in SUMO2/3. SUMO1 Glu93 contacts SAE2 Arg119 and Tyr159 and is conserved as Glu in SUMO1 or Gln in SUMO2 or -3. Additionally, SUMO1 Gln94 is strictly conserved among SUMO isoforms and contacts SAE2 Ala142 and Leu145 (13). These differences on how SUMO1 or SUMO2/-3 interact with SAE2 would explain the findings that the K_ms of SUMO2 (3.42 ± 0.91 μM) and SUMO3 (2.76 ± 0.75 μM) are about four to five times higher than those of SUMO1 (0.7458 ± 0.1105 μM).

Using the values of k_{cat}/K_m ratio, we can compare the utilization of different substrates for SUMO E1. The k_{cat}/K_m ratios for SUMO1, SUMO2, and SUMO3 are not significantly different and indicate no difference in substrate specificity of the SUMO E1 enzyme to SUMO1, -2, or -3 paralogs (Table 1). However, notably, SUMO1 is mostly bound to RanGAP1 in cells, whereas SUMO2 and SUMO3 are mostly unbound (6,41).

In this study, we demonstrated the application of a quantitative FRET assay in determining the SUMO1, -2, -3 and ATP affinity in SUMOylation activation. As we described, the advantages of FRET technology in determining K_m include the ability to monitor reaction progress in real-time, high throughput, high sensitivity and by an environmentally friendly assay. This quantitative FRET assay method can be used to determine the enzyme kinetics of other ubiquitin-like protein pathways. Additionally, the quantitative FRET assay can be used to determine the mode of action for small-molecule inhibitors that may perturb the interaction between an enzyme and its

substrates in a high-throughput manner. These results extend the utility of quantitative FRET in characterizing protein-protein interaction and enzyme kinetics.

STE is a non-competitive inhibitor of the SUMO E1 enzyme

In characterizing the STE mode of inhibition of the SUMO E1 enzyme, we used the quantitative FRET assay to measure the apparent Km and V_{max} in the presence of various concentrations of STE. STE treatment decreases the V_{max} but does not change the apparent Km value. This is indicative that STE is a non-competitive inhibitor for the SUMO E1 enzyme. Since noncompetitive inhibitors do not compete with substrate for binding to the free enzyme, this result suggests that STE binds to the E1 enzyme at a site distinct from the active site and does not bind to the adenylation site nor thioester site of the E1 enzyme. Another characteristic of noncompetitive inhibition is that inhibition cannot be overcome by increasing substrate concentration. Therefore, it implies that STE can be used to inhibit the SUMO E1 enzyme even in the presence of high concentrations of SUMO. This would be important to applications as a cancer therapy.

Due to the high Ki value of 1.9μM, STE may serve as a lead structure for the design of more potent analogues. Affinity and selectivity can be improved by ensuring more perfect geometric and noncovalent interactions with the binding site. Structural modifications to better occupy a hydrophobic pocket can improve potency from the millimolar to the nanomolar range(42).

Inhibiting E1 is a good strategy for inhibiting the whole SUMOylation pathway because only one SUMO E1 has been found in this pathway. In our docking simulation, we selected the STE binding position based on the calculated free binding energy. Based on the highest free binding energy, STE appears to be bound close to the second crossover loop containing Zn motif (Cys441-X-X-Cys444) which links the catalytic Cys and UbL domains (11,13). On a closer look, STE binding

pocket consists of three different part of Uba2 chain: amino acid 127-131, 443-447, and 525-527. This binding pocket is distant from the adenylation site and the Cys 173 catalytic site. This allosteric binding can be beneficial in modulating the SUMO E1 enzyme by increasing selectivity against other E1 in ubiquitin and ubiquitin-like pathways because there are many elements in the E1 domains that are conserved at the level of sequence and structure among the E1 enzymes among ubiquitin and the ubiquitin like pathways.

In conclusion, our candidate compound, STE, was found as a small molecule that inhibits the SUMOylation pathway in a high-throughput screening. Our biochemistry assay results showed that STE inhibits the SUMO E1 enzyme. To establish the mode of inhibition, we first established a quantitative FRET assay to determine the Km of the SUMO E1 enzyme for its different substrates, SUMO1, SUMO2, SUMO3, and ATP. We then used the quantitative FRET assay to determine the mode of SUMO E1 inhibition and calculated the inhibition constant of STE. From the quantitative FRET assay, it was determined that STE inhibits the SUMO E1 enzyme non-competitively because in the presence of increasing concentrations of STE, the V_{max} value decreased, while the K_m values were relatively constant. Additionally, from these assays, we calculated the inhibition constant to be 1.90 μM. We also performed a docking simulation using AutoDock and found that the lowest binding energy was -7.69 kcal/mol with an inhibition constant of 2.30 μM. Taken together, these data suggest that STE binds to an allosteric site and may interfere with the conformational changes of the Uba2 necessary for activation of SUMO. Additionally, this allosteric binding site could increase specificity of STE binding to SUMO E1. More definitive experiments such as X-ray crystallography or NMR spectroscopy are needed to confirm these studies.

3.6 References

1. Hay RT. SUMO: a history of modification. Molecular cell 2005;18(1):1-12.
2. Cubeñas-Potts C, Matunis Michael J. SUMO: A Multifaceted Modifier of Chromatin Structure and Function. Developmental cell 2013;24(1):1-12.
3. Jackson Stephen P, Durocher D. Regulation of DNA Damage Responses by Ubiquitin and SUMO. Molecular cell 2013;49(5):795-807.
4. Woo C-H, Abe J-i. SUMO—a post-translational modification with therapeutic potential? Current Opinion in Pharmacology 2010;10(2):146-55.
5. Bettermann K, Benesch M, Weis S, Haybaeck J. SUMOylation in carcinogenesis. Cancer letters 2012;316(2):113-25.
6. Saitoh H, Hinchey J. Functional Heterogeneity of Small Ubiquitin-related Protein Modifiers SUMO1 versus SUMO2/3. Journal of Biological Chemistry 2000;275(9):6252-58.
7. Tatham MH, Jaffray E, Vaughan OA, Desterro JMP, Botting CH, Naismith JH, et al. Polymeric Chains of SUMO2 and SUMO3 Are Conjugated to Protein Substrates by SAE1/SAE2 and Ubc9. Journal of Biological Chemistry 2001;276(38):35368-74.
8. Walden H, Podgorski MS, Schulman BA. Insights into the ubiquitin transfer cascade from the structure of the activating enzyme for NEDD8. Nature 2003;422(6929):330-4.
9. Haas AL, Warm JV, Herschko A, Rose IA. Ubiquitin-activating enzyme Mechanism and role in protein-ubiquitin conjugation. The Journal of biological chemistry 1982;257:2543-48.
10. Olsen Shaun K, Lima Christopher D. Structure of a Ubiquitin E1-E2 Complex: Insights to E1-E2 Thioester Transfer. Molecular cell 2013;49(5):884-96.
11. Olsen SK, Capili AD, Lu X, Tan DS, Lima CD. Active site remodelling accompanies thioester bond formation in the SUMO E1. Nature 2010;463(7283):906-12.

12. Truong K, Lee TD, Chen Y. Small ubiquitin-like modifier (SUMO) modification of E1 Cys domain inhibits E1 Cys domain enzymatic activity. The Journal of biological chemistry 2012;287(19):15154-63.

13. Lois LM, Lima CD. Structures of the SUMO E1 provide mechanistic insights into SUMO activation and E2 recruitment to E1. EMBO J 2005;24(3):439-51.

14. Bernier-Villamor V, Sampson DA, Matunis MJ, Lima CD. Structural Basis for E2-Mediated SUMO Conjugation Revealed by a Complex between Ubiquitin-Conjugating Enzyme Ubc9 and RanGAP1. Cell 2002;108(3):345-56.

15. Wang J, Hu W, Cai S, Lee B, Song J, Chen Y. The intrinsic affinity between E2 and the Cys domain of E1 in ubiquitin-like modifications. Molecular cell 2007;27(2):228-37.

16. Chung CD, Liao J, Liu B, Rao X, Jay P, Berta P, et al. Specific Inhibition of Stat3 Signal Transduction by PIAS3. Science 1997;278:1803-5.

17. Liao J, Fu Y, Shuai K. Distinct roles of the NH2- and COOH-terminal domains of the protein inhibitor of activated signal transducer and activator of transcription (STAT) 1 (PIAS1) in cytokine-induced PIAS1–Stat1 interaction. Proceedings of the National Academy of Sciences 2000;97(10):5267-72.

18. Tang Z, Hecker CM, Scheschonka A, Betz H. Protein interactions in the sumoylation cascade: lessons from X-ray structures. The FEBS journal 2008;275(12):3003-15.

19. Clegg RM. Fluorescence resonance energy transfer. Current Opinion in Biotechnology 1995;6(1):103-10.

20. Nguyen AW, Daugherty PS. Evolutionary optimization of fluorescent proteins for intracellular FRET. Nature biotechnology 2005;23(3):355-60.

21. Song Y, Rodgers VGJ, Schultz JS, Liao J. Protein interaction affinity determination by quantitative FRET technology. Biotechnology and Bioengineering 2012;109(11):2875-83.

22. Liu Y, Song Y, Madahar V, Liao J. Quantitative Förster resonance energy transfer analysis for kinetic determinations of SUMO-specific protease. Analytical biochemistry 2012;422(1):14-21.

23. Jiang L, Liu Y, Song Y, Saavedra A, Pan S, Xiang W, et al. Internal Calibration Förster Resonance Energy Transfer Assay: A Real-Time Approach for Determining Protease Kinetics. Sensors 2013;13(4):4553-70.

24. Tatham MH, Hay RT. FRET-based *in vitro* assays for the analysis of SUMO protease activities. Methods in molecular biology (Clifton, NJ) 2009;497:253-68.

25. Song Y, Liao J. An *in vitro* Forster resonance energy transfer-based high-throughput screening assay for inhibitors of protein-protein interactions in SUMOylation pathway. Assay and drug development technologies 2012;10(4):336-43.

26. Xie S. Enzyme Kinetics, Past and Present. Science 2013;342:1457-9.

27. Copeland RA. Enzymes: A Practical Introduction To Structure, Mechanism And Data Analysis. 2nd ed. New York: Wiley; 2000.

28. Wang J, Chen Y. Role of the Zn(2+) motif of E1 in SUMO adenylation. J Biol Chem 2010;285(31):23732-8.

29. Burch TJ, Haas AL. Site-Directed Mutagenesis of Ubiquitin. Differential Roles for Arginine in the Interaction with Ubiquitin-Activating Enzyme. Biochemistry 1994;33(23):7300-08.

30. Bruzzese FJ, Tsu CA, Ma J, Loke HK, Wu D, Li Z, et al. Development of a charcoal paper adenosine triphosphate:pyrophosphate exchange assay: kinetic characterization of NEDD8 activating enzyme. Analytical biochemistry 2009;394(1):24-9.

31. Wee KE, Lai Z, Auger KR, MA J, Horiouchi KY, Dowling RL, et al. Steady-state kinetic analysis of human ubiquitin-activating enzyme (E1) using a fluorescently labeled ubiquitin substrate. J Protein Chem 2000;19(6):489-98.

32. Jiang L, Saavedra AN, Way G, Alanis J, Kung R, Li J, et al. Specific substrate recognition and thioester intermediate determinations in ubiquitin and SUMO conjugation cascades revealed by a high-sensitive FRET assay. Molecular BioSystems 2014.

33. Schneider CA, Rasband WS, Eliceiri KW. NIH Image to ImageJ: 25 years of image analysis. Nat Meth 2012;9(7):671-75.

34. Morris GM, Huey R, Lindstrom W, Sanner MF, Belew RK, Goodsell DS, et al. AutoDock4 and AutoDockTools4: Automated docking with selective receptor flexibility. J Comput Chem 2009;30(16):2785-91.

35. Humphrey W, Dalke A, Schulten K. VMD-Visual Molecular Dynamics. J Molec Graphics 1996;14:33-38.

36. Wang J, Cai S, Chen Y. Mechanism of E1-E2 interaction for the inhibition of Ubl adenylation. The Journal of biological chemistry 2010;285(43):33457-62.

37. Dixon M. The determination of enzyme inhibitor constants. The Biochemical journal 1953;55(1):170-1.

38. Bossis G, Chmielarska K, Gärtner U, Pichler A, Stieger E, Melchior F. A Fluorescence Resonance Energy Transfer - Based Assay to Study SUMO Modification in Solution. In: Raymond JD, editor. Methods in Enzymology. Volume Volume 398: Academic Press; 2005. p 20-32.

39. Stankovic-Valentin N, Kozaczkiewicz L, Curth K, Melchior F. An *In Vitro* FRET-Based Assay for the Analysis of SUMO Conjugation and Isopeptidase Cleavage. In: Ulrich H, editor. SUMO

Protocols. Volume 497, METHODS IN MOLECULAR BIOLOGY™: Humana Press; 2009. p 241-51.

40. Tokgoz Z, Siepmann TJ, Streich F, Jr., Kumar B, Klein JM, Haas AL. E1-E2 interactions in ubiquitin and Nedd8 ligation pathways. The Journal of biological chemistry 2012;287(1):311-21.

41. Becker J, Barysch SV, Karaca S, Dittner C, Hsiao HH, Berriel Diaz M, et al. Detecting endogenous SUMO targets in mammalian cells and tissues. Nature structural & molecular biology 2013;20(4):525-31.

42. Smith AJ, Zhang X, Leach AG, Houk KN. Beyond picomolar affinities: quantitative aspects of noncovalent and covalent binding of drugs to proteins. Journal of medicinal chemistry 2009;52(2):225-33.

CHAPTER 4. THE EFFECT OF STE TREATMENT ON NON-SMALL CELL LUNG CANCER CELL LINES

4.1 Abstract

The function and survival of normal and malignant cells depends on fine-tuning of the ubiquitin-proteasome system. STE is a small molecule inhibitor of the SUMOylation pathway discovered through FRET-based high-throughput screening. Previous studies in our lab have found that STE inhibits the E1 enzyme and that this inhibition is specific to the SUMOylation pathway. We also showed that STE acts as a non-competitive inhibitor, with an inhibitor constant of 1.9 μM. Since SUMOylation is important in genome integrity, we hypothesize that inhibition of the SUMOylation pathway may decrease cancer cell viability. To test this hypothesis, we treated HEK cells and non-small cell lung cancer cell lines with STE and observed cell viability and cell cycle progressions. Our results showed that STE induces cell death in non-small cell lung cancer cell lines, independent of their p-53 status. Additionally, STE treatment of cells inhibited cell cycle progression in HEK cells. Taken together, these results suggest that STE may have anti-cancer activity.

4.2 Introduction

Lung cancer is the most lethal malignancy in both females and males, resulting in an estimated 224,210 new cases in 2014 and accounting for approximately 27 percent of all cancer deaths in the US (1). For the purpose of treatment, lung cancer is classified as small cell (14%) or non-small cell (84%). For early stage non-small cell lung cancers (NSCLC), the treatment of choice is usually surgery. However, approximately 85% of lung cancers have already metastasized by the time of diagnosis, necessitating treatment with chemotherapy, targeted drugs, or some combination of the two (1). Currently, there are a few targeted therapies available for NSCLC: epidermal growth factor receptor (EGFR) tyrosine kinase inhibitors, an anti-vascular endothelial growth factor (VEGF) antibody, and EML4-ALK (echinoderm microtubule-associated protein-like 4 (EML4) - anaplastic lymphoma kinase (ALK)) inhibitors in patients with EML-ALK translocations (2). Reck et al. recommended the assessment of the presence of activating EGFR mutations and ALK rearrangement in patients with non-squamous NSCLC in order to effectively utilize the inhibitors of these oncogenic alterations (3). These therapies help a large percentage of patients experience remission, although the cancer often returns. Thus, the 1- and 5-year survival rates for lung cancer are 43% and 17% respectively(1). Thus, improving response and overcoming resistance to chemotherapy are important goals to increase the relative survival rates for lung cancer.

The SUMOylation pathway involvement in non-small cell lung carcinoma has been described in previously published literature: Kessler et al. described how SAE2 is required for growth of Myc-dependent tumors and that low SAE1/SAE2 abundance in Myc-high human breast cancer correlates with longer metastasis-free patient survival (4). Rabellino et al. showed that SUMOylation of the tumor suppressor, promyelocytic leukemia (PML) protein, promoted ubiquitin

proteasome mediated degradation of PML and attenuated PML tumor suppressor functions. In non-small cell lung carcinoma, the SUMOylation of PML requires PIAS1 E3 ligase (5). Non-small cell lung cancer patients with high expression of the E2 conjugating enzyme, Ubc9, were found to be more likely to have advanced-stage disease compared to those with low Ubc9 expression (6). Specifically, Ubc9 expression is altered only in adenocarcinomas (7). Additionally, the expression of Ubc9 correlated with the invasive ability of lung cancer cells (6). In regard to pharmacogenomics, Han et al. showed that genetic variations of Ubc9 gene, Ubc9 10920CG, enhances sensitivity to irinotecan chemotherapy in advanced NSCLC through upregulation of SUMO1 in tumor cells (8). The involvement of both SUMO andUbc9 in NSCLC suggests that inhibition of the SUMO E1 enzyme could be an effective new treatment for NSCLC.

In comparison to RNA-mediated silencing such as with small interfering RNA (siRNA) and RNA interference (RNAi), a small molecule inhibitor offers inhibition of protein that is physically intact (9). Thus, if a target protein has scaffolding functions, these may be preserved while inhibiting other functions. This could be advantageous.

In our effort to find small molecule inhibitors of the SUMOylation pathway, we chose STE as our lead compound. STE is a small molecule inhibitor that selectively inhibits the SUMO E1 activating enzyme (Aos1/Uba2). In addition, this inhibition is specific to the SUMOylation pathway and had no effect on ubiquitin E1 or NEDD8 E1. We also showed that STE acts as a non-competitive inhibitor with an inhibitor constant of 1.9 μM. The object of investigation discussed here was to evaluate the activity of STE against non-small cell lung cancer cell lines. Since p53 is a SUMO substrate, we investigated whether STE-induced cell death was dependent on p53 status. We utilized two NSCLC cell lines, H460 p53WT and H358 p53-/-. We found that STE, as a single agent,

induces cell death in these two non-small cell lung cancer cell lines regardless of p53 status. However, the mechanism for cell death is not known and requires further exploration. We also found that STE treatment inhibited cell cycle progression in HEK cells.

4.3 Materials and Methods

Cell Lines and Cell Culture

The H358 and H460, NSCLC cell lines, established from patients with bronchioalveolar carcinoma and large cell carcinoma respectively, were obtained from the American Type Culture Collection (ATCC, Manassas, VA). Human Embryonic Kidney 293 cells were obtained from the ATCC. The HEK293 cells were grown in DMEM (Life Technologies, Inc., Grand Island, NY) supplemented with 10% fetal bovine serum (Life Technologies, Inc.). The H358 and H460 cells were grown in RPMI 1640 (Life Technologies, Inc.) with 10% fetal bovine serum. All of the cell lines were maintained at 37°C in a 5% CO_2 atmosphere.

MTS Assay

An MTS (3-(4,5-dimethylthiazol-2-yl)-5-(3-carboxymethoxyphenyl)-2-(4-sulfophenyl)-2H-tetrazolium) assay was used to screen for viable cell number. To evaluate the effect of STE treatment on cell number, we quantified the change in the number of viable cells per well at 24, 48, 72, and 96 hour. The CellTiter 96® AQueous One Solution Cell Proliferation Assay was used according to the manufacturer's instructions (Promega, Madison, WI). For cell viability analysis, HEK 293 and H460 cells were plated at a density of 7×10^3 cells/well on 96-well culture plates. The next day, cells were treated with different concentration of ST025091 (0.1, 0.5, 1, 2.5, 5, and 10 μM) or with DMSO. At the end of treatment, the incubation medium was removed, and each well

of 96 well plates was incubated with 100µl DPBS with 4.5% D-glucose. Twenty microliters of the dye reagent was added to each well and plates were incubated for an additional 2 h. The absorbance at 490nm was recorded using a 96-well plate reader (Victor2). For quantification, three independent experiments with three samples each were analyzed.

Cell Cycle Distribution Analysis

Propidium iodide (PI) staining was used to analyze DNA content. HEK293, H358, and H460 cells were plated in 10-cm culture dishes at $5x10^6$ cells to yield 50-60% confluence within 24h. Cells were then treated with either DMSO (0.1-0.3%) or STE (5µM). After 6, 16, 24, and 48h of treatment, both adherent and floating cells were harvested. After washing with PBS, the cells were fixed in 70% ethanol and kept at -20^{o}C until the DNA staining process. Cells were washed twice with PBS before staining process. To stain the DNA, cells were stained with PI staining solution containing 40 ug/ml PI and 3.8mM sodium citrate in PBS with 0.5µg/ml RNase A. After 3h incubation at 4^{o}C, the DNA content was measured using a FACScan flow cytometer with a 488-nm line of an argon-ion laser for excitation and data were collected using CellQuest software (Becton-Dickinson, Franklin Lakes, NJ). For all assays, 10,000 events were counted. Cells with various amounts of DNA from the 2N (G0/G1) amount to the 4N (G2/M) were observed.

4.4 Results

MTS assays showed a reduced number of H460 and H358 cells with STE treatment

We investigated the effects of STE treatment on the growth of HEK293 and H460 large-cell lung cancer carcinoma cells. Figure 1 shows the growth of HEK and H460 cells in the presence of various concentrations of STE compared to vehicle control. A dose-dependent inhibition of cell

growth was observed at concentrations of 1µM or more. Forty-eight hours after treatment, the growth of H460 cells was completely inhibited by 2.5µM STE.

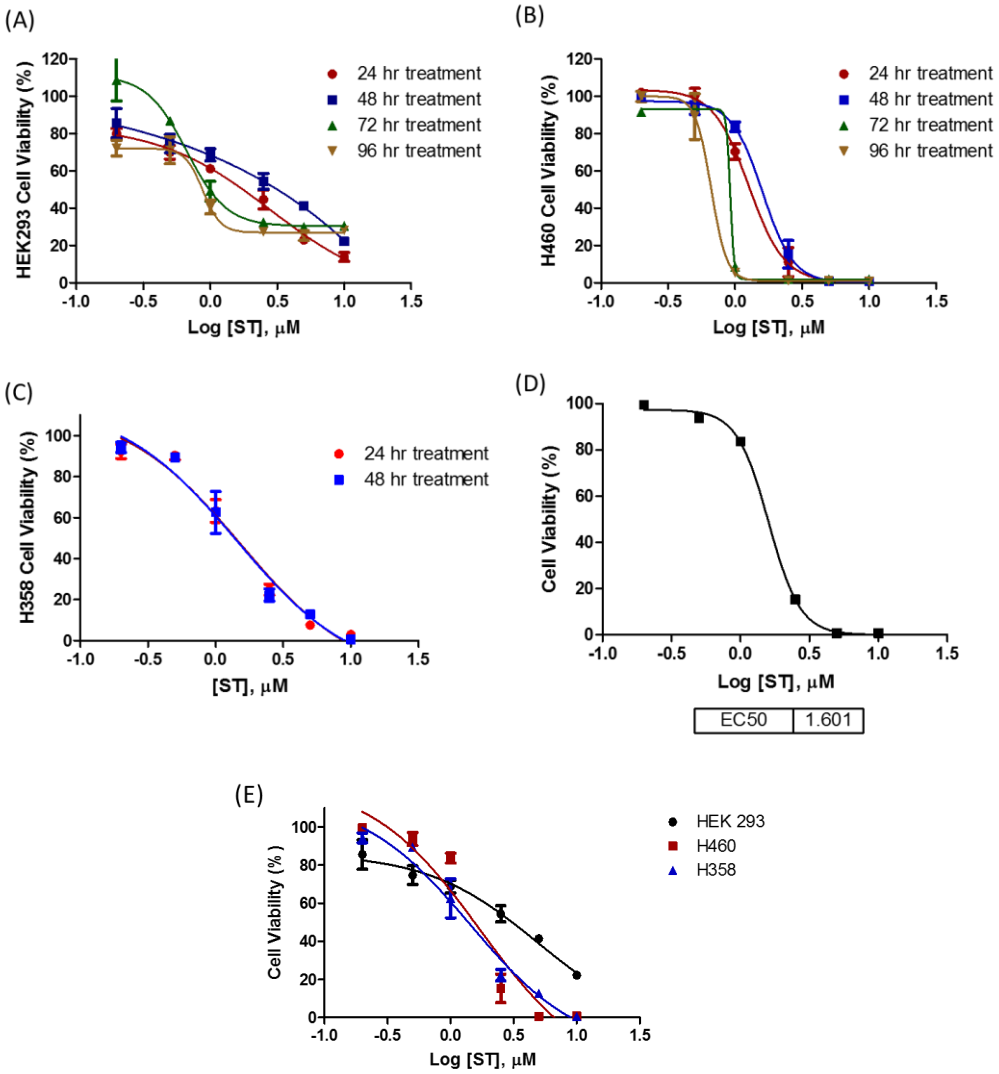

Figure 4.1 MTS assay to assess cell viability in vitro in HEK and H460 cells. STE reduced the viability of (B) H460 and (C) H358 lung cancer cells by 40% compared to HEK 293(A). The percentage of growth was calculated, with 100% representing control cells treated with 0.3% DMSO alone. (D) Based on the MTS assay, the EC_{50} = 1.60 µM for the H460 NSCLC cell lines. (E) HEK cell viability versus H460 and H358 to illustrate the difference of STE treatment for 48h.

The viability of H460 cells was inhibited to 98, 70, 11, 0.6% of the control level by 0.5, 1, 2.5, and 5 µM respectively 48 hour after the addition of STE. STE reduced the viability of the H460 and the H358 cells by 40% compared with the controls (Figure 4.1A - C). This reduced cell viability is dose dependent and the effective concentration where 50% of the cells remained viable was 1.6µM (Figure 4.1D). The result of this assay indicated that STE treatment at the dose of 1µM significantly reduced H460 cell viability after 48 hour of treatment compared to HEK 293 cells.

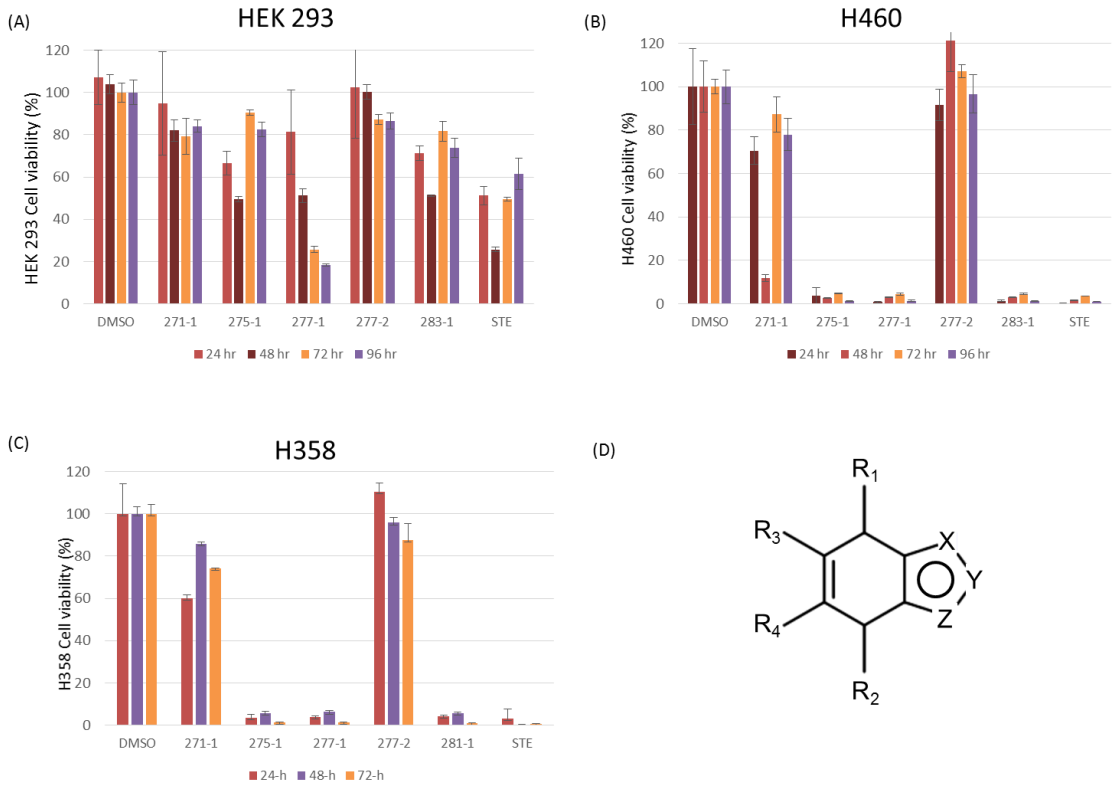

Figure 4.2 MTS assay to assess cell viability in vitro in HEK, H460, and H358 to compare STE derivatives' activities. To determine structure-activity relationship of STE and its derivatives, the MTS assay was employed to observe cell viability after DMSO or 5µM of compounds (271-1, 275-1, 277-1, 277-2, 283-1, and STE. 275-1, 277-1, and 283-1 exhibited similar activity to the STE treatment and induced cell death in both H460 (B) and H358 (C) cell lines.

We developed derivatives from our lead compound, STE, to investigate structure- activity relationships. To explore the phenotypical function of these compounds, each compound was used to treat HEK, H460, and H358 cells at a 5 μM concentration and the MTS assays were performed after 24-hour treatments. The results indicated that 275-1, 277-1, and 283-1 had similar activities to the STE and induced cell death more profoundly in the NSCLC, H460 (Figure 4.2B) and H358 (Figure 4.2C) compared to the HEK cells (Figure 4.2A). The 275-1, 277-1, and 283-1 induced H358 and H460 cell death within 24 hours. Since 275-1, 277-1, and 283-1 were derivatives of the STE, these findings suggested the replacement of R1, R2, R3, or R4 side chains of STE have similar activities in inducing cell death in lung cancers.

STE Induces S-phase Cell Cycle Arrest in HEK 293

To elucidate the effect of STE on cell cycle progression in exponentially dividing cultures of the HEK cell line, subconfluent cultures of cells were treated with either DMSO alone or with STE (5μM). After 6 hours of treatment, cells were labeled with PI and the DNA content of the nuclei of HEK 293 cells was measured by flow cytometric analysis. As shown in Fig. 2B, treatment with 5μM STE markedly induced S-phase cell cycle arrest. FACS analysis revealed that a 6-hour exposure to STE increased the population of S-phase cells. Cells at the S-phase increased from 11.92% to 23.39%. As shown in Fig 4.2C, the increase of S-phase cells was accompanied by a decrease in G1 phase cells. Additionally, 16% of the cells were undergoing apoptosis after 6 hours of treatment, as detected as an increase in the sub-G1 apoptotic peak. Therefore, our results demonstrate that STE inhibits S-phase cell cycle progression.

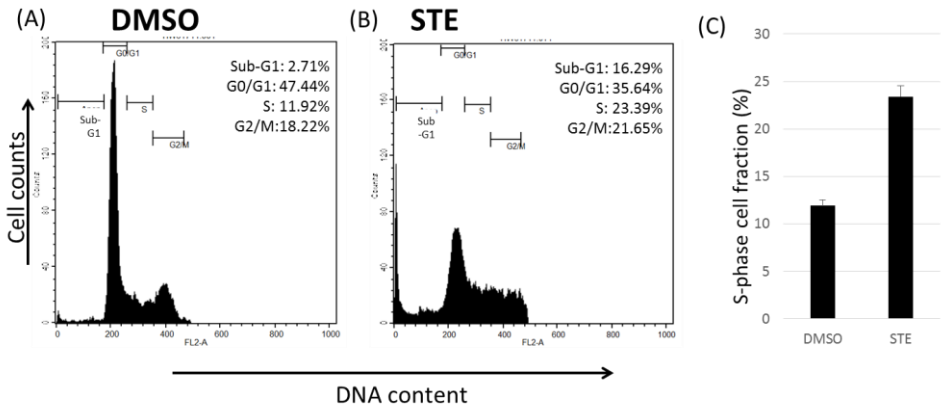

Figure 4.3 The effect of STE on cell cycle progression in HEK 293 cells. HEK293 were treated with (A) DMSO and (B) 5µM STE for 16 hour. The DNA content of propidium iodide-stained nuclei was analyzed by FACScan flow cytometry. (C) The percentage of cells in G1S phase was doubled in the STE treatment group.

STE Treatment Induces Cell Death in H460 and H358 NSCLC cell lines

To further investigate the effect of STE treatment, we performed cell cycle analysis after 5µM of STE treatment in the H460 p53WT and H358 P53$^{-/-}$. Flow cytometric measurement of cell-cycle distribution of the HEK293, H460, and H358 cells after incubation with ST025091 (5 µM) showed that both non-small lung cancer cell lines were sensitive to ST025091 treatment and ST025091 treatment induced cell death in both cell lines as early as 6 hours after treatment. Both H460 and H358 showed a decreased cell number in the G0/G1, S, and G2/M phases in 6 hours and >90% cells were in the sub-G1 by 16 hours. This result also indicated that STE induced cell death in the presence of both wild type and mutant p53.

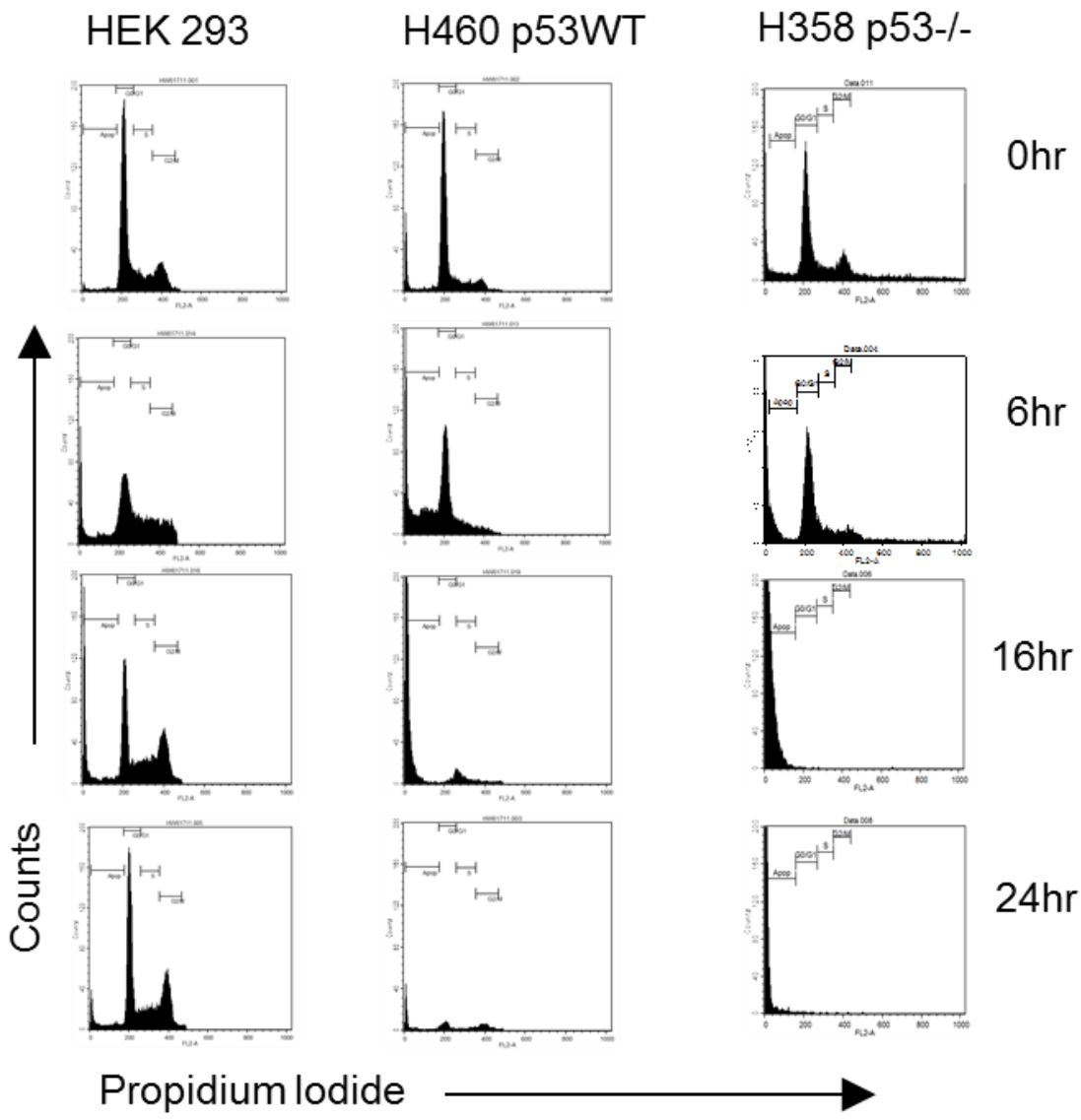

Figure 4.4 Flow cytometry to assess HEK293, H460, and H358 cell cycle after 5µM STE treatment for indicated period. Flow cytometry indicated that the level of SubG1 was 97% in H460 and 99.2% in H358 cells 16 hour after exposure to 5µM STE.

4.5 Discussion

In Chapter 3, we measured the STE inhibition constant using in vitro FRET-based SUMO E1 kinetic assays. To complement this experiment, we performed MTS assays to measure the concentration required to inhibit SUMOylation in cells. Our first goal was to determine whether there was a correlation between in vitro protein-protein interaction assays and the effective concentration in the cellular assays. In our MTS assay, we determined that the effective cellular concentration (EC50) of 1.60μM which is close to the value determined in a previous FRET based kinetic assay experiment, which showed a 1.90 μM inhibition constant. The similarity between these two numbers provides a rational correlation between in vitro biochemically measured affinity and effective cellular concentration.

The data from MTS assay suggest that STE treatment caused up to 60% reduction in HEK 293 cell viability. However, STE markedly reduced NSCLC cells viability up to 100% in a dose dependent manner. The viability of the H460 NSCLC cells decreased from 98% to 0.6% of the control level as the STE dosage increased from 0.5 to 5 μM as indicated by the MTS assay. This set of data showed that both H460 and H358 NSCLC cell lines are sensitive to the STE-induced cell death. However, since there is some cell toxicity in a non-cancer cell lines, further explorations on the mechanism of cell death is needed to identify the target protein that is affected by STE treatment.

To determine structure-activity relationships of the derivative compounds that we developed in the lab, MTS assay were used to determine the activity of those compounds. Out of 5 STE derivatives that were synthesized, only 3 compounds had similar effects to the STE in term of inducing cell death in H358 and H460 cells: 275-1, 277-1, and 283-1. Compound 275 contains

two hydroxide substitution on R1 and R2 which carries a negative charge. This electrostatic interactions may increase binding affinity between 275-1 inhibitor and the SUMO E1 enzyme. This is an example how determination of key structural components in the inhibitory mechanism shared by a series of related compounds is important to correlate structural changes with inhibitor potency.

To further explore the effect on cell proliferation, the propidium iodide uptake assay was used to identify the cell distribution during the various phases of the cell cycle. In this assay, the number of cells of four distinct cell phases was counted: the sub-G1, G1, S (DNA synthesis phase), and G2/M (mitosis phase). Consistent with the MTS assay, our results indicated at the H460 and H358 cells were mostly apoptotic, as evidenced by the sub-G1 DNA content in our cell-cycle analysis. In our attempt to probe for the pathways that were affected by the inhibition of SUMOylation pathway, we used H358 p53-null and H460 p53WT because p53 is one of SUMO substrate that are involved in carcinogenesis. Since there was no difference between these two cell lines both in the cell viability and cell cycle analysis, the STE likely affects cell viability by mechanisms that do not involve p53.

In contrast to both H358 and H460 cells, the HEK 293 seemed to show a transient S-phase cell cycle arrest following STE treatment, as indicated by doubling of the number of cells in the S-phase. The S-phase is the phase where cells duplicate their DNA. Entry into each phase of the cell-cycle is carefully regulated by cell-cycle checkpoints. Targeting these checkpoints has been utilized to develop small molecule inhibitors to regulate the quality and rate of cell division of cancer cells. Defects in checkpoints may lead a cancer cell to enhance proliferation, and efforts to correct these

problems may slow growth and induce cell death(10). Our data suggest that STE induces S-phase cell cycle arrest which in turns may induce apoptosis in cancer cells.

Since the S-phase is the phase of DNA synthesis where chromosome duplication occurs, any problems with DNA replication trigger a checkpoint that puts the phase on hold until the problem is resolved(11). One of the problems that a cell may encounter during the S-phase is double-stranded breaks (DSBs). Since DSB ruin the replication fork, it is a catastrophic event that has to be successfully repaired before DNA replication can resume(11). Multiple DSB repair proteins are targeted by a SUMOylation wave that is triggered by the DNA-bound SUMO ligase, Siz-2, and ssDNA is resected (12). Since our results show that STE inhibits SUMO E1 and induces S-phase cell cycle arrest, we propose a new hypothesis that inhibiting the SUMOylation pathway can have a detrimental effect on the DSB repair process in S-phase, resulting in induction of apoptosis. This new hypothesis needs to be tested in order to further elucidate the specific mechanism of action of STE in inducing cancer cell death.

The propidium iodide uptake assay has limited value in determining the cause of cell death. The “sub G1” peak may represent apoptotic cells, mechanically damaged cells, or cells with a lower DNA content for other reasons. Therefore, to examine whether STE treatment induces cell death through apoptosis or necrosis process, a set of subsequent experiments such as Terminal deoxynucleotidyl transferase dUTP nick end labeling Terminal deoxynucleotidyl transferase dUTP nick end labeling (TUNEL) or Annexin-V/PI to detect apoptosis should be performed.

In conclusion, our data show that STE treatment in NSCLC H358 and H460 cell lines induces cell death with an EC50 of 1.6μM. In the assays used, more than 90% of H358 and H460 cells were found in the Sub-G1 population after 16 hour of STE treatment.

4.6 References

1. AmericanCancerSociety. Cancer Facts & Figures 2014. Atlanta: American Cancer Society; 2014.
2. NationalCancerInstitute. 2014 PDQ® Non-Small Cell Lung Cancer Treatment. National Cancer Institute <http://www.cancer.gov/cancertopics/pdq/treatment/non-small-cell-lung/healthprofessional>.
3. Reck M, Heigener DF, Mok T, Soria J-C, Rabe KF. Management of non-small-cell lung cancer: recent developments. The Lancet 2013;382(9893):709-19.
4. Kessler JD, Kahle KT, Sun T, Meerbrey KL, Schlabach MR, Schmitt EM, et al. A SUMOylation-Dependent Transcriptional Subprogram Is Required for Myc-Driven Tumorigenesis. Science 2011;335(6066):348-53.
5. Rabellino A, Carter B, Konstantinidou G, Wu S-Y, Rimessi A, Byers LA, et al. The SUMO E3-ligase PIAS1 Regulates the Tumor Suppressor PML and Its Oncogenic Counterpart PML-RARA. Cancer research 2012;72(9):2275-84.
6. Li H, Niu H, Peng Y, Wang J, He P. Ubc9 promotes invasion and metastasis of lung cancer cells. Oncol Rep 2013;29(4):1588-94.
7. McDoniels-Silvers AL, Nimri CF, Stoner GD, Lubet RA, You M. Differential Gene Expression in Human Lung Adenocarcinomas and Squamous Cell Carcinomas. Clinical Cancer Research 2002;8(4):1127-38.
8. Ronchi VP, Klein JM, Haas AL. E6AP/UBE3A Ubiquitin Ligase Harbors Two E2∼ubiquitin Binding Sites. Journal of Biological Chemistry 2013;288(15):10349-60.

9. Yang Y, Kitagaki J, Dai RM, Tsai YC, Lorick KL, Ludwig RL, et al. Inhibitors of ubiquitin-activating enzyme (E1), a new class of potential cancer therapeutics. Cancer research 2007;67(19):9472-81.

10. DiPaola RS. To Arrest or Not To G2-M Cell-Cycle Arrest : Commentary re: A. K. Tyagi et al., Silibinin Strongly Synergizes Human Prostate Carcinoma DU145 Cells to Doxorubicin-induced Growth Inhibition, G2-M Arrest, and Apoptosis. Clin. Cancer Res., 8: 3512–3519, 2002. Clinical Cancer Research 2002;8(11):3311-14.

11. Das-Bradoo S, Bielinsky A-K. Dna Replication and Checkpoint Control in S Phase. Nature Education 2010;3(9):50.

12. Psakhye I, Jentsch S. Protein Group Modification and Synergy in the SUMO Pathway as Exemplified in DNA Repair. Cell 2012;151(4):807-20.

CHAPTER 5. CONCLUSION & FUTURE DIRECTION

5.1 Conclusion

Small Ubiquitin-like Modifiers (SUMOs) are small proteins from the ubiquitin family that have been implicated in many physiological cellular mechanisms as well as pathological conditions such as cancer and infectious diseases. To date, no specific small molecule inhibitor of the SUMOylation pathway has been found. We performed a high-throughput screening to find inhibitors of the SUMOylation pathway and discovered a lead compound, STE, active in a mammalian cell line. Throughout this dissertation, I have described the discovery from screening to validated hit. We determined that STE acts as a specific non-competitive inhibitor of the E1 enzyme and is capable of inducing cell death in non-small cell lung cancer cell lines. This last chapter is dedicated to drawing a general conclusion based on the research data and to suggesting the future research directions.

5.2 Future Directions

There are many factors that make it challenging to find a small molecule compound to inhibit protein-protein interactions. These factors include the lack of small-molecule starting points for drug design, a relatively large surface area is buried on each side of the interface, the difficulty of distinguishing real from artefactual binding, and the size and character of typical small-molecule libraries (1). We pioneered the search for small molecule inhibitors of the SUMOylation pathway and determined that STE can be used as a starting point for SUMO E1 inhibitor designs. To find a potent inhibitor for the SUMO E1 enzyme, the next steps will be identification of binding site and determination of structure-activity relationships to improve the compound. Additionally, we can implement a combination of methods in high-throughput screening to increase the probability of finding more hit compounds.

5.2.1 Binding site exploration

To identify hot spots, compact and centralized regions of residues that are crucial for the affinity of the protein-protein interaction, both X-ray crystallography and site-directed mutagenesis can be used (1). Since the SUMO E1 protein binds to both SUMO and ATP, it can be categorized as an allosteric protein as it contains two or more topologically distinct binding sites that interact functionally with each other(1). STE acts as a non-competitive inhibitor of this allosteric protein; however, the exact binding site is yet to be confirmed even though the molecular modeling is highly suggestive of a particular site. There are several methods that could be used to identify the STE binding site on the E1 enzyme. These include analytical ultracentrifugation (AUC), nuclear magnetic resonance (NMR), and X-ray crystallography.

Analytical ultracentrifugation (AUC) is commonly used to characterize interactions of purified proteins in dilute solutions. The centrifuge is equipped with an absorbance detector that measures the ultraviolet-visible spectrum of a sample placed in a specially designed rotor. The protein is centrifuged for several hours at 3,000–50,000 RPM until equilibrium is reached. The small molecule now sediments with an apparent molecular weight equal to that of the protein. From the shape of the protein sedimentation curve at equilibrium, the molecular weight of the protein species can be determined. The sedimentation profile of the small molecule can be detected at 300 nm in the presence of the protein(1).

Crystal structures are often considered the “gold standard” for learning about the geometry of proteins, including protein and small molecule interactions. To prepare the sample, one of two methods can be used: soaking and co-crystallization. However, these different sample preparation techniques can lead to different interaction structures (2). Since E1 undergoes significant conformational changes during adenylation and thioester formation, the sample

preparation method for identification of the STE binding site should be chosen carefully. Co-crystallization is a more suitable option because the protein-ligand complexes are formed by equilibrating them in solution and then the assembled complex is crystalized (2). Lois and Lima obtained the structure of SAE1/SAE2-SUMO-ATP complex by co-crystallization (3) indicating that the E1 enzyme complex structure is stable to be crystalized and that this method can be used to identify STE inhibitor binding site. The crystal or NMR structure of an enzyme with a bound inhibitor provides structural details such as hydrogen bonding, salt bridge formation, other electrostatic interactions, and hydrophobic interactions (4). These crystal structure data will be useful in determining the structure-activity relationships relevant to the design of a higher affinity to E1 enzyme.

5.2.2 Structure activity relationships

The Rule of Five, by Lipinski et al., proposed that compounds that have a molecular mass <500Da, a calculated logP (cLogP) <5, a number of hydrogen-bond donors<5, and a number of hydrogen-bond acceptors <10 are more likely to be soluble and permeable and thus more likely to be developed as oral drugs(5). STE meets all the Rule of Five criteria, however, due to its low binding affinity, we need to find a better derivative that has a higher affinity to the enzyme.

Since STE is the first characterized small-molecule inhibitor of the SUMO E1 enzyme, it can serve as the starting point for the fragment-based synthesis of compounds. Measures of inhibitor potency such as Ki or IC50 are useful in elucidating the stereochemical and physicochemical features of inhibitory molecules that allow them to bind well to the enzyme (4). There are four main types of physicochemical forces that are important in protein inhibitor interactions: hydrophobic interactions, hydrogen bondings, electrostatic interactions and van der Waals forces (6). An understanding of these physicochemical forces is important in predicting the structure of

a compound that would interact better with the enzyme. This iterative structure-based inhibitor design method can be used to search for additional changes to improve STE potency.

5.2.3 Mechanism of cancer cell sensitivity to STE

Myc hyperactivation in human cancer now approaches 70%, suggesting that this event is important for tumorigenesis (7). Activation of Myc occurs through diverse mechanisms, including translocations, amplifications, enhanced translation or protein stability (7). An emerging approach to cancer treatment is the targeting of the cellular machineries not directly involved in DNA replication or cell division, but which are essential for cancer growth and survival , such as SUMO E1 (8). Since STE inhibits SUMO E1 and the inactivation of SAE2 leads to mitotic catastrophe and cell death upon Myc hyperactivation (9), we hypothesized that STE inhibition of SAE would induce apoptosis in Myc-overexpressing cancer cells. To test this hypothesis further, we can investigate gene expression in the LP-1 and Raji cell lines to see if Myc is expression downregulated by STE treatment. This approach is especially promising because LP1, the human myeloma cell line, bears increased expression of c-myc protooncogene (10). Similarly, in Raji cells, which carry a t(8;14) chromosome translocation, the c-myc oncogene is translocated to a switch region of the gamma heavy chain, S gamma (11). Additionally, we can treat the LP-1 and Raji cells with control vehicle or increasing doses of STE and measure the expression of Myc using quantitative PCR at different time points to see if there is a dose-dependent suppression of Myc by STE. As a control, we will use isolated human B cells and treat them with vehicle control or various concentration of STE. These experiments will answer the questions if STE treatment downregulated Myc pathway and if this treatment also induce cytotoxicity in isolated human B cells.

In addition to cell-based assays, STE can also be tested on animal models of solid tumors, such as 4T1 breast carcinomas, to investigate its anti-cancer effect in vivo. Since STE was found as

an inhibitor of the SUMOylation pathway, it will be interesting to test the effects of STE on SUMOylation activity in vivo by staining tumor sections with SUMO antibodies to measure target protein modification by SUMO. Additionally, it will be beneficial to determine if STE induces apoptosis or necrosis in vivo. These observations will be useful as a proof of concept of targeting the SUMOylation pathway as a new approach to cancer treatment.

5.3 Significance

Posttranslational modification by SUMO has emerged as one of the pathways supporting carcinogenesis. We successfully performed a FRET-based high-throughput screening to identify small molecules inhibitor of SUMOylation pathway. We identified STE as a small molecule inhibitor of the SUMOylation pathway and characterized the mechanism of action of this inhibitor. Mechanistically, STE impaired SUMOylation by inhibiting the E1~SUMO thioester formation. I developed quantitative FRET assays to measure the kinetics of the SUMO E1 enzyme and found the Km of SUMO1, SUMO2, SUMO3, and ATP. By employing this innovative assay, I determined STE to be a non-competitive inhibitor of the SUMO E1 enzyme with an inhibition constant of 1.90 μM. Additionally, STE caused more death in non-small cell lung cancer cell lines compared HEK 293 cells. Further elucidation of the molecular mechanisms by which STE induces cell death will provide a basis for targeting SUMOylation for cancer treatment.

5.4 References

1. Arkin MR, Wells JA. Small-molecule inhibitors of protein-protein interactions: progressing towards the dream. Nature reviews Drug discovery 2004;3(4):301-17.
2. Klebe G. Virtual ligand screening: strategies, perspectives and limitations. Drug Discovery Today 2006;11(13–14):580-94.
3. Lois LM, Lima CD. Structures of the SUMO E1 provide mechanistic insights into SUMO activation and E2 recruitment to E1. The EMBO journal 2005;24(3):439-51.
4. Copeland RA. Reversible Inhibitors. Enzymes: John Wiley & Sons, Inc.; 2002. p 266-304.
5. Lipinski CA, Lombardo F, Dominy BW, Feeney PJ. Experimental and computational approaches to estimate solubility and permeability in drug discovery and development settings. Advanced Drug Delivery Reviews 2001;46(1–3):3-26.
6. Copeland RA. Chemical Bonds and Reactions in Biochemistry. Enzymes: John Wiley & Sons, Inc.; 2002. p 11-41.
7. Nilsson JA, Cleveland JL. Myc pathways provoking cell suicide and cancer. Oncogene 2003;22(56):9007-21.
8. Dobbelstein M, Moll U. Targeting tumour-supportive cellular machineries in anticancer drug development. Nature reviews Drug discovery 2014;13(3):179-96.
9. Kessler JD, Kahle KT, Sun T, Meerbrey KL, Schlabach MR, Schmitt EM, et al. A SUMOylation-Dependent Transcriptional Subprogram Is Required for Myc-Driven Tumorigenesis. Science 2011;335(6066):348-53.
10. Pegoraro L, Malavasi F, Bellone G, Massaia M, Boccadoro M, Saglio G, et al. The human myeloma cell line LP-1: a versatile model in which to study early plasma-cell differentiation and c-myc activation. Blood 1989;73(4):1020-7.

11. Nishikura K, Erikson J, ar-Rushdi A, Huebner K, Croce CM. The translocated c-myc oncogene of Raji Burkitt lymphoma cells is not expressed in human lymphoblastoid cells. Proceedings of the National Academy of Sciences of the United States of America 1985;82(9):2900-4.